64-003
B

UNITED STATES
NAVAL POSTGRADUATE SCHOOL

THESIS

AN INVESTIGATION OF THE WEAR AND FRICTION CHARACTERISTICS OF A HIGH TEMPERATURE SOLID FILM LUBRICANT IN HIGH VACUUM AND IN AIR

BY

Donald W. Flage

AN INVESTIGATION OF THE WEAR AND FRICTION CHARACTERISTICS OF A HIGH TEMPERATURE SOLID FILM LUBRICANT IN HIGH VACUUM AND IN AIR

* * * * * * *

Donald W. Flage

AN INVESTIGATION OF THE WEAR AND FRICTION CHARACTERISTICS OF A HIGH TEMPERATURE SOLID FILM LUBRICANT IN HIGH VACUUM AND IN AIR

by

Donald W. Flage

Lieutenant, United States Navy

Submitted in partial fulfillment of
the requirements for the degree of

MASTER OF SCIENCE
IN
MECHANICAL ENGINEERING

United States Naval Postgraduate School
Monterey, California

1964

AN INVESTIGATION OF THE WEAR AND FRICTION CHARACTERISTICS OF A HIGH TEMPERATURE SOLID FILM LUBRICANT IN HIGH VACUUM AND IN AIR

by

Donald W. Flage

This work is accepted as fulfilling
the thesis requirements for the degree of
MASTER OF SCIENCE
IN
MECHANICAL ENGINEERING
from the
United States Naval Postgraduate School

ABSTRACT

With a specially designed machine, the wear and friction characteristics of high temperature SFL #1000, manufactured by Electrofilm Incorporated, North Hollywood, California, were investigated.

The lower wear specimen, a stainless-steel annular disc, coated at the factory to a thickness of 0.0003 to 0.0005 in., was the rotating member. The upper non-rotating specimen, identical to the lower, was uncoated. These mating wear and friction annular surfaces were tested under the following controlled variables:

1. Temperatures room temperature, 500°F, and 1000°F
2. Speed 250 and 350 RPM
3. Load 10.29, 20.55, and 30.35 lbs.
4. Environment 10^{-5} - 10^{-6} mm Hga, and ambient pressure.

The results of these tests clearly indicated this lubricant to have poor lubricating characteristics. Specifically, SFL #1000, a ceramic bonded high temperature solid film lubricant using molybdenum disulphide combined with synthetic graphite, was found to have:

1. Unacceptably high dynamic coefficient of friction (prior to film break-through) in high vacuum as well as in air. Typical values ranged from 0.30 to 0.40.

2. Undesirable "stick-slip" phenomenon, occurring when the static friction coefficient exceeds the dynamic coefficient.

3. Excessively high wear rates, (change in film thickness (μ in.)/elapsed run time (min.)). Typical rates ranged from 10 to 50 μ in./min.

4. Low wear lives. Film failure occurred usually between one to 10 minutes.

The results of these tests clearly indicated that this lubricant would make a poor candidate for any practical engineering application where moderate rubbing speed and running time were needed.

SUMMARY

The objectives of this thesis were as follows:

A. The design and fabrication of a high vacuum wear-and-friction machine capable of yielding repeatable results; speed, temperature, and load as variable parameters.

B. Investigation of the wear and friction characteristics of Electrofilm's high temperature SFL #1000 in high vacuum and in air.

The following conclusions were reached:

A. SFL #1000 produced the following:

1. Unacceptably high dynamic coefficient of friction, with the additional bad feature of a "stick-slip" phenomenon.
2. Excessively high wear rates (low wear life) rendering it an unsatisfactory lubricant.
3. Non-repeatable results.

B. With Teflon (TFE) wear samples, the wear-and-friction machine yielded consistent results for the following reasons:

1. Teflon (TFE) Tests #1 and #2, were reproducible with an average μ_d of 0.20.
2. Teflon (TFE) Tests #3 and #4, were also reproducible with an average μ_d of 0.175.
3. These results compared favorably with values of the coefficient of friction found in the literature [9, 11, 23].

4. The most favorable runs using SFL #1000 produced coefficients of friction in reasonable comparison to those values quoted in Electrofilm's Technical Bulletin #2048 [8].

The experimental work was performed from February through March 1964 at the United States Naval Postgraduate School, Monterey, California.

ACKNOWLEDGMENTS

The author is indebted to Professor E. K. Gatcombe for his assistance in securing the necessary funds for this project. Professor J. R. Clark of the Department of Metallurgy and Chemistry is also thanked for his advice and assistance. Laboratory technicians K. S. Smith and H. E. Herriman were most helpful in the author's efforts to learn about high vacuum techniques. The wear-and-friction machine was designed by the author and built in the machine shops of the Naval Postgraduate School. Mr. N. Walker and Mr. H. F. Perry are thanked for producing excellent machine components, and special acknowledgment is due Mr. August B. Rasmussen who worked hand-in-hand with the designer to make the machine's timely completion possible.

TABLE OF CONTENTS

LIST OF ILLUSTRATIONS

LIST OF TABLES

I

INTRODUCTION

Man's ideas and ambitions have always been far in advance of the materials to fulfill them. His greatest ambition today is to leave the Earth and travel throughout the universe. In any vehicle traveling through space, control of friction, wear, and lubrication may well constitute the greatest materials problem.

The growing interest in the exploration of the universe makes mandatory new machines that must operate under the extreme temperatures and the high vacuum of outer space. A critical problem is that of developing bearings that will operate for long unattended periods. Conventional bearings cannot be used because the liquid lubricants evaporate quickly at the low pressure.

The use of solid film lubricants is one answer to this problem. Certain properties of SFL make them attractive in outer space environs. These properties are:

1. Low wear rate,
2. Low coefficient of friction, and
3. Low evaporation rate.

Solid lubricants generally consist of fine powders having inherent lubricating properties. The types that will be described are mixed with a binder (generally a resin selected because of its high shear strength and abrasion resistance) and

applied to a metallic surface with heat. Promising solid lubricants are molybdenum disulfide and graphite. There has been a considerable amount of data presented in the past showing that graphite is not a satisfactory lubricant in high vacuum. Savage [18, 19] has said, in his two papers, that graphite lubricates by virtue of adsorbed water. This water is lost in a vacuum. This leaves only one well-known solid lubricant, molybdenum disulfide, for use in a vacuum. There has been considerable amount of data presented on the chemistry, melting point, etc., of molybdenum disulfide. In a vacuum, it should theoretically be usable at as high a temperature as its melting point. Cannon [4] has shown that molybdenum disulphide melts in excess of 1650°C. This indicates that in a good vacuum where there is no oxygen to oxidize the molybdenum disulphide to molybdenum trioxide, the material should be capable of lubricating to this temperature.

This lubricant derives its special properties from its unique laminar-lattice crystal structure that imparts low shear strength and makes it possible to form a regenerative lubricating film on mating surfaces. The crystal structure of molybdenum disulphide is shown in Figure I-1. The entire atomic forces on each plane are much greater than the forces between planes, resulting in a low shear strength between planes and therefore a low coefficient of friction [6].

The solid film lubricant to be tested under vacuum for wear and friction is SFL #1000 produced by Electrofilm Incorporated, North Hollywood, California. It is a ceramic bonded high

temperature solid film lubricant currently in use in the 800-2000°F range. It uses molybdenum disulphide combined with synthetic graphite to yield low friction and high load carrying capabilities at high temperature. It has never been tested under vacuum, and it is the author's intention to measure the performance of this high temperature solid lubricant with a specially designed high vacuum wear-and-friction machine.

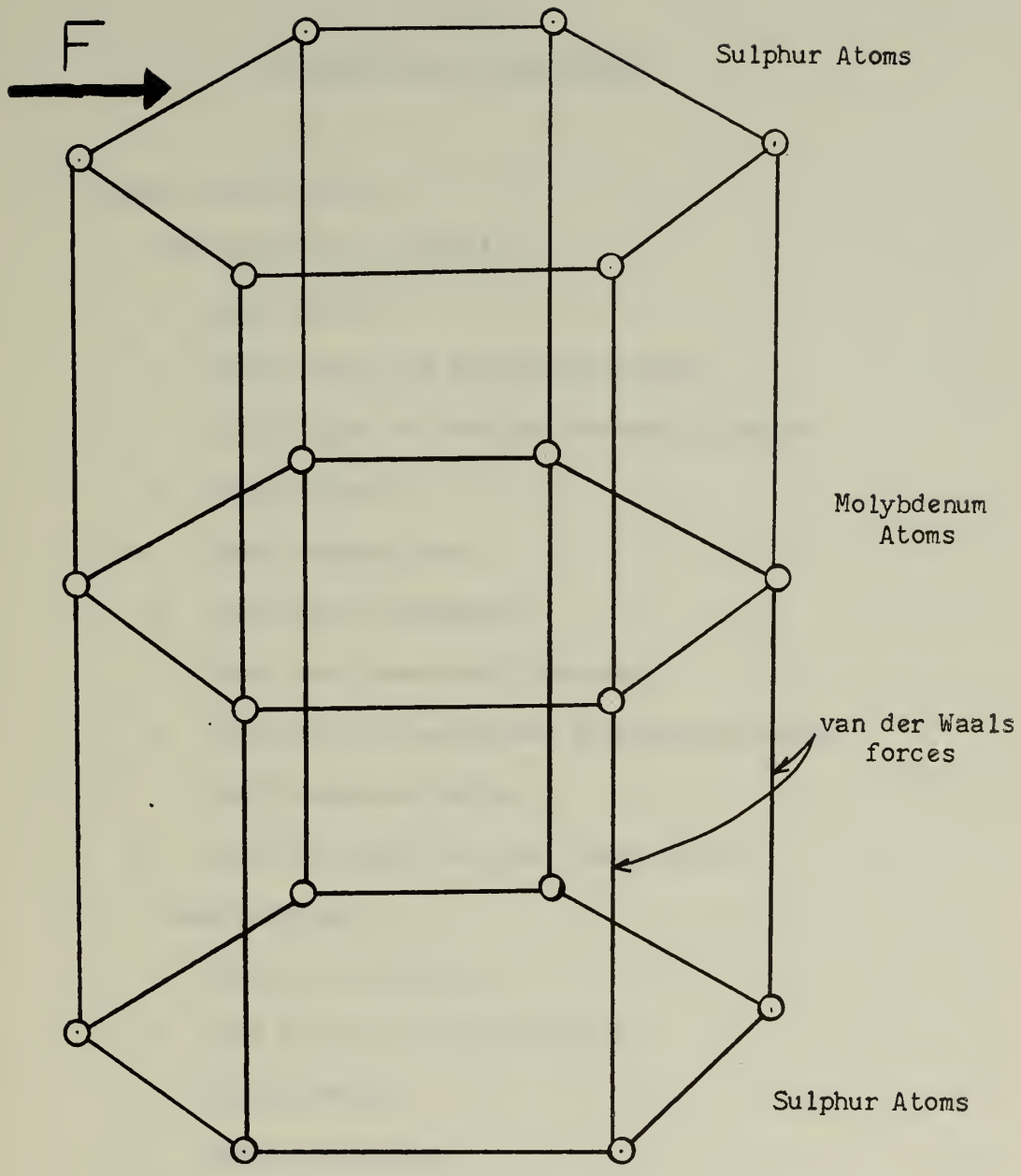

Figure I-1

Crystal structure of molybdenum disulphide. Low shear strength and low coefficient of friction is a result of atomic forces on each plane being stronger than those between planes.

II

DESCRIPTION OF EQUIPMENT

I. General Description

A. Wear-and-Friction Machine

1. Heat Source
2. Static Load and Non-Rotating Shaft
3. Coefficient of Friction Measuring Device
4. Rotary Shaft
5. Speed Sensing Unit
6. Structural Components
7. Upper and Lower Wear Specimen
8. Temperature Sensing and Indicating Devices
9. Wear Measuring Device
10. Variable Speed Unit and Power Drive

B. Vacuum System

1. Bell Jar and Hoist
2. Base Plate and Feed-Throughs
3. Vacuum Pumps
4. Seals and Valves
5. Gages
6. Safety Devices

II. Detailed Descriptions

A. Wear-and-Friction Machine

1. Heat Source

A high-vacuum furnace was designed and built by the author to provide a maximum steady state temperature of 1500°F on the rotating wear specimens. The heater was of the resistance type using an aluminum-chromium-iron based alloy for the heated wire. This wire, commercially known as KANTHAL A-1, was wound around $\frac{1}{8}$ in. alumina tubing and then cemented in place on the innermost radiant shield. The capacity of the heater was a nominal 1.25 kw using single phase AC 115-volt power supply. The shape of the heater was cylindrical; diameter 9 in., and height 8 in. In order to minimize heat loss by radiation (at high vacuum, convective losses are negligible, [5]), four concentric heat shields of AISI 316 stainless-steel were used along with a partial inner shield of pure sheet molybdenum (extremely low emmisivity). Two $1\frac{1}{2}$ in. holes were centrally located through the shielded top and bottom of the heater through which the non-rotating and rotating shafts entered. The heater "lid" was cut in two and handles were installed to facilitate mounting and demounting of the wear specimens. Temperature control was accomplished by using a chromel-alumel

thermocouple introduced radially through a hole in the heater shields and positioned in the upper non-rotating wear specimen $\frac{1}{8}$ in. from the wear surface. The specimen temperature was monitored by a Honeywell-Brown heat controller (Serial #872 608) which had been previously calibrated by the author using a null potentiometer made by the Rubicon Company (Serial #2732).

2. Static Load and Non-Rotating Shaft

AISI 304 stainless-steel, disc-type weights were machined to vary the normal load applied to the $\frac{1}{2}$ in. annular surfaces of the wear and friction specimens. These weights (10.29, 20.55, and 30.35 lbs.) were positioned concentrically over the non-rotating shaft and were located above the wear machine. The loading weights included non-rotating shaft, upper wear specimen, ball joint, and torque arm.

The non-rotating shaft was fabricated from two materials; these were AISI 304 stainless-steel and a high temperature ceramic called Lavite. The overall length was 22 in. with a nominal $\frac{5}{8}$ - in. diameter. A $\frac{3}{4}$ - in. stainless-steel ball was placed at the end of the shaft and mounted in a spherically ground container. Two inches above the ball, a $\frac{3}{16}$ - in. stainless-steel torque pin, 1.70 in. long, was driven radially through the shaft. The Lavite and the steel were fastened together by two $\frac{7}{16}$ - in. threaded steel

studs. Six inches above the ball, a $\frac{1}{16}$ - in. slot was machined through the entire shaft to accommodate a 5 x 0.5 x 0.050 in. cantilever arm manufactured from high grade spring steel. The shaft was threaded at the top section to secure a disc-type platform permitting placement of the larger weights.

This Lavite is naturally-occurring hydrous aluminum silicate as furnished by the American Lavite Corporation of Chattanooga, Tennessee. It was first machined in the ordinary manner, slightly under sized, then fired in a metallurgical furnace by raising the temperature slowly to 1800°F, holding that temperature for about one hour, after which the furnace cooled. It is credited by the supplier with 2500 psi ultimate tensile strength, 40,000 psi compressive strength, and a thermal conductivity of 0.003 (cal./cm.sec.°C).

3. Coefficient of Friction Measuring Device

Recorded torque arm strain caused by torque induced in the non-rotating shaft by the rotating wear-and-friction specimen, enabled the coefficient of dynamic friction to be determined.

The cantilever beam was carefully located and secured in a $\frac{3}{16}$ - in. milled slot in the stainless-steel portion of the upper shaft $\frac{1}{4}$ in. above the lower ball bearing. At a point 1.667 in. from the center line of the shaft, four high temperature

Bakelite strain gages were longitudinally installed, two on each side of the beam. The gages were purchased from the Baldwin-Lima-Hamilton Corporation, Waltham, Massachusetts, and were of the AB-5 type having a nominal resistance of 75 ± 0.3 ohms and a gage factor of 2.06 ± 0.01, with overall dimensions of $\frac{1}{8}$ in. wide and $\frac{1}{2}$-in. long. These gages were attached to the torque arm using a phenolic Bakelite cement allowing the gage area to dry sufficiently before curing. The cement was cured by slowly raising the temperature to 100°F, holding for one hour; final cure at 350°F for one hour, with the heating rate not to exceed 100°F per hour. Number 10 gage constantan wire was soft soldered to the strain gage leads, insulated with alumina sleeving. The insulated leads were then fed through a 1-in. stainless-steel tube, 20-in. long. A vacuum tight feed-through (8 pronged) in the base plate enabled the leads to be connected to a BLH Type N portable strain indicator (type SR-4). The dynamic coefficient of friction was related to the longitudinal strain of the cantilever beam by equation $\mu d = K(\epsilon l/3)$. (See Appendix E for detailed analysis.)

A chromel-alumel thermocouple was placed near the four active strain gages, connected for full temperature compensation.

4. Rotary Shaft

The rotary shaft driving the lower wear sample was made in three distinct parts. These were:

a. Lower steel section

A six-in. length of AISI 304 stainless-steel was machined to slip through two $\frac{3}{4}$ - in. medium-duty ball bearings, spaced 4-in. apart. These bearings were made by New Departure, Bristol, Connecticut. For vacuum use, they were thoroughly cleaned and lubricated with Dow Corning High Vacuum Grease (stable up to +400°F at pressures of at least 10^{-6}mm Hga). A $1\frac{1}{4}$ in. diameter collar was machined integral with the rotary shaft to transmit axial load to the upper thrust ball bearing.

b. Middle ceramic section

A cylinder of Lavite, $2\frac{7}{8}$ x $1\frac{1}{4}$ in. was machined, and on each end a $\frac{9}{16}$ - in. hole, $\frac{5}{8}$-in. long was tapped. This portion of the shaft connected the upper stainless-steel wear specimen support with the lower steel shaft and provided the necessary thermal conduction barrier from the heater core to the critical bearing areas that had to be maintained at $\leq$ 400°F.

c. Upper steel section

Fabricated from the same type of stainless-steel as the lower section, it was designed to serve two purposes:

(1) Transmit torque to the lower wear sample,

(2) Act as a rigid base to support the lower wear specimen.

The base was machined in circular steps to conform to the contour of the under side of the lower wear sample. To transmit torque, two $\frac{1}{8}$ in.diam. pins were pressed into the outer portion of the base and protruded approximately $\frac{1}{8}$ -in. The stepped sections enabled each specimen to be concentrically located on the base.

The power shaft was connected to the vacuum rotary seal by a specially designed Oldham flexible coupling, machined from AISI 304 stainless-steel and Teflon, (TFE). It enabled vibration-damped torque to be transmitted from the $\frac{5}{16}$ - in. rotary seal shaft through the middle coupling component made of Teflon (TFE), and finally to the hollow $\frac{3}{4}$ - in. stainless-steel specimen shaft. The Teflon, having excellent damping properties, was used to dampen out torque pulses produced in the speed controller and electric motor. It also had the additional feature of low outgassing (10^{-6}mm Hga) at high temperatures (up to 500°F). [23].

5. Speed Sensing Unit

The determination of the wear specimen shaft speed was accomplished by a system of gears, an electric tachometer, and a remote speed sensing meter.

A six-in. diameter aluminum spur gear (110 teeth) was press fitted on the output shaft of the Vickers Speed Controller. This large gear drove a $2\frac{1}{4}$ -in. diameter aluminum gear of 49 teeth, increasing the speed 2.222 to 1. The small gear drove the tachometer generator made by Ideal Industries Incorporated, Sycamore, Illinois (Serial #50-001). The voltage produced was applied across a speed sensing meter located on the side of the wear machine just above the speed control knob. The meter had a low and a high scale.

Low scale 0 - 1250 RPM

High scale 0 - 2500 RPM

The generator was housed in an aluminum block that was connected to a "cantilever" type aluminum angle, firmly bolted to the wear-machine frame. Between each metal-to-metal connection, a $\frac{1}{4}$ - in. rubber isolator to absorb some of the vibrations caused by the rotating power unit, was placed. This rubber isolation scheme was also applied to the speed sensing unit.

6. Structural Components

The structural components of the machine were made primarily out of various types of stainless-steel. This was done to reduce significantly the outgassing rate and make possible an early attainment of the operating pressure (10^{-5} -10^{-6} mm Hga). The wear machine

consisted of 5 platform-type discs held in place by four $\frac{3}{4}$-in. threaded columns. Each platform served a special purpose:

a. The bottom platform was $\frac{1}{2}$ - in. thick, 13 in. in diameter with a five-in. inner hole through which the power shaft operated. Four $\frac{3}{4}$ - 10 - N.C. threaded holes were placed 1-in. from the outer periphery of the plate (45° apart) and served as a foundation for the threaded columns. Four aligning pins were located on the bottom of the disc to position the wear-and-friction machine on the base plate.

b. The next higher platform was $\frac{1}{2}$-in. thick, and 12-in. in diameter. This platform served to house the lower ball bearing which was a medium-duty, single-row, unshielded bearing, press-fitted into a machined bearing housing that was screwed in place at the center of the platform. Four $\frac{7}{8}$ - in. slots were milled on the edges of the platform to enable the threaded columns to support the plate and to align the center bearing.

c. The third highest platform served two functions. The vacuum heater rested on this $\frac{1}{2}$ - in. thick plate and was positioned centrally on the platform by four aligning pins. Its second function was to house the upper thrust bearing. This bearing was a medium-duty, double-row, ball bearing and served to

absorb the axial thrust of the 10-, 20-, and 30-lb. weights.

d. The fourth highest platform was similar to the ones previously mentioned, but it was $\frac{1}{4}$-in. thick. Its function was to house the lower ball bearing that supported the non-rotating shaft. Alignment of this bearing with the power shaft ball bearings was accomplished by the enlarged slots milled on the edges of the platform. Another purpose of this member was to serve as a foundation for the stainless-steel knife edge which was positioned and locked in place five-in. from the center line of the non-rotating shaft. Throughout the structure, $\frac{3}{4}$-10-NC stainless-steel nuts were used to lock the various platforms in place.

e. The fifth and final platform was identical to the one just mentioned and housed the upper ball bearing. Alignment of the bearing was again accomplished using the enlarged slot method.

Attached to the machine were two 1-in. stainless-steel tubes designed to carry all the thermocouples and strain gage leads. Wherever a thermocouple was required, a "branch" tube was screwed into the main tube and served as a radiation shield. Inside this "branch" tube was another stainless-steel tube, slightly larger than the alumina sleeving, capable of sliding in and out. Once the thermocouple was

correctly positioned, the various tubes were locked in place with stainless-steel set screws. In this way, all the thermocouples were protected from physical damage and the effects of radiation were thus minimized.

7. Upper and Lower Wear Specimens

The upper and lower wear specimens were machined accurately from AISI 410 cold-rolled stainless-steel. The two specimens were machined into 2-in. diameter discs, $\frac{3}{4}$ - in. in height. A cut, 1-in. in diameter, $\frac{1}{16}$ - in. deep, was made on both samples to create a $\frac{1}{2}$ - in. annular wear surface. The deep sections of the specimen insured minimum warping at operating temperatures. The lower sample was coated with SFL #1000. The coating procedure was as follows:

a. Degrease the 20 RMS surface with MIL-T-7003,

b. Chemically etch (Bondente "SS"),

c. Inspect,

d. Apply SFL #1000 by spraying,

e. Cure at 250°F for $\frac{1}{2}$ hour, then at plus 1000°F for 15 min.,

f. Inspect.

The upper annular wear surface (non-lubricated) was machine ground flat to a 8 RMS finish. A $\frac{1}{8} \times \frac{1}{4}$ - in. hole was drilled $\frac{1}{8}$-in. up from the wear surface to accommodate the shielded chromel-alumel thermocouple. A spherical seat of $\frac{3}{8}$-in. radius was ground $\frac{1}{4}$-in. into the top of the upper specimen to house the ball-end-jointed, non-rotating shaft. To transmit torque, a stainless-steel forked component was

secured by four #8-32 stainless-steel screws around the spherical seat.

Torque transmission from the rotating power shaft to the lower wear specimen was via two $\frac{1}{8}$ - in. stainless-steel pins, 4-in. apart, fitting into a $\frac{3}{16}$-in. keyway on the specimen. Machined on the under side of the test specimen were two concentric "concave" cavities 1.25 x 0.150 and 0.750 x 0.100 in. These stepped cavities insured colinearity between platform and test specimen.

8. Temperature Sensing and Indicating Devices

Chromel-alumel thermocouples were used to sense the temperatures at the following locations on the wear machine:

a. Upper non-rotating wear specimen,

b. Outer race of the thrust ball bearing,

c. Ball bearing (one nearest furnace),

d. Adjacent to strain gages,

e. Vacuum base plate;

The reasons for this choice of temperature monitoring were as follows:

a. The temperature of the mating wear surfaces was necessary because it was a controlled parameter in the testing.

b. The double-row, medium-duty, thrust bearing was lubricated with Dow Corning Silicone grease which had an upper stability limit of 400°F.

c. The lower ball bearing that supported the non-rotating shaft was also lubricated with this high temperature vacuum grease.

d. To calibrate the torque arm accurately for the various operating temperatures, it was necessary to know the temperatures at the strain gage location. It was decided to attach the thermocouple to the knife-edge member rather than to the cantilever arm which had to be raised and lowered periodically.

e. The numerous Viton and Silicone "O" rings located on the under side of the base plate could withstand temperatures up to 400-500°F. However, since the Viton "O" rings outgass above 300°F, this temperature limit was necessary if a high vacuum of 10^{-5}- 10^{-6}mm Hga was to be maintained. The thermocouples, b. through e. above, were insulated with either alumina beading or tubing and were soldered to the Swedgelock thermocouple feed-through. The thermocouple leads were cemented to a Bakelite terminal board on the side of the wear machine. Through a thermocouple selector switch, absolute potential from any of the four thermocouples (referenced against an ice junction) was accurately registered on a Rubicon precision potentiometer (#2732). The common ice junction was housed in a stainless-steel tube inserted in a standard vacuum bottle that was filled with crushed ice and located near the thermocouple terminal board.

The thermocouple, controlling the temperature of the upper wear specimen, was connected to a Honeywell-Brown heat controller (#872-608), which had been previously calibrated by the author. Thus temperature control from 100 to 1500°F was achieved.

9. Wear Measuring Device

A Mikrokator, made by C. E. Johansson Gage Co., Dearborn, Michigan, was used to detect dimensional loss of the solid-film lubricant. This Mikrokator (Serial #7V510 E-7) had a sensitivity of 0.000005-in. per division with a complete scale range of 0.0004-in. It was a frictionless mechanical device having a patented mechanism providing amplification of 100,000 to 1 without the use of gears, levers, air, or electricity.

The heart of the Mikrokator, its amplifying mechanism, was a twisted bronze band to which the indicating pointer was attached. The twist was permanently set into the metal band by clamping both ends and rotating the center beyond its elastic limit. When this band was stretched, it tended to straighten out. The rotation of its center point was proportional to the tensile load imposed. By these means, a pointer attached to the center of the band would be rotated through a considerable angle by a very small increase in the band's length. Connection of the measuring tip to the twisted band was accomplished through a rigid spindle, supported between two slotted steel diaphragms and attached at its upper end

to a right-angle spring knee. The movable end of the twisted band was attached to the second arm of the spring knee. Displacement of the tip produces an exactly proportional, but greatly amplified, movement of the pointer. Other necessary Mikrokator accessories were:

a. Lifting lever (Serial #511)

b. Measuring plate (3.15-in. diameter)(Serial #518-2)

c. Flat cemented carbide measuring point (Serial #PM-512)

d. Stand (Serial #513A)

10. Variable Speed Unit and Power Drive

A variable speed unit of the fluid coupling type was used to transmit up to 30 in.lb. torque to the wear specimens. It had a speed range from 0 to $\pm$ 1800 RPM, and speed was controlled by turning a knurled aluminum knob located on the side of the machine directly under the tachometer. After the desired speed was set, the speed control shaft was locked in place by an Allen set screw. The Vickers speed controller, manufactured by Vickers Incorporated, Division of Sperry Rand Corp., Detroit, Michigan, was driven by a 1-HP capacitor-start induction motor. Two Oldham flexible couplings were used in the power drive; one between the induction motor and the speed controller, and the other from the speed controller to the vacuum rotary seal.

B. Vacuum System

1. Bell Jar and Hoist

An AISI 304 stainless-steel bell jar (16-in. diameter, 33-in. high) was fabricated by the Steinmetz Machine Company, Pacific Grove, California. The side walls of $\frac{1}{4}$-in. plate were rolled and electric-arc welded. A highly finished (30 RMS) 5-in. flange was welded to the bottom of the "can" as was the $\frac{3}{8}$-in. stainless-steel top. Finally, a large bolt was welded to the top of the drum for lifting purposes.

The drum was then checked for leaks and the welded seams were found to be extremely porous. To remedy the leakage problem, the can was cleaned externally by wire brushing; and then black Glyptal sealant was applied over the entire bell jar while a rough vacuum was applied inside. This sealant was able to withstand a temperature up to 200°F without appreciable outgassing. With the sealant at 200°F, high vacuum of 10^{-6}mm Hga was claimed by the manufacturer.

The hoist was designed to raise and lower the 187 lb. bell jar and to swing the raised jar 90 degrees to the right or left. To accomplish these tasks, the hoist was fabricated in the following manner. A 9-ft. length of steel pipe ($2\frac{1}{2}$-in. diameter, $\frac{1}{4}$-in. wall) was fastened to the wear machine table by two

aluminum blocks (15-in. apart), serving as bearings to support the radial load, and by a thrust bearing located at the bottom of the table. This heavy-duty Timken tapered roller bearing, housed in an aluminum block, reduced the effort to turn the drum.

To raise and lower the drum, a boat trailer winch was securely fastened to the pipe just above a 1-ft. long turning handle. Steel cable ($\frac{5}{16}$-in. diameter) was used to lift the weight and was fed through two 4-in. steel pulleys located on a welded steel arm on top of the pipe. Three safety features were used to prevent the raised jar from falling; they were:

a. Steel rachet engaging the teeth of the driving pinion gear permitted one-way motion.

b. Stainless-steel tube fitted over the driving shaft prevented the driving handle from rotating.

c. Extra cable clamp reduced the possibility of a clamp failure.

Two 1-in diameter bullet-nosed aluminum rods were attached to the wear machine parallel with the longitudinal axis of the bell jar. These guiding rods were fitted through two "wings" extending radially from the bell jar, 8-in. from the bottom flange. The holes in the "wings" were fitted with Teflon

bushings to prevent sticking and chatter as the jar was raised and lowered.

2. Base Plate and Feed-Throughs

The circular vacuum base plate was made from aluminum, and the two surfaces were machined to a 50 RMS finish. The "O" ring grooves ($17\frac{1}{8}$ and $19\frac{1}{8}$ in. inside diameter) were machined on one side of the $\frac{5}{8}$ -in. plate for normal 0.275-in. diameter "O" rings. This base plate rested on a $\frac{5}{8}$ -in. aluminum supporting plate. A $3\frac{1}{2}$ -in. hole was bored in the plate to house the diffusion-pump manifold. Various holes were bored for the vacuum feed-throughs as follows:

a. Rotary vacuum seal

This device, made by the MRC Manufacturing Corporation, Orangeburg, New York, permitted the transmission of rotary motion into high-vacuum systems without leakage. Leak proof to 2000 RPM and ideal for systems operating up to 10^{-7}mm Hga, it possessed a patented floating seal and double-ball-bearing construction with a $\frac{5}{16}$ -in. stainless-steel power shaft. A $1\frac{1}{8}$ -in. diameter hole was drilled 1 inch off center to allow for the rotary seal. To prevent leakage, a $\frac{1}{8}$ -in. Viton "O" ring was used, with the "O" ring flange secured to the under side of the base plate with 8, #10-24 steel Allen screws.

b. Thermocouple feed-through

A brass Swagelok fitting (Serial #1210-1-OR) made by the Crawford Fitting Company, Cleveland, Ohio, feeds 8 chromel-alumel thermocouple leads through the base plate. The $\frac{3}{4}$-in. stainless-steel tube was capped at one end with an 8-pronged insulation feed-through disc; the tube was placed in the tube fitting, and two Viton "O" rings sealed the tube and the $1\frac{1}{16}$-in. threaded hole in the plate.

c. Strain gage feed-through

An 8-pronged insulated feed-through cap was soft soldered to a stainless-steel "O" ring flange ($2\frac{1}{2}$-in. diameter, $\frac{3}{16}$-in. thick). A $\frac{3}{4}$-in. hole was drilled through the base plate for passage of the strain gage leads, and leakage was prevented by using a $\frac{1}{8}$-in. Viton "O" ring.

d. Vacuum heater electrical feed-throughs

Two heavy-duty power feed-throughs carried the necessary 10 to 15 amperes of heater current. These feed-throughs were furnished by the Physics Department of the U. S. Naval Postgraduate School, Monterey, California. The vacuum seal was achieved using Buna "N" washers between the bottom surface of the base plate and the stainless-steel head of the electrical feed-through. Two $\frac{3}{4}$-in. holes

were drilled into the plate to house these fittings. Heavy-gage copper buss bars connected the vacuum heater terminals to the electrical feed-through terminals.

3. Vacuum Pumps

a. Mechanical pumps

Two Welch Duo-Seal pumps were used in the vacuum system:

(1) Roughing pump

A 1402B Welch pump, two stage, was used to secure rough vacuum in the large stainless-steel bell jar. This pump was able to pump 140 liter/min. and was driven by a $\frac{1}{2}$ HP capacitor-start induction motor.

(2) Fore pump

A large capacity Welch pump (type 1397B) was used to back the oil diffusion pump. This pump had a free air capacity of 425 liter/min. and was driven at 365 RPM by a $\frac{3}{4}$ HP induction motor. With the aid of a 4-in. quick-acting valve located between the diffusion pump and the vacuum chamber, it was possible to keep a high vacuum (10^{-6} mm Hga) localized in this vicinity, while the vacuum bell jar was hoisted to allow for easy access to the wear machine. In this way, the time

required for the necessary vacuum to be achieved in the jar was reduced.

b. Diffusion pump

A MCF-300 pump, manufactured by Consolidated Vacuum Corporation, Rochester, New York, was used to bring the vacuum in the bell jar down to 10^{-5} - 10^{-6}mm Hga. The ultimate pressure for this pump was 2×10^{-7}mm Hga, with a maximum pumping speed of 290 liters/sec. at 4×10^{-4} - 9×10^{-4}mm Hga with Dow Corning DC-704 diffusion-pump oil. The limiting forepressure at full load was 220 microns and at no load was 480 microns of mercury.

4. Seals and Valves

Much use was made of the "O" ring seal, and two specific kinds of "O" ring materials were used, Silicone and Viton. Silicone rubber "O" rings, red in color, maintain their stability in the presence of a high vacuum at temperatures as high as 400°F. They have two other interesting features:

a. Negligible outgassing at elevated temperatures;

b. High air permeability at elevated temperatures.

The Viton "O" rings, black in color, had the reverse features of Silicone "O" rings. Thus, the bell jar was sealed by double "O" rings; Silicone on the inner and Viton on the outer groove.

The following openings to the vacuum system were sealed by Viton "O" rings:

a. Rotary shaft

b. Thermocouple feed-through

c. Strain gage feed-through

d. Vacuum furnace leads

e. Diffusion pump manifold

f. Fore line connection

An STV-4, quick-acting manual gate valve, manufactured by Consolidated Vacuum Corporation, Rochester, New York, isolated the bell jar from the diffusion pump. The body and valve plate were constructed of aluminum and the working parts were steel. This valve opened fully with no restriction to the flow area, and was individually leak tested with a mass spectrometer leak detector. The "O" flanges were drilled to mate with the MCF-300 series diffusion pump.

A valve made by Vacuum Electronics Corporation, Long Island, New York, was used to isolate the bell jar from the roughing mechanical pump. It was a bellows sealed, brass body valve using a Viton "O" ring and gasket. Two 6-in. pieces of $\frac{1}{2}$-in. stainless-steel pipe were silver soldered to the manually operated valve, one pipe soldered directly to the diffusion pump manifold, the other to the mechanical pump via vacuum rubber tubing.

5. Gages

A type 07-1031-01 ionization/thermocouple gage, manufactured by the National Research Corporation, Cambridge, Massachusetts, was used to monitor the pressure at various points in the vacuum system. This gage included:

a. Two thermocouple gage circuits with switching so that neither, either, or both gages were operative. One gage was located in the low-vacuum side of the diffusion pump to indicate foreline pressure, and the other gage on the high-vacuum side of the diffusion pump to indicate roughing pressure and also indicate when the pressure was low enough to turn on the ionization gage.

b. An emission regulating ion gage circuit with grid emission values of one, five, and ten milliamperes.

c. A DC amplifier giving full scale measurements of ion currents corresponding to pressures of 5 microns, 1 micron, 0.1 micron, 0.01 micron, and 0.001 micron of mercury (1 micron = 1^{-3} mm Hga), when used with an NRC type 05-700 gage. This hot filament ionization gage was located in the high-vacuum side and indicated operating pressure.

d. A high pressure cutout in the ion gage filament circuit which automatically turned off the gage if the pressure exceeded approximately $1\frac{1}{2}$ times the full scale on any scale.

e. One instrument meter having two scales; (1) the upper scale calibrated in tenths from zero to one for use in reading the thermocouple gage input, the ionization gage grid current, and the ionization gage output from the DC amplifier, and (2) the lower scale calibrated in microns of mercury absolute from 1000 to one micron for use in reading the output of the thermocouple gage.

6. Safety Devices

a. Three safety devices were used to protect the equipment from damage:

(1) Thermal controller

A thermally operated switch was located against the cooling coils of the diffusion pump. The thermal controller, normally closed, would open-circuit the diffusion pump heater at 250 $\pm$ 5°F. This controller was also connected in series with the vacuum heater because with a loss of cooling water, the pumping would essentially stop and a gradual increase in pressure in the bell jar would cause large temperature rises due to convective heat transfer.

(2) A second similar type thermal switch was positioned in an aluminum housing and fastened to the underside of the aluminum base plate. If a leak occured overnight, the temperature of

the base plate would rise, and the "O" rings' seals would be damaged.

(3) Vacuum gage relay

This relay, housed in the ionization/thermocouple console, controlled the diffusion pump heater. The heater circuit was opened when the pressure on any scale of the ion range selector was increased by 150 percent. Thus, the hot diffusion pump oil was protected against the atmosphere.

III

EXPERIMENTAL PROCEDURES

A. Vacuum System

Because of anticipated troubles in obtaining a satisfactory vacuum, this system was put into operation first. It was built in steps to facilitate trouble shooting. The fore pump was connected to the diffusion pump. Minor leaks were discovered from a mass spectrometer leak detector.

Subsequently, the system as a whole was unsuccessfully operated. The stainless-steel bell jar was then tested individually, and the welded seams and major portions of the tank were found porous. It was then decided to coat the entire outside of the bell jar with black Glyptal while under rough vacuum. This sealing technique solved the leakage problem, and high vacuum was then achieved.

B. Test Procedures

1. Vacuum Runs

The fore pump and the vacuum gage were turned on. When 25 microns of mercury were indicated on the gage, the diffusion pump heater was energized.

A wear sample was checked for temperature and placed on the Mikrokator. Four scribed numbered lines were made on the side of the specimen (45° apart) to insure consistent readings. Starting with line one, a reading was taken for each line. This procedure

was repeated four times. To determine the mean initial reading, the numbered line readings were separately averaged, and these results were in turn averaged over the total number of lines.

The method for testing the wear samples was as follows:

a. Lower wear specimen placed on power shaft.

b. Upper wear specimen positioned on lower wear sample and thermocouple installed.

c. Non-rotating shaft lowered to engage upper wear specimen.

d. Loading weights placed on non-rotating shaft and heater cover positioned.

e. Bell jar lowered over wear machine.

f. Roughing pump operated to evacuate bell jar.

g. At rough vacuum of 50 microns, quick-acting gate valve opened, bringing entire system to a high vacuum.

h. At 10^{-5} mm Hga, vacuum heater turned on to desired temperature setting.

i. At thermal equilibrium, initial strain gage reading recorded, and power drive operated.

j. Speed control knob adjusted to desired speed.

k. Strain gage readings versus time recorded until audible evidence that SFL #1000 had worn away at which time test ended.

To remove the worn specimen, the vacuum gate valve was closed and the ion gage turned off. The bell jar was

slowly vented to the atmosphere, whereupon the hoist lifted the bell jar off the wear machine. After removal of the heater cover, an industrial blower quickly cooled the specimen. To insure that the temperature of the specimen was the same as when the initial readings were made, the wear specimen was placed on a copper cooling block. With the aid of a thermocouple and a null potentiometer, the initial specimen temperature was duplicated. Final readings were then made using the Mikrokator.

2. Air Runs

To shift from vacuum to air runs, the vacuum system was shut down by turning off the diffusion pump heater, and allowing the oil to cool. The fore pump was stopped and air was slowly admitted to the system. Then the bell jar was raised over the wear machine, turned 90° to the left, and locked in place. After removal of the base plate "O" rings, the apparatus was ready for tests in air. The method for testing the wear specimens in air was identical to that used in vacuum, except for the procedures dealing specifically with vacuum.

IV

SOURCES OF ERROR IN THE DYNAMIC COEFFICIENT OF FRICTION

A. Mean Frictional Radius ($\bar{r}$)

The arithmetic mean of 0.75-in. was used as the effective frictional radius in all calculations. This was valid if the coefficient of friction was assumed not to be a function of linear velocity and the wear was uniform. However, in this test, the solid film lubricant broke down exposing bare metal very early in most test runs, and the resulting "composite" coefficient of friction became larger and larger, approaching the coefficient of friction for steel-on-steel. By visually inspecting the specimen after each run, it was possible to estimate the uncertainty in the value of $\bar{r}$. This was determined to be $\pm$ 0.10-in.

B. Calibration Moment (M_p)

It was assumed that the net strain produced by the calibration moment would be the same under actual test conditions. The possible discrepancy was that under test conditions a "pure" couple made up the moment, while in the calibration test, a force and a couple were produced. This additional force, imposed at the lower ball bearing, might have produced a greater frictional torque than encountered in actual testing.

C. Extrapolation of the Calibration Curve

The calibration curve was valid for $3 \leq M_p \leq 13$ (in.lb.). In some runs, however, large and small net strains were encountered corresponding to large and small moments. Thus, it was necessary to extrapolate the curves linearly.

D. Initial Strain Gage Reading (ε_b)

During air tests, it was possible to press the torque arm against the knife edge repeatedly to check for consistent initial readings just prior to testing. However, this check could not be used in the vacuum runs. The initial readings were checked for consistency before the bell jar was lowered, and it was some time before the actual run was conducted (especially the 1000°F runs).

E. Final Strain Gage Readings (ε_a)

The values of ε_a were accurately determined in the early part of each run (no chatter due to break-through of film). However, as the SFL #1000 began breaking down at various sections on the wear surface, excessive chatter occurred, causing marked fluctuations in the strain gage indicator needle. Consequently, the uncertainty in the final readings was approximately $\pm$ 30 to 40 μ in./in. The greatest uncertainty in the net reading of strain was calculated to be about 40 to 50 μ in./in. which was equal to two divisions on the vertical scale of the calibration curve. Thus, very flat (horizontal) elliptical error regions surrounded each calibration point.

F. Frictionless Pulley

Nylon (20-lb. test) monofilament fishing line was used to connect the lever arm to the various calibration weights. A "frictionless" pulley was needed because the shaft was vertically located. The pulley consisted of a 2-in. long $\frac{5}{16}$-in. diameter steel shaft suspended by two precision ball bearings housed in an aluminum frame. The pulley was clamped rigidly to the machine platform directly above the heater. Although some pulley friction obviously did exist, it was neglected in the calibration test.

EXPERIMENTAL OBSERVATIONS

TEST 2A (W - 20.55 lb., S - 350 RPM, T - Htr. off, In Air) (Three runs)

With a pronounced increase in the strain reading as a criterion for failure, it appeared that the SFL #1000 successfully lubricated for 14 min. at which time a marked increase in strain reading accompanied by excessive chatter and squeak indicated film break through. The test had to be stopped at 18 min.

After run 2B-A, some SFL #1000 "dust" was found in the wear sample's inner annular cavity. Some lubricant had been deposited on the uncoated upper wear specimen; it was easily rubbed off.

At the conclusion of run 2C-A (which had to be terminated after one minute's duration due to excessive deflection of the torque arm), 60 to 70% of the wear sample was showing bare steel. Again a moderate amount of SFL #1000 "dust" was found in the inner annular cavity.

TEST 3A (Same as 2A) (Two runs)

After 5 min., at which time test 3A-A was concluded, little change in strain gage readings was evident, and no major film break-through observed. However, localized scuffing of the film (to bare metal) was seen when closely inspected, and a moderate amount of film "dust" was again

found in the inner cavity. A dark band of SFL #1000, approximately $\frac{1}{4}$-in. wide and at a mean radius of $\frac{3}{4}$-in. was noticed.

Run 3B-A was similar to 3A-A. The duration was again 5 min, and stable strain readings were recorded. However, severe grabbing occurred when the drive motor stopped (the non-rotating shaft had to be held to prevent torque arm damage). The dark band explained above was wider, and general scuffing of the film (exposing bare metal) was observed. Less "dust" was present and a fine bright steel ring inside the dark band existed.

TEST 4A (W - 10.29 lb., S - 250 RPM, T - 1000°F, In Air)
(Two Runs)

Temperature of 1000°F was achieved before rotation of wear sample (load fully applied). The chatter phenomenon for run 4A-A occurred after 1 min, resulting in ever-increasing strain gage readings. At 4 $\frac{1}{2}$ min, severe vibration occurred causing erratic strain gage readings. This run was terminated at 7 $\frac{1}{2}$ min. Upon inspection of the upper wear surface, a hard pale-grey annular existed (deposited SFL #1000) that covered 60 to 80% of the total wear surface. This film was not easily removed. The lower wear sample had the identical wear band, and small flakes of SFL #1000 (not dust) were observed in the inner cavity. Some local scrubbing of the film (to bare metal) was also observed.

Run 4B-A lasted 2 $\frac{1}{2}$ min.; it was terminated due to excessive grabbing. All or most of the SFL #1000 had been evenly worn off (there were no major scuff marks or rings of steel observable). Again a small amount of flakes appeared in the inner cavity.

TEST 5A (Same as 4A) (Two Runs)

Run 5A-A lasted 4 min. and was smooth running (no squealing or chattering). There were 3 or 4 bad scuff marks, but bare metal was not exposed.

The first 2 min. of run 5B-A was as smooth running as the previous test. However, after this period, chatter commenced and progressively worsened (manual speed control had to be used to maintain constant speed). The strain readings did not vary significantly. General scuffing of the lower wear specimen (not as large as run 5A-A), and a $\frac{1}{8}$-in. band of SFL #1000 on the upper wear specimen was observed. The film deposited on the upper wear annulus was again not easily removed, while many flakes of lubricant were observed in the inner cavity.

TEST 6A (W - 30.35 lb., S - 350 RPM, T - 500°F, In Air) (Two Runs)

Run 6A-A had to be terminated in 2 min. because of excessive chatter. After 1 min. of operation, the chattering commenced and caused a large increase in the strain reading. The upper wear sample displayed a large band of SFL #1000 ($\frac{1}{4}$-in. wide) in the center of the annular. The lower wear sample contained a similar wear band

that was encircled (both inside and outside) by two thin shiny metal grooves.

Run 6B-A was more unsuccessful than 6A-A because after 3 $\frac{1}{2}$ min. of operation there was tremendous chatter, grabbing, and squealing associated with large deflections of the torque arm.

A large wear band was observed on the lower annular surface (80 to 90% of total), and general scuffing was predominant. Bare metal, scattered through-out the worn surface with the absence of metal grooves, was observed.

TEST 7A (Same as 6A) (Two Runs)

Run 7A-A lasted 6 $\frac{1}{2}$ min.; the first 5 min. was essentially free of chatter and large strain fluctuations. At 6 min., excessive squealing was noted. The lower wear specimen was unevenly worn with two bare metal rings surrounding a generally scuffed area exposing bare metal.

Run 7B-A had to be terminated in 1 $\frac{1}{2}$ min. of operation because of severe chatter causing dangerous torque arm deflection. The lower wear specimen looked as it did after run 7A-A (except for more scuffing and wider metal rings). Approximately 50% of the SFL #1000 was worn off with some of this lubricant being deposited as "dust" in the inner cavity.

TEST 2V (W - 20.55 lb., S - 350 RPM, T - Htr. off, Vac ~ 5 mm Hga) (Two runs)

Smooth operation was observed while conducting run 2A-V which lasted 16 $\frac{1}{2}$ min. No visible break-through of

the film was noted although a moderate amount of "dust" was observed in the inner cavity. Strain gage readings were free from fluctuations and did not vary significantly. There was, however, a definite increase in readings at $5\frac{1}{2}$ min.

Run 2B-V was also smooth in operation; it lasted 13 min. There were some scuffed areas visible, but none of these exposed bare steel. Again a small amount of "dust" was observed. Strain gage readings fluctuated because of minor chatter.

TEST 3V (Same as 2V except Vac - 9.6×10^{-5} mm Hga) (Two Runs)

Run 3A-V was considered a good test because of chatter-free operation. There were no break-throughs of the SFL #1000 although a moderate amount of flakes were observed within the inner specimen cavity, and some lubricant had been deposited on the upper wear sample. It appeared that the lubricant had scrubbed off some areas and had been redeposited on other areas either on the lower or upper wear surfaces. This run lasted $16\frac{1}{2}$ min. as did run 2A-V.

There was even wear in run 3B-V lasting 13 min. Some flakes of SFL #1000 were visible in the inner cavity (less than in run 3A-V), and minor scuff marks were observed throughout the lower wear surface. It appeared that the bare steel was "just underneath" the highly worn solid film lubricant.

TEST 6V (W = 30.35 lb., S = 350 RPM, T = 1000°F, Vac = 8$\times 5$mm Hga) (One Run)

After 7 min. of running test 6A-V, it was necessary to stop because of severe chatter and vibration. The SFL #1000 was evenly worn off, exposing large areas of bare steel. Flaked lubricant was visible in the inner cavity, and the upper wear sample was smeared with lubricant and partially scored. Progressively higher strain gage readings were recorded.

TEST 7V (Same as 6V) (One Run)

Run 7A-V was terminated at 13 min. because of excessive chatter. Progressively higher strain readings were again observed. The lower wear specimen was heavily scored exposing large areas of bare steel, and large quantities of flaked lubricant were noticed. Run 7A-V differed from 6A-V in that the film was not worn evenly.

VI

DISCUSSION OF RESULTS

The results of the various runs were placed in Appendix D. These results consisted of the average dynamic coefficient of friction (μ_d) for both the theoretical and calibration methods. Since it was difficult to determine precisely when the solid film lubricant failed, the following criterion was used. A plot of μ_d versus time was made for each "new specimen" run. The film failure point occurred when a pronounced increase in the coefficient of friction was noticed. The preceding values were then averaged to yield a mean μ_d.

The dimensional loss and the wear rate were also determined for each run. To check for reproducible results, each test was duplicated.

It was the opinion of the author, that only the "new specimen" runs should be used in determining the effective dynamic coefficient of friction. In many cases the lubricant had broken down sufficiently to invalidate the "Second use" runs as far as friction data were concerned. The later runs were made primarily to investigate wear and wear rate. The purpose of the wear and friction tests were two-fold.

A. Check for Comparable Results.

B. Investigate Wear and Friction Characteristics of SFL #1000.

Therefore, the discussion of results was divided into two parts; i.e., (1) The reproducibility of matched runs and (2) A general discussion of any trends observed in the wear-and-friction experiment.

A. Comparable Results of Matched Runs

Since SFL #1000 was applied to the bare metal lower samples by Electrofilm, Incorporated, there was no assurance that each wear specimen was equal in wear-and-friction characteristics to any other specimen. For this experiment, however, it was assumed that each was identical.

Although each wear sample was at about the same temperature when dimension loss was determined, there was no temperature control on the Mikrokator itself. However, the comparator was shielded against direct sun light and the ambient temperature of the laboratory seldom varied 5°F.

Considering these remarks, the following matched tests will be discussed:

TESTS 2A and 3A

Test 3A had a higher μ_d (0.415) than 2A (0.330). However, if the error "flags" were noted, the highest value of μ_d 2A and the lowest value of μ_d 3A were comparable.

Although test 2A had a lower average value of μ_d, the wear rate was about double that of 3A. Normally, a

high coefficient of friction is associated with high wear rate. According to Crump [7],

> Wear life and wear rate are dependent on lubricant film thickness and as resin binder to solid lubricant pigment ratio increases wear life increases.

Electrofilm's Technical Bulletin #2048 [8] indicated that coefficients of friction ranging from 0.119 to 0.380 were expected at room temperature for various coated metals.

TESTS 4A and 5A

If the failure criterion was used on test 4A, the first value of 0.180 was the only valid coefficient of friction. The gradient of μ_d was large even at the onset of the run and a correspondingly high wear rate was calculated (222 μin./min.). It was of interest to note that the lowest value of μ_d for 4A was nearly the same for the majority of values calculated in test 5A. Because of the low values of μ_d for 5A, the wear rate (7.68 μin./min.) was much less than 4A. Bowden and Tabor [1] stated that the coefficient of friction for steel sliding on steel could vary from 0.6 to 1.0 depending on the amount of oxide present. Since the $\mu_{d_{max}}$ for 4A was 0.754, it can be concluded that a major portion of the lower wear sample surface was bare steel. This was verified by the microphotograph of Spec. 10.

TESTS 6A and 7A

Using the failure criterion on test 6A, the average μ_d (0.288) was determined from the first two values only,

since severe chatter occurred after 1 min. operation. The high wear rate of 36 μin./min. was probably caused by the accelerated decomposition of the SFL #1000 after initial break-through.

Run 7A, on the other hand, showed a gradual increase in the coefficient of friction (0.16 to 0.26 in 5 min.) before failure occurred. The average μd was calculated to be 0.228 and the corresponding wear rate was considerably lower (6.74 μin./min.) than the wear rate of test 6A.

TESTS 2V and 3V

Although test 3A-V had low constant values of μd (0.355 average), the corresponding wear rate of 8.13 μin./min. was about 10 times that of 4A-V which had a higher average coefficient of friction (0.450). For this test μd was initially high but decreased slowly to the failure point when a large change in μd was noted. Thus, a "healing" of the broken film might have occurred. In general, these matched tests were most inconsistent.

TESTS 6V and 7V

The coefficient of friction (μd) for 6A-V gradually increased from 0.350 to 0.440 in $3\frac{1}{2}$ min. when failure occurred. Then the μd gradient increased with a resulting μd of 0.770 (steel-on-steel) in 7 min.

The corresponding wear rate was so great that the wear loss could not be determined from the Mikrokator. It was at least 300 μ in., and probably much more. In terms of wear rate the loss was greater than 43 μin./min.

Test 7A-V was very similar to 6A-V. The gradual increase of μ_d (0.350 to 0.430) elapsed 9 min. instead of $3\frac{1}{2}$ min., at which time a large friction factor gradient occurred reaching a final value of 0.675.

Since the maximum value of μ_d for 7A-V was less than 6A-V, it was reasonable that the wear rate was less (214 μ in./min.)

The average coefficient of friction for both tests (up to the respective failure points) was very comparable; 0.393 for 6A-V and 0.390 for 7A-V.

Although matched tests 4A and 5A and 6V and 7V were partially comparable, it was felt by the author that nothing conclusive was reached by these series of tests. It was then decided to check for repeatable results by testing another wear sample. Teflon (TFE) was chosen for three reasons:

1. The Teflon sample was thick enough (0.25-in.) so that no film break-through phenomenon would occur.
2. Much data was available concerning the coefficient of friction. Thus, repeatable results for comparable runs could be checked, and these values of μ_d could further be compared with values found in the literature [9, 11, 23].
3. The static coefficient of friction was lower than the dynamic coefficient, and thus the problem of "stick-slip," in which higher break-away friction

causes undesirable vibration, was eliminated. It was possible then to determine if the SFL #1000 originated the excessive chatter and vibration, witnessed in the machine's operation, or if the machine itself caused the vibration.

Test Procedures for Teflon (TFE)

Two identical Teflon samples were used, from which four comparison runs were made in air at 73°F. and at a speed of 350 RPM. Tests #1 and #2, using a 10.29 lb. load, were run for 10 min., while Tests #3 and #4 were loaded to 30.35 lb. and run for 5 min.

After the completion of Test #1, the 10.29 lb. load was removed and the 30.35 lb. weight was applied, at which time Test #3 commenced.

With the other Teflon wear sample, Tests #2 and #4 were likewise run.

Experimental Observations

1. No audible chatter observed in any of the 4 runs.
2. Speed control not used after the initial desired speed indicated.
3. Strain gage readings varied at the most ± 5 μin./in.

Comments on Results

1. Tests #1 and #2 were reproducible with an average value of μ_d equal to 0.20. As time elapsed the value of μ_d for both runs was observed to decrease slightly.
2. Tests #3 and #4 were reproducible, with an average calculated value of 0.175. In the first minute of operation, Test #4 had a slightly higher μ_d, but by $1\frac{1}{2}$ min, both values of μ_d for each remaining time interval were identical.
3. With a greater normal load, the coefficient of friction decreased (0.20 for Tests#1 and #2; 0.175 for Test #3 and #4). According to engineering data concerning the frictional properties of Teflon [9], the coefficient of friction of these fluorocarbon resins increases at lower loads, and they exhibit their greatest superiority at loads greater than 10 lb.
4. H. S. White [23] observed the frictional behavior of TFE--fluorocarbon resins in a journal bearing application. He had a $\frac{1}{4}$-in. stainless-steel shaft supported by and revolving in a bearing made of Teflon (TFE) (5-lb. normal load). Under such conditions, he reported the coefficient of friction to be in the range of 0.20 to 0.27. Bowden and Tabor [1] stated that under moderate loading (75-lb.), the value of the coefficient of friction was expected to fall within the range of 0.11 to 0.14.

Thus, for Teflon, the wear-and-friction machine did produce consistent results with these results comparing favorably with the values of friction found in the literature.

B. Observed Trends in the Wear and Friction of SFL #1000

1. Wear

a. Initial wear rate was high but slowed down as the surface was compressed and burnished. Initial dimension loss was probably due to film compression rather than material removal. Crump [67] stated that the wear rate of solid film lubricants decreases rapidly after about 30 min. of operation, at which time a moderate wear rate is established that remains essentially constant until film failure. He further said,

> Part of the initial weight loss is caused by the sloughing off of loose surface particles. During the first few seconds of operation, the film thickness decreases rapidly. The dimensional loss is not accompanied with a proportionate weight loss indicating that the film is being compressed rather than worn away.

b. At elevated temperatures (1000°F) film wear rate in vacuum markedly increased over the wear rate in air. Since SFL #1000 was composed of synthetic graphite and molybdenum disulfide bonded with a high temperature ceramic binder, it was possible that under high vacuum the synthetic graphite

may have lost its lubrication characteristics as does natural graphite. Savage [18, 19] has said, in his two papers, that graphite lubricates by virtue of adsorbed water. This water is lost in high vacuum (especially at elevated temperatures).

c. Film failure occurred earlier when the coefficient of friction was higher.

According to Crump [7], there is a dependency of wear rate and wear life upon the coefficient of friction. He states that wear life increases when there is a reduction in the coefficient of friction.

2. Friction

a. The coefficient of friction was essentially constant and independent of time for all runs where film failure did not occur.

b. The coefficients of friction both in air and in high vacuum at room temperature were comparable.

c. At elevated temperatures (1000°F), μ_d in high vacuum was significantly higher than in air.

VII

CONCLUSIONS AND RECOMMENDATIONS

A. Conclusions

1. High temperature SFL #1000 manufactured by Electrofilm, Incorporated, North Hollywood, California was, on the basis of this experiment, found to be a poor lubricant for use in air as well as in high vacuum for the following reasons:
   a. The extremely short wear life made SFL #1000 a poor candidate for any practical engineering application where moderate rubbing velocities are needed.
   b. The dynamic coefficient of friction was, in the author's opinion, unacceptably high with the undesirable "stick-slip" phenomenon occuring.

   These conclusions were reached after verifying the consistency of the machine's friction results using Teflon (TFE) wear samples.

   The Mikrokator was assumed to be in good working order; it was a new expensive comparator made by C. E. Johansson Gage Company, Dearborn, Michigan, one of the leading manufacturers of this kind of instrument.

B. Recommendations

1. This project be continued with some refinements in the equipment made. They are:

a. Install a water baffle in the vacuum system. This will minimize back streaming of the diffusion oil.

b. Install a liquid air cold trap. This will yield a better ultimate pressure and higher outer space altitudes can be simulated.

c. Further leak detection of the vacuum system with the mass spectrometer.

d. Fabricate a new upper wear sample of the pivoted "slipper" design.

e. Attach an oscillograph to the Type N portable strain indicator, thus directly yielding important friction-time characteristics.

With these modifications made, it is the author's firm belief that new and valuable information can be gained on the subject of wear and friction of solid lubricants in a space simulated environment.

BIBLIOGRAPHY

1. Bowden, F. P. and Tabor, D. The Friction and Lubrication of Solids. Oxford Press, 1958, pp 162-175.

2. Bowden, F. P., and Young, J. E. Friction of Diamond, Graphite and Carbon and the Influence of Surface Films. Proc. Roy. Soc., A, vol. 20, 1951, pp. 444-455.

3. Campbell, W. E. Solid Lubricants, paper presented before the ASLE. Boston, April 1953.

4. Cannon, P. Melting Point and Sublimation of Molybdenum Disulphide. General Electric Research Laboratory reprint 3280.

5. Clauss, F. J. Materials Evaluation under High Vacuum and Other Satellite Environmental Conditions. Lockheed Space and Missiles Division, Tech. Report 3-77-61-23, Jan. 1962.

6. Crump, R. E. Solid Film Lubricants. Product Engineering, February, 1956, pp. 200-205.

7. Crump, R. E. Solid Film Lubricants--Factors Influencing their Mechanism of Friction and Wear. Paper presented before the Joint Lubrication Conference of the ASME-ASLE, Oct. 9, 1956.

8. Electrofilm Incorporated, Tech. Bulletin on Solid Film Lubrication #2048, pp. 2-4.

9. Freeman, P. Lubrication and Friction. Pitman and Sons Ltd., 1962, pp 149-151.

10. Fuller, D. D. Theory and Practice of Lubrication for Engineers. John Wiley and Sons, Inc., 1956, pp 328-335.

11. Hanford, W. E. and Joyce, R. M. Journal of American Chemical Society, vol. 68, 1946, p 2082.

12. Johnson, R., Godfrey, D., and Bisson, E. Friction of Solid Films on Steel at High Sliding Velocities. National Advisory Committee for Aeronautics, Tech. Note #1578, Washington, April, 1948.

13. McAdams, W. H. Heat Transmission. McGraw-Hill Book Co., Inc., 1954, Chapter 4.

14. Materials Selector. Materials in Design Engineering, Mid-October, 1961, vol. 54.

15. Moore, M. B. Theory and Application of Mechanical Engineering Measurements. D. Van Nostrand Co., Inc., 1960, Chapters 6 and 8.

16. Perry, C. C. and Lissner, H. R. The Strain Gage Primer, McGraw-Hill Book Co., Inc., 1955.

17. Rabinowicz, E. and Imai, M. Friction and Wear at Elevated Temperatures. Report #WADC-TR-59-603, Surface Laboratory, M.I.T., Cambridge, Mass., March, 1963.

18. Savage, R. H. Graphite Lubrication. Journal of Applied Physics, vol. 19, #1, January, 1948.

19. Savage, R. H. Physically and Chemically Adsorbed Films in the Lubrication of Graphite Sliding Contacts. Annals of the New York Academy of Sciences, vol. 53, Art. 4, June 27, 1951.

20. Schenck, H. Theories of Engineering Experimentation, McGraw-Hill Book Co., Inc., 1961, pp. 40-53.

21. Shigley, J. E. Machine Design. McGraw-Hill Book Co., Inc., 1956, pp. 415-417.

22. Timoshenko and MacCullough. Elements of Strength of Materials. D. Van Nostrand Co., Inc., 1941.

23. White, H. S. Engineering Facts about Teflon. Published by the Plastic Sales Division, Polychemicals Dept., E. I. Du Pont de Nemours and Co., Inc., Wilmington, Delaware.

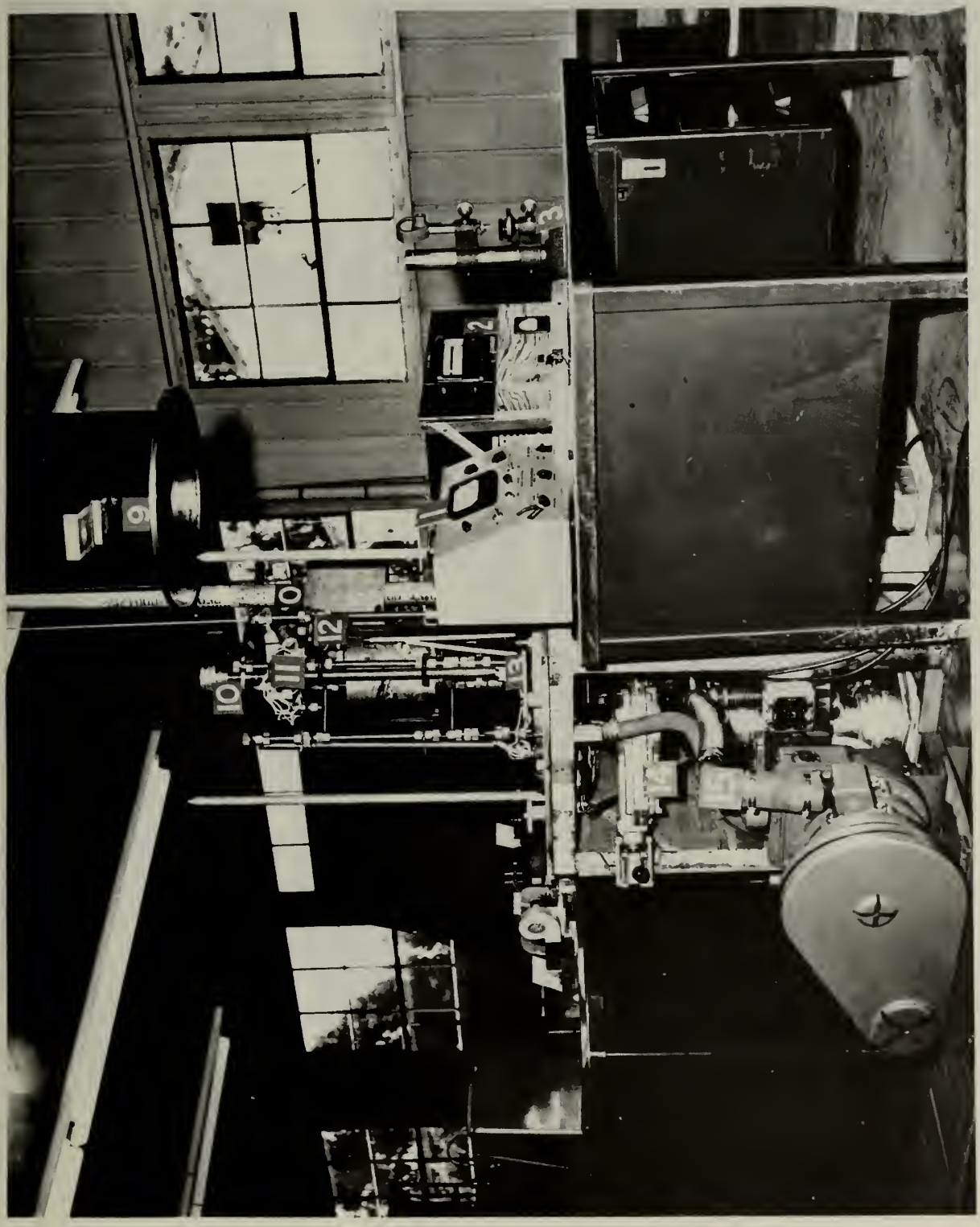

GENERAL VIEW OF WEAR/FRICTION MACHINE

FIGURE A I

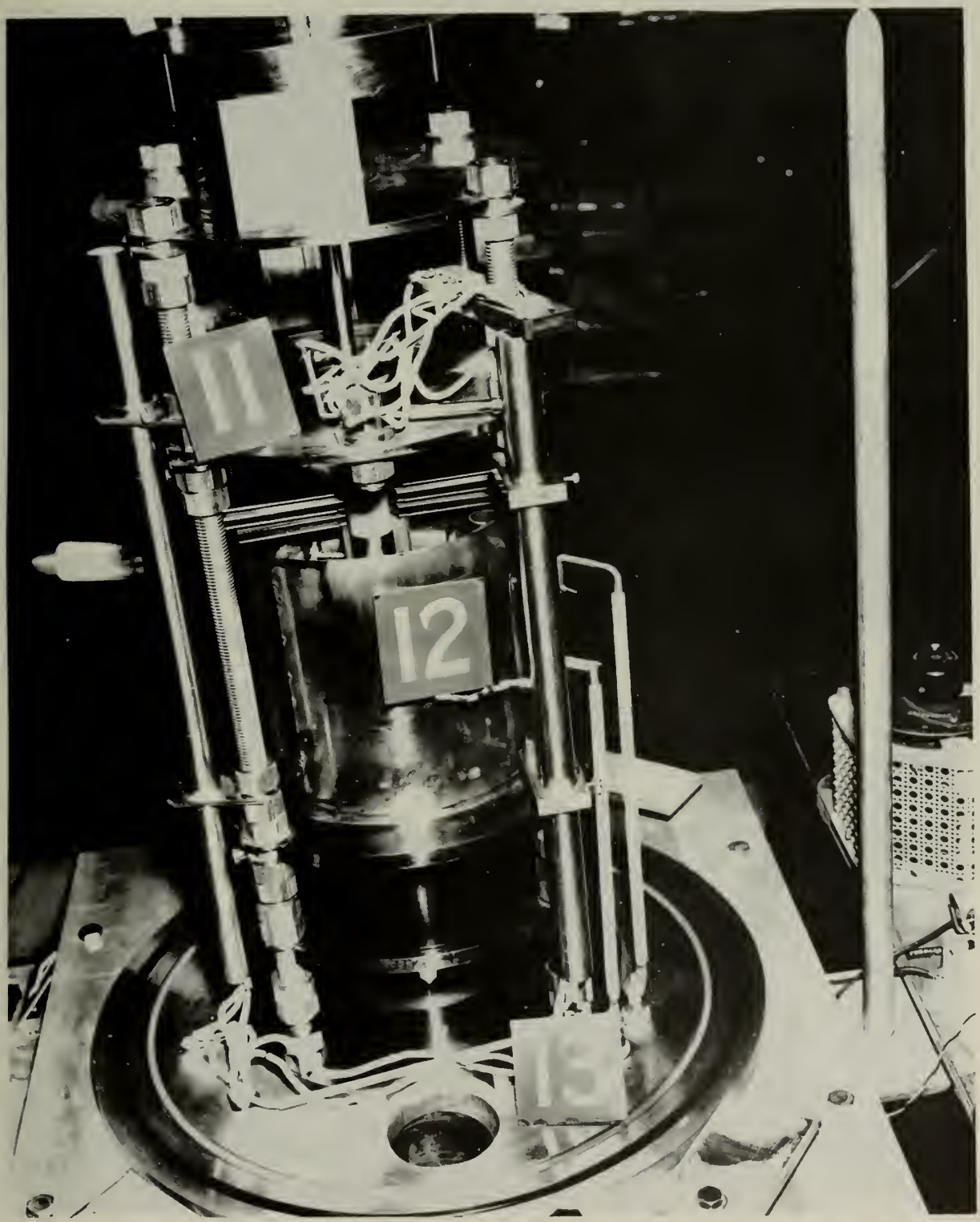

VACUUM BASEPLATE AND WEAR/FRICTION MACHINE

FIGURE A 2

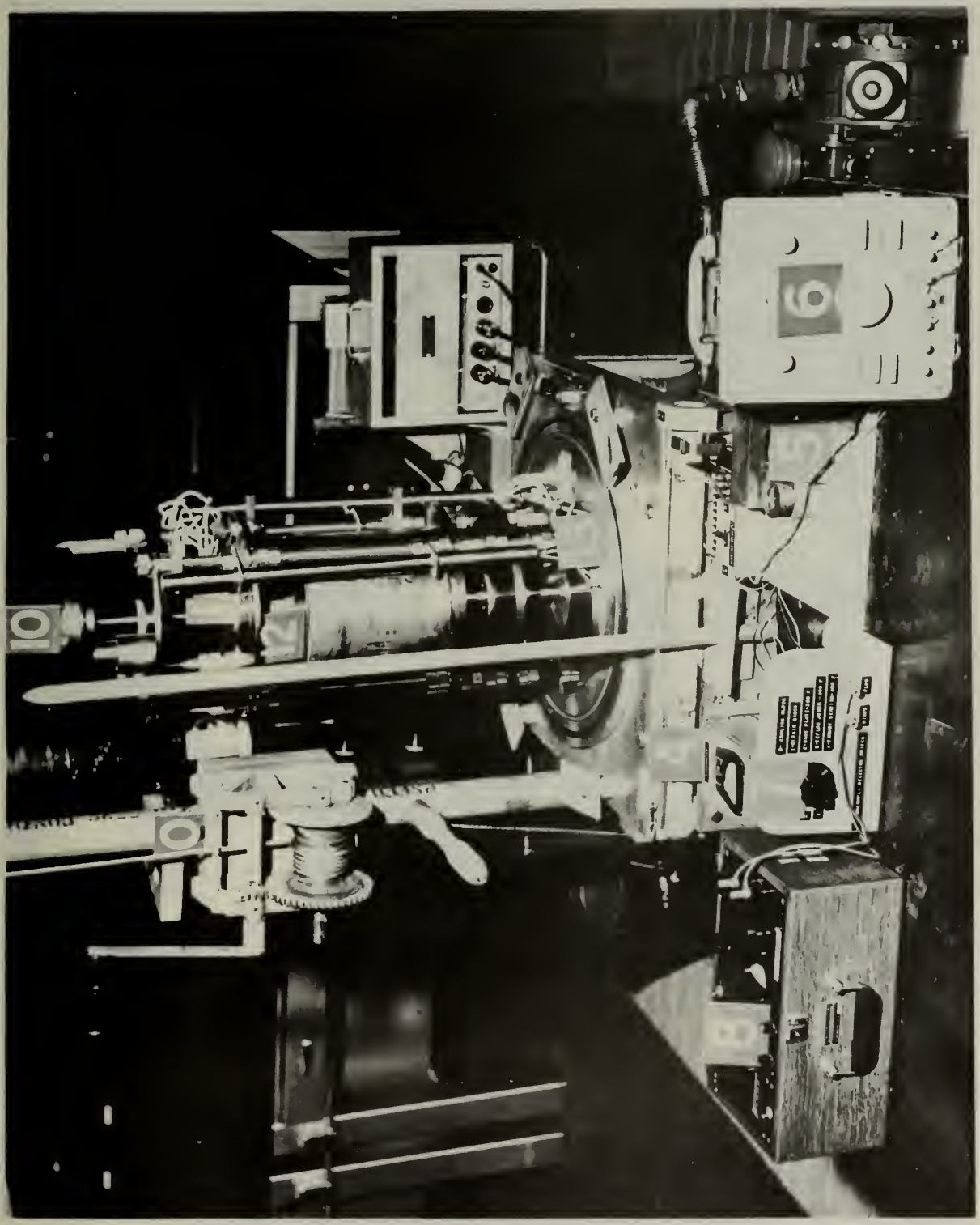

INSTRUMENT TABLE NO 1 AND WEAR/FRICTION MACHINE

FIGURE A 3

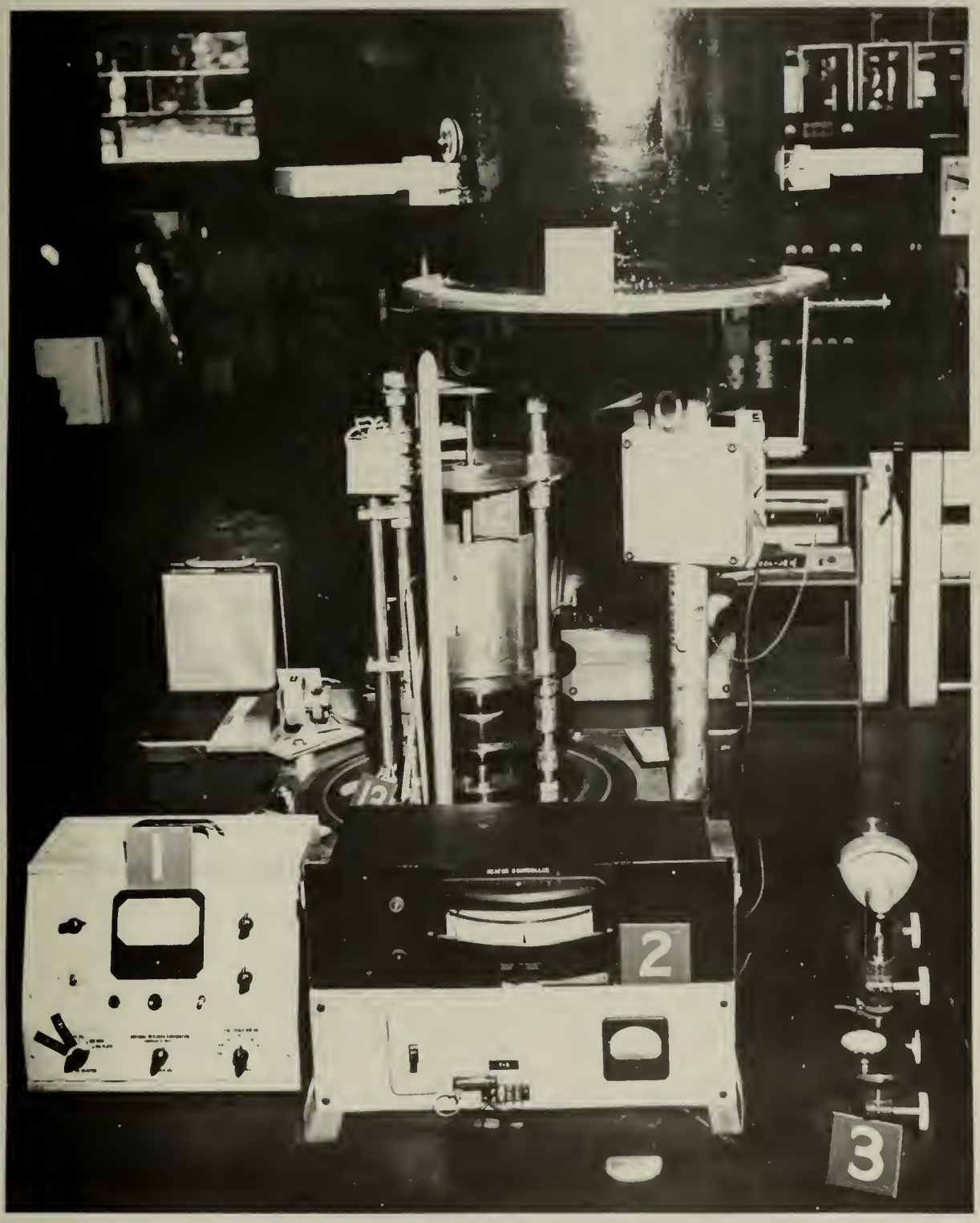

INSTRUMENT TABLE NO 2 AND WEAR/FRICTION MACHINE

FIGURE A 4

EQUIPMENT SYMBOLS

0. Hoist Assembly
1. Vacuum Gage
2. Heat Controller
3. Mikrokator
4. Speed Sensor
5. Cooling Block Assembly
6. Strain Gage Indicator
7. Thermocouple Selector Switch
8. Null Potentiometer
9. Bell Jar
10. Loading Weights
11. Torque Arm Assembly
12. Radiant Heater Assembly
13. Base Plate and Feed-through Connections
14. Diffusion Pump
15. Fore Pump
16. Hydraulic Variable Speed Device

Figure A-5

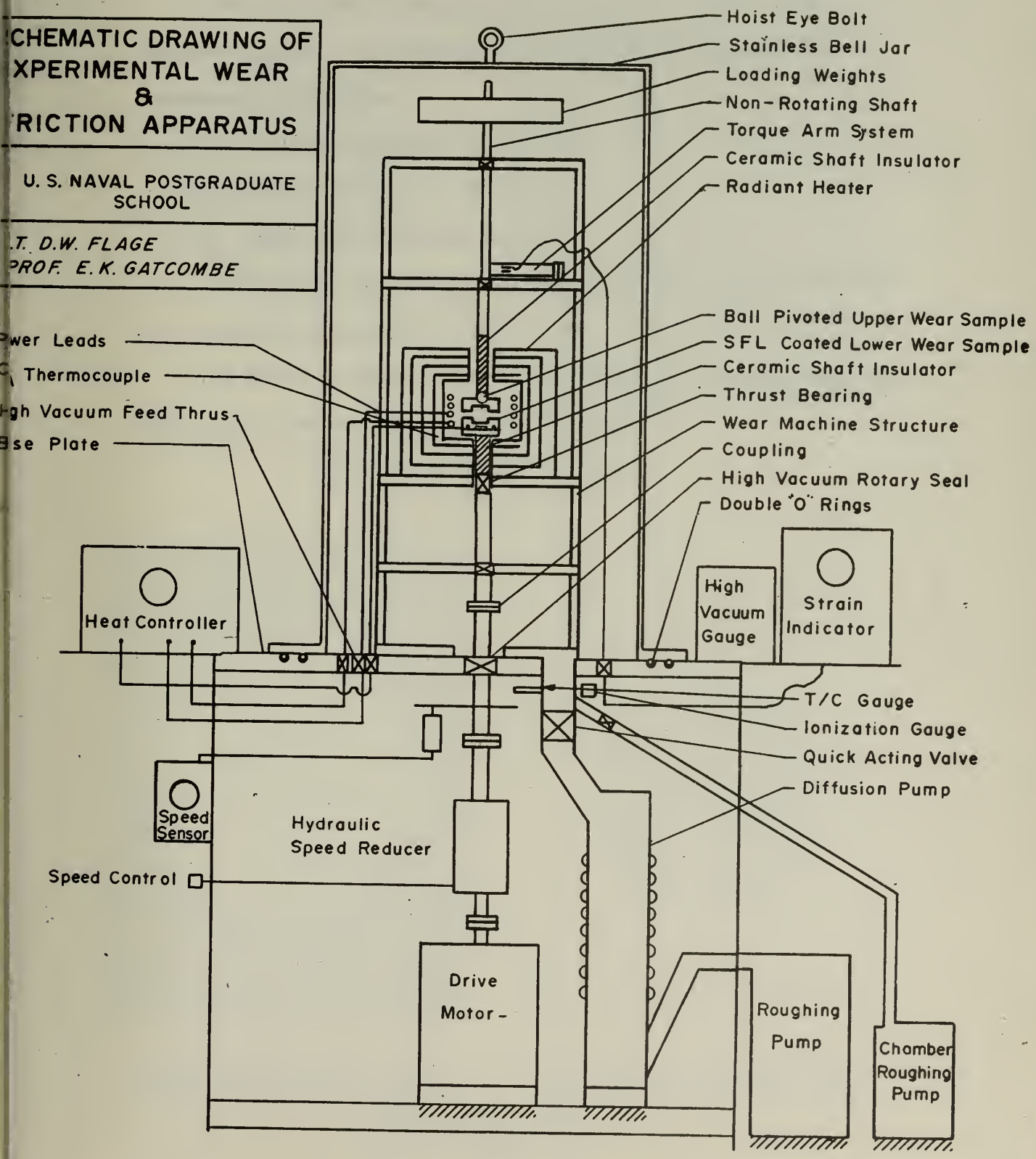
CHEMATIC DRAWING OF
XPERIMENTAL WEAR
&
RICTION APPARATUS
U. S. NAVAL POSTGRADUATE SCHOOL
.T. D.W. FLAGE
PROF. E.K. GATCOMBE
Hoist Eye Bolt
Stainless Bell Jar
Loading Weights
Non-Rotating Shaft
Torque Arm System
Ceramic Shaft Insulator
Radiant Heater
Ball Pivoted Upper Wear Sample
SFL Coated Lower Wear Sample
Ceramic Shaft Insulator
Thrust Bearing
Wear Machine Structure
Coupling
High Vacuum Rotary Seal
Double "O" Rings
wer Leads
Thermocouple
gh Vacuum Feed Thrus
se Plate
Heat Controller
High Vacuum Gauge
Strain Indicator
T/C Gauge
Ionization Gauge
Quick Acting Valve
Diffusion Pump
Speed Sensor
Hydraulic Speed Reducer
Speed Control
Drive Motor
Roughing Pump
Chamber Roughing Pump

Figure A-6

Specimen Photographs

Two (2) Poloroid photographs were taken for each wear specimen tested. In addition to these, the following photographs were also taken:

1. Untested specimen (SFL #1000)
2. Teflon (TFE) wear specimen
3. Upper wear specimen (steel)

A white ring was placed over a section of the wear specimen to be photomicrographed (x 150).

The white or light grey areas on these photographs represent bare steel, and the black matrix, SFL #1000.

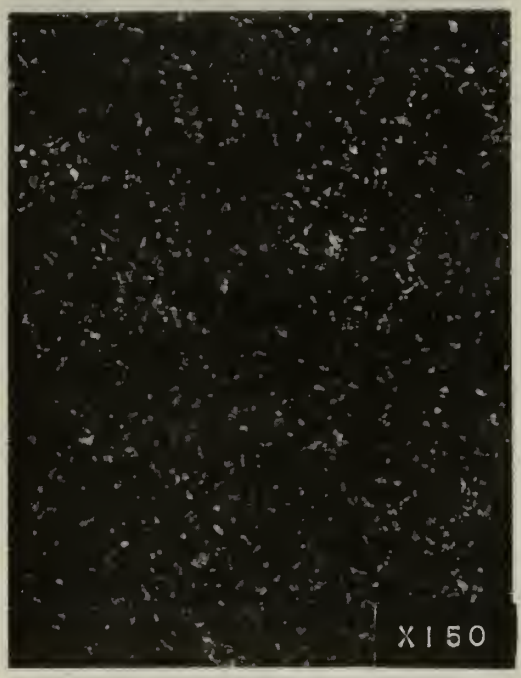

UNTESTED SPEC. 17

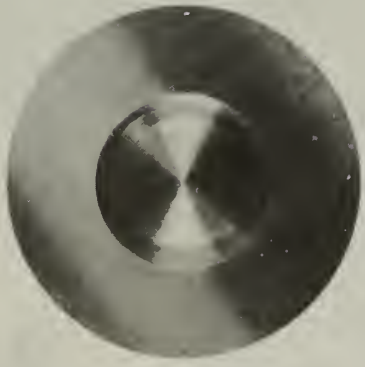

TEFLON WEAR SPEC.

UPPER WEAR SPEC.

FIG. B 1

TEST 2A SPEC. 4

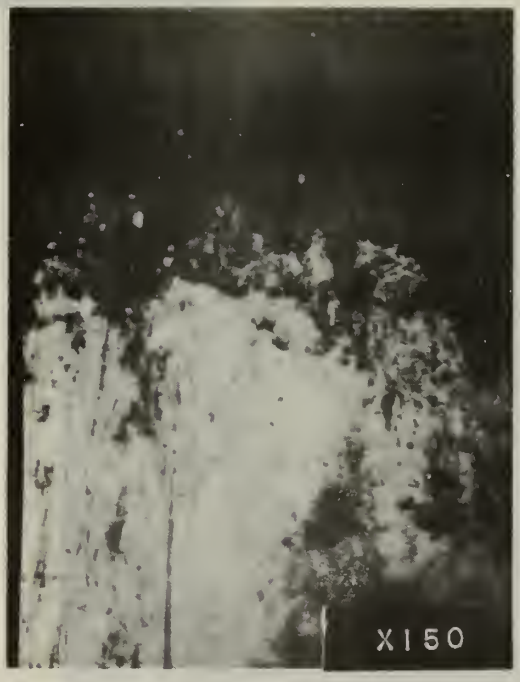

TEST 3A SPEC. 5

FIG. B 2

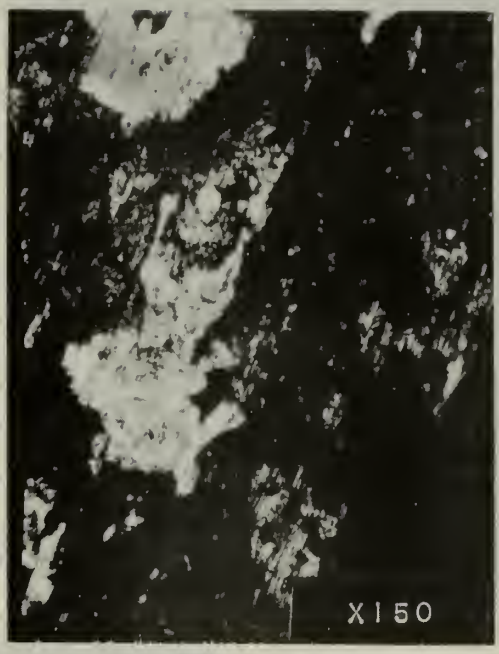

TEST 4A SPEC. 6

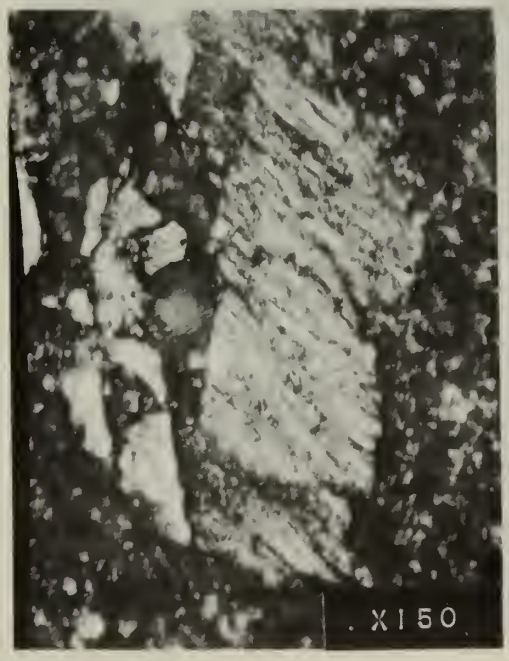

TEST 5A SPEC. 10

FIG. B 3

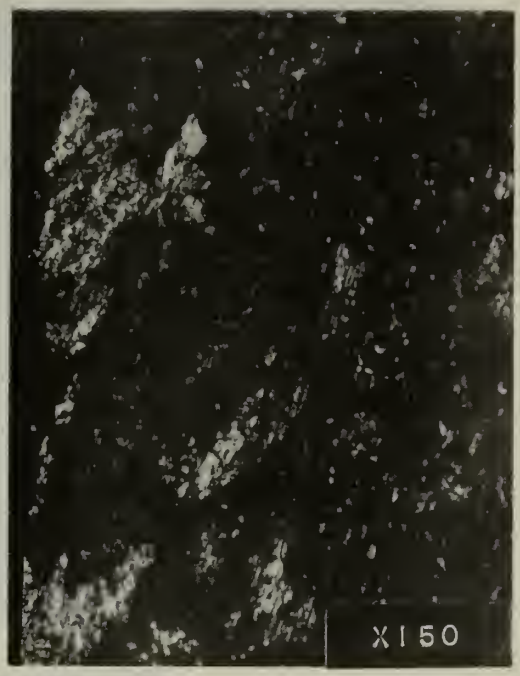

TEST 6A SPEC. 8

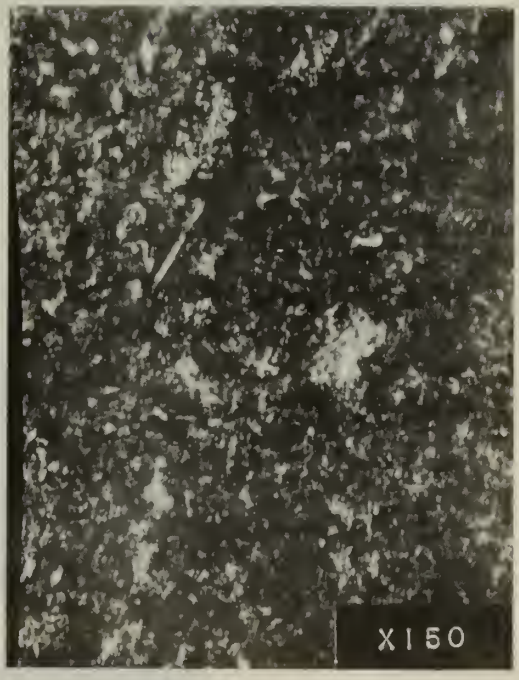

TEST 7A SPEC. 9

FIG. B 4

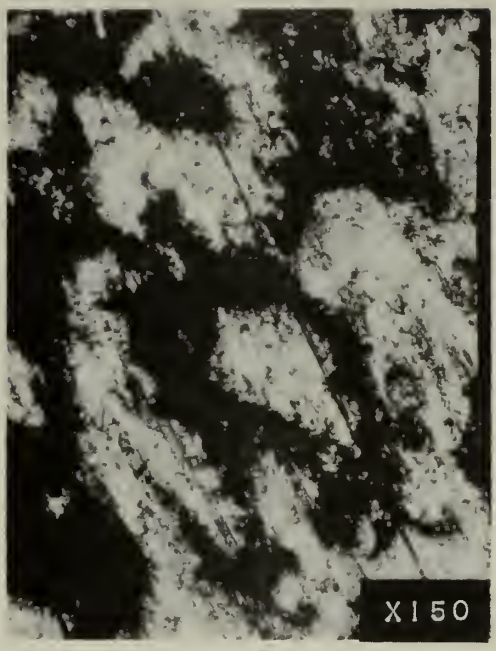

TEST 2V SPEC. 11

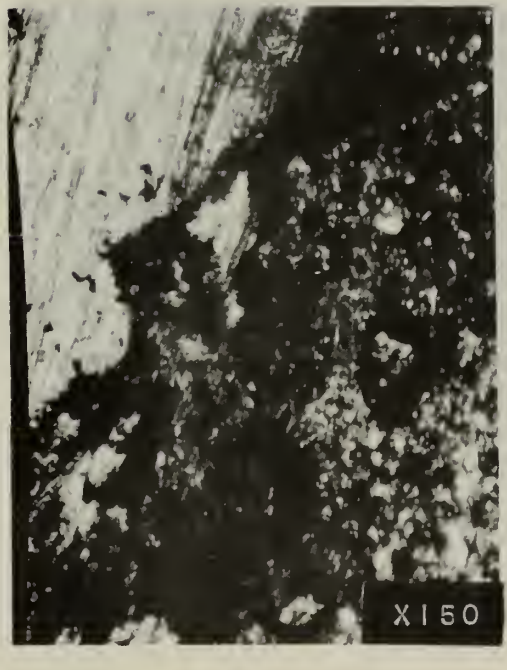

TEST 3V SPEC.. 13

FIG. B 5

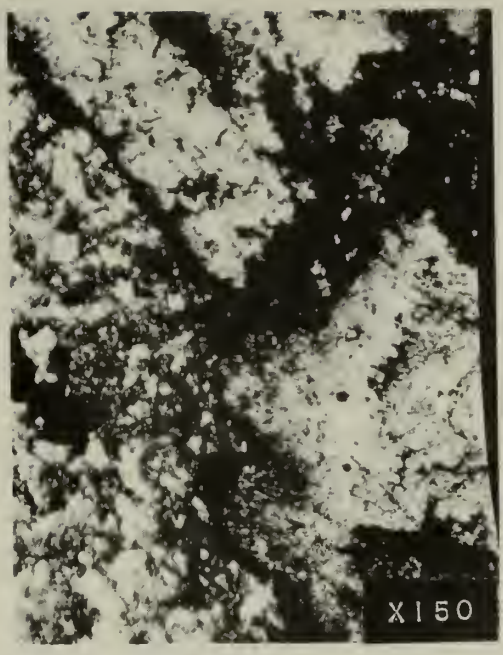

TEST 6V SPEC. 14

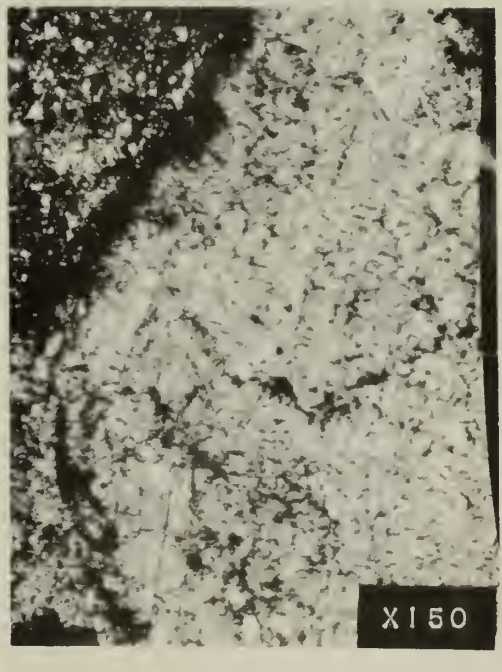

TEST 7V SPEC. 15

FIG. B 6

TABLE C-1

MIKROKATOR READINGS*

TEST	Before $(\Delta B)10^5$ in. 1	2	3	4	After $(\Delta A)10^5$ in. 1	2	3	4
2A-A	0.8	-8.5	-1.5	-1.2	-17.5	-17.0	-16.4	-17.4
	-2.8	-4.8	-0.5	-5.5	-12.6	-17.0	-14.6	-14.6
Spec.4	1.5	-2.0	-3.2	-3.2	-11.9	-14.0	-11.0	-14.2
	0.0	-4.0	-6.2	-7.3	-15.5	-15.5	-16.4	-15.0
2B-A	13.7	11.9	15.4	14.0	12.7	13.3	13.1	9.8
	18.0	17.9	16.2	11.0	15.8	17.8	12.7	12.7
Spec.4	16.6	19.0	17.8	19.3	16.2	15.4	15.0	15.5
	17.1	20.0	13.5	15.2	16.4	15.0	15.4	15.3
2C-A	12.7	13.3	13.1	9.8	6.7	5.8	4.5	5.0
	15.8	17.8	12.7	12.7	10.6	9.4	7.6	5.6
Spec.4	16.2	15.4	15.0	15.5	15.1	15.0	11.1	10.5
	16.4	15.0	15.4	15.3	8.7	8.2	7.9	9.6
3A-A	17.0	15.1	16.6	21.0	9.6	14.4	12.5	11.0
	20.8	20.0	20.0	16.6	11.2	8.4	14.6	10.3
Spec.5	16.4	18.2	13.2	17.4	1.8	2.1	1.5	7.6
	13.5	14.4	10.0	19.0	5.0	6.4	7.1	4.9
3B-A	9.6	14.4	12.5	11.0	12.3	6.5	7.2	8.3
	11.2	8.4	14.6	10.3	7.5	5.8	7.2	7.6
Spec.5	1.8	2.1	1.5	7.6	2.1	7.6	0.7	0.0
	5.0	6.4	7.1	4.9	4.2	5.0	6.2	4.2
4A-A	13.1	9.4	15.2	17.7	0.4	-3.6	5.0	-7.3
	14.2	15.4	9.7	8.0	-1.0	-7.2	-3.4	1.0
Spec.6	11.0	13.7	14.0	6.0	-4.8	-3.5	-6.4	4.2
	12.0	7.7	3.8	7.2	-5.5	-5.3	-9.8	-9.2
5A-A	3.4	0.0	2.0	-0.5	1.6	2.5	-4.1	-3.3
	20.0	17.4	18.6	17.7	12.8	12.0	13.0	12.0
Spec.10	12.1	12.7	11.2	11.0	18.5	9.0	10.5	11.3
	0.2	-1.5	0.3	-3.1	1.2	-10.5	-5.7	-5.0

* Row data - readings at same position

Column data - readings at different stations

MIKROKATOR READINGS

TEST	Before $(\Delta B)10^5$ in. 1	2	3	4	After $(\Delta A)10^5$ in. 1	2	3	4
5B-A	1.6	2.5	-4.1	-3.3	0.8	5.0	-2.7	3.8
	12.8	12.0	13.0	12.0	12.3	14.0	10.9	8.0
Spec.10	18.5	9.0	10.5	11.3	13.5	13.6	11.6	7.1
	1.2	-10.5	-5.7	-5.0	-8.1	-2.9	-8.4	-4.7
6A-A	13.5	11.6	4.1	7.8	-4.4	1.1	-2.3	0.0
	9.0	10.1	12.0	12.9	8.1	7.6	4.9	1.7
Spec.8	10.1	4.0	5.6	10.3	7.6	3.9	4.8	6.4
	10.4	4.4	5.4	8.9	4.1	1.0	0.9	3.0
6B-A	8.4	12.0	10.0	9.6	5.0	12.3	6.5	5.6
	20.2	14.8	17.6	21.0	11.7	7.1	10.0	10.8
Spec.8	16.8	15.0	15.7	19.5	14.0	10.0	4.5	4.5
	9.5	12.9	17.4	16.4	7.0	5.7	3.9	1.6
7A-A	11.0	7.4	16.7	16.4	7.6	9.2	8.5	9.5
	-8.4	-8.8	-10.1	-7.6	-14.1	-16.1	-15.3	-15.4
Spec.9	2.2	-2.2	-0.4	-3.3	-1.6	-3.8	-2.5	-2.1
	21.0	21.0	22.0	22.0	19.5	16.1	15.0	14.4
7B-A	7.6	9.2	8.5	9.5	5.6	10.5	1.2	2.6
	-14.1	-16.1	-15.3	-15.4	-21.0	-19.8	-21.0	-18.8
Spec.9	-1.6	-3.8	-2.5	-2.1	-2.0	-3.0	-5.0	-6.1
	19.5	16.1	15.0	14.4	7.4	11.7	9.1	11.1
2A-V	7.0	4.9	5.5	4.5	5.0	8.9	10.0	0.0
	5.0	2.7	4.0	7.4	5.5	4.0	1.5	10.3
Spec.11	16.6	14.0	14.2	11.8	12.1	9.0	13.3	9.5
	17.2	17.0	13.0	13.6	14.9	14.7	7.3	9.7
2B-V	5.0	8.9	10.0	0.0	-3.0	-2.3	-1.0	0.0
	5.5	4.0	1.5	10.3	-4.0	-2.7	-4.7	-4.8
Spec.11	12.1	9.0	13.3	9.5	3.5	3.7	3.5	3.4
	14.9	14.7	7.3	9.7	5.0	5.8	5.6	4.1
3A-V	10.4	5.0	6.9	14.1	-4.2	-5.2	-6.3	-5.2
	7.3	2.4	4.1	5.7	-7.6	-8.2	-7.8	-9.3
Spec.13	0.5	3.0	3.3	1.8	-6.4	-6.8	-7.0	-8.3
	12.3	15.8	15.0	15.1	-2.4	-2.9	-1.4	-3.6

MIKROKATOR READINGS

TEST	Before (ΔB)10^5 in. 1	2	3	4	After (ΔA)10^5 in. 1	2	3	4
3B-V	-4.2	-5.2	-6.3	-5.2	-10.0	-9.4	-10.5	-9.8
	-7.6	-8.2	-7.8	-9.3	-10.2	-6.9	-7.8	-5.5
Spec.13	-6.4	-6.8	-7.0	-8.3	-10.6	-10.5	-9.2	-10.2
	-2.4	-2.9	-1.4	-3.6	-6.6	-3.9	-2.9	-5.2
6A-V	17.4	17.4	17.1	17.4				
	14.5	10.6	11.4	12.8				
Spec.14	1.0	1.0	0.0	0.0	(off scale)			
	4.7	6.7	5.6	7.5				
7A-V	8.2	12.8	11.4	11.4	-15.5	-20.0	-21.0	-19.6
	0.5	2.3	5.1	4.2	-23.0	-22.0	-24.0	-24.0
Spec.15	6.5	9.5	5.0	6.4	-24.0	-23.0	-24.0	-25.0
	17.8	18.8	20.5	17.5	-3.5	-6.0	-5.0	-6.8

TABLE C-2

FRICTION DATA

TEST	Time (min)	ϵ_a (μin/in)	TEST	Time (min)	ϵ_a (μin/in)
(W - 20.55 lb, T - Htr. off, S - 350 RPM, in air)					
2A-A			3A-A		
ϵ_b = 11035	1.0	8675	ϵ_b = 11160	0.67	8100
	2.0	8615		1.0	8000
	3.0	8660		2.0	8200
	4.0	8600		2.5	8170
				3.0	8110
2B-A				3.5	8095
ϵ_b = 11170	1.0	8905		4.0	8075
	2.0	9040		5.0	8070
	3.0	9200			
	4.0	9250	3B-A		
	5.0	8550	ϵ_b = 11245	0.5	8030
	10.0	8730		1.0	8000
	15.0	7000		2.0	8150
				3.0	8020
2C-A				4.0	8030
ϵ_b = 11210	1.0	6850		5.0	8030
(W - 10.29 lb, T - 1000°F, S - 250 RPM, in air)					
4A-A			4B-A		
ϵ_b = 11074	0.5	10440	ϵ_b = 10810	0.5	8510
	1.0	10000		1.0	8570
	1.5	9600		1.5	8460
	2.0	9230		2.0	8420
	2.5	9360		2.5	8420
	3.0	9400			
	3.5	9210	5A-A		
	4.0	9140	ϵ_b = 14250	0.25	13560
	4.5	8820		0.5	13540
	5.0	8630		1.0	13560
	5.5	8575		1.5	13560
	6.0	8530		2.0	13520
	6.5	8420		2.5	13540
	7.0	8410		3.0	13520
	7.5	8360		3.5	13489
				4.0	13400
5B-A			5B-A		
ϵ_b = 14270	0.25	13930	(Cont.)	3.0	12990
	0.5	13930		3.5	12990
	1.0	13930		4.0	12950
	1.5	13842		4.5	12950
	2.0	13190		5.0	12930
	2.5	12990		5.5	12230
				6.0	12950

TEST	Time (min)	ϵ_a (μin/in)	TEST	Time (min)	ϵ_a (μin/in)
(W - 30.35 lb, T - 500°F, S - 350 RPM, in air)					
6A-A			7A-A		
ϵ_b = 10750	0.5	7410	ϵ_b = 10675	0.25	8950
	1.0	7900		0.5	8740
	1.5	6600		1.0	8600
	2.0	6190		1.5	8490
				2.0	8490
6B-A				2.5	8430
ϵ_b = 10750	0.5	7500		3.0	8300
	1.0	7555		3.5	8190
	1.5	7360		4.0	8120
	2.0	7260		4.5	8110
	2.5	7100		5.0	7830
	3.0	6770		5.5	7550
	3.5	6360		6.0	7310
				6.5	6960
			7B-A	0.25	10312
			ϵ_b = 14112	0.5	9632
				1.0	9262
(W - 20.55 lb, T - Htr. off, S - 350 RPM, in vacuum)					
2A-V			2B-V		
ϵ_b = 18335	0.25	15080	ϵ_b = 18000	0.5	14300
	0.5	15080		1.0	14960
Vac-9x10^{-5} mm Hg	1.0	14810	Vac-8x10^{-5} mm Hg	1.5	15500
	1.5	15210		2.0	15720
	2.0	15210		2.0	15820
	2.5	15010		3.0	15940
	3.0	15370		3.5	16020
	3.5	15250		4.0	15780
	4.0	15310		4.5	15700
	4.5	15350		5.0	15020
	5.0	--		5.5	14700
	5.5	15230		6.0	14180
	6.0	14450		6.5	14700
	6.5	14430		7.0	15100
	7.0	14450		7.5	14820
	7.5	15285		8.0	14780
	8.0	14530		9.0	15140
	8.5	14930		9.5	15300
	9.0	14930		10.0	15660
	9.5	14610		11.0	16060
	10.0	14610		12.0	16300
	10.5	14610		13.0	16480
	11.0	14200			
	11.5	14170			

TEST	Time (min)	ϵ_a (μin/in)
2A-V (Cont.)	12.0	14745
	13.0	14310
	14.0	14930
	15.0	15170
	15.5	14950
	16.0	14930
	16.5	14850
3B-V		
ϵ_b = 18305	0.25	15820
	0.50	15700
	1.0	15880
	1.5	15620
	2.0	15960
	2.5	15980
	3.0	16140
	3.5	16140
	4.0	15780
	4.5	15780
	5.0	16180
	5.5	15780
	6.0	16100
	6.5	15500
	7.0	16020
	7.5	15420
	8.0	15900
	8.5	16020
	9.0	15900
	9.5	16080
	10.0	16080
	10.5	16300
	11.0	15960
	11.5	15420
	12.0	16620
	12.5	16460
	13.0	15060

TEST	Time (min)	ϵ_a (μin/in)
3A-V	0.25	15700
ϵ_b = 18295	0.5	15700
	1.0	15860
	1.5	15740
	2.0	15800
	2.5	15860
	3.0	15880
	3.5	15820
	4.0	15740
	4.5	15820
	5.0	15860
	5.5	15780
	6.0	15780
	6.5	15740
	7.0	15780
	7.5	16180
	8.0	15700
	8.5	15700
	9.0	15940
	9.5	15860
	10.0	15700
	10.5	15900
	11.0	15820
	11.5	15780
	12.0	15580
	13.0	15820
	14.0	15420
	15.0	15780
	16.0	15740
	16.5	15740

(W - 30.35 lb, T - 1000°F, S - 350 RPM, in vacuum)

TEST	Time (min)	ϕ_a (μin/in)	TEST	Time (min)	ϕ_a (μin/in)
6A-V			7A-V		
ϕ_b = 18450	0.25	14770	ϕ_b = 18100	0.25	15260
	0.5	15050		0.5	14580
Vac-1.5 $\times 10^{-4}$ mm Hg	1.0	14530	Vac-6.3 $\times 10^{-5}$ mmHg	1.0	14260
	1.5	14290		1.5	13820
	2.0	14450		2.0	13410
	2.5	14180		2.5	13740
	3.0	13845		3.0	14260
	3.5	13930		3.5	13740
	4.0	13090		4.0	13940
	4.5	12400		4.5	13660
	5.0	11770		5.0	14220
	5.5	11050		5.5	14260
	6.0	10890		6.0	14380
	6.5	10650		6.5	14020
	7.0	10250		7.0	14140
				7.5	13820
				8.0	13660
				8.5	13580
				9.0	13410
				9.5	12500
				10.0	12100
				10.5	10900
				11.0	12500
				11.5	12500
				12.0	11810
				12.5	11020
				13.0	10900

TABLE C-3

TABULATED WEAR CALCULATIONS

TEST	Time (min.)	$\overline{\Delta B}_1$	$\overline{\Delta B}_2$	$\overline{\Delta B}_3$	$\overline{\Delta B}_4$	$\overline{\Delta B}$	$\overline{\Delta A}_1$	$\overline{\Delta A}_2$	$\overline{\Delta A}_3$	$\overline{\Delta A}_4$	$\overline{\Delta A}$	$\overline{\Delta(\mu\text{-in.})}$	Wear Rate (μ in./min.)
2A-A	4.0	-2.60	-2.57	-1.75	-4.38	-2.83	-17.08	-17.02	-12.71	-15.60	-15.50	127.0	31.8
2B-A	13.0	13.75	14.75	18.18	16.45	15.79	12.21	14.73	15.51	15.51	14.48	13.1	1.01
2C-A	1.0	12.21	14.73	15.51	15.51	14.48	5.50	8.20	12.90	8.60	8.80	56.8	56.8
3A-A	5.0	17.42	19.32	16.29	14.21	16.80	11.86	11.12	3.24	5.84	8.02	87.8	17.6
3B-A	5.0	11.86	11.12	3.24	5.84	8.02	8.57	7.03	2.60	4.90	5.77	22.5	4.50
4A-A	7.5	13.85	11.83	11.17	7.67	11.13	-1.37	-1.43	-0.89	-7.45	-5.57	167.0	22.2
4B-A	2.5	-1.37	-1.43	-0.89	-7.45	-5.57	(	no readings			)	--	--
5A-A	4.0	0.65	18.40	11.74	-0.98	7.70	-0.83	12.45	12.32	-5.30	4.63	30.7	7.68
5B-A	6.0	-0.83	12.45	12.32	-5.30	4.63	1.73	11.30	11.45	-6.03	4.60	0.30	0.05
6A-A	2.0	9.25	11.00	7.50	7.27	8.75	-1.39	5.58	5.67	2.25	1.55	72.0	36.0
6B-A	3.5	10.00	18.37	16.79	14.05	14.80	7.35	9.90	8.25	4.55	7.51	72.9	20.8
7A-A	6.5	12.86	-8.73	-0.93	21.50	6.18	8.70	-15.23	-2.50	16.25	1.80	43.8	6.74
7B-A	1.0	8.70	-15.23	-2.50	16.25	1.80	4.98	-20.15	-4.03	9.83	-2.35	41.5	41.5
2A-V	16.5	5.47	4.78	14.15	15.20	9.90	5.97	5.20	10.89	11.61	8.41	14.9	0.90
2B-V	13.0	5.97	5.20	10.89	11.61	8.41	-1.58	-4.05	3.52	5.12	0.75	76.6	5.89
3A-V	16.5	9.10	4.88	2.15	14.55	7.67	-5.22	-8.22	-7.12	-2.58	-5.78	135.0	8.13
3B-V	13.0	-5.22	-8.22	-7.12	-2.58	-5.78	-9.92	-7.60	-10.10	-4.65	-8.06	22.8	1.75
6A-V	7.0	17.33	12.32	0.50	6.12	9.07	(	off scale			)	>300.0	>43.0
7A-V	13.0	10.93	3.03	6.85	18.65	9.85	-19.00	-23.25	-24.00	-5.32	-17.90	278.0	21.4

TABLE D-1

TABULATED WEAR RESULTS**

TEST	W(lb)	T(°F)	S(RPM)	Run time (min)	Wear Loss (Δ)μ-in.)	Wear Rate (μin/min.)
2A	20.55	Htr.off	350	18.0	207.0	11.5
3A	20.55	Htr.off	350	10.0	110.0	11.0
4A	10.29	1000	250	7.5	167.0	22.2
5A	10.29	1000	250	10.0	31.0	3.10
6A	30.35	500	350	5.5	145.0	26.4
7A	30.35	500	350	7.5	85.0	11.3
2V	20.55	Htr.off	350	29.5	92.0	3.12
3V	20.55	Htr.off	350	29.5	158.0	5.35
6V	30.35	1000	350	7.0	>300*	>43
7V	30.35	1000	350	13.0	278.0	21.4

** - Includes all runs of each test

* - Off scale, an estimation

INITIAL FILM THICKNESS , 300-500 μin.

TABLE D-2

"NEW SPECIMEN" WEAR-AND-FRICTION RESULTS

TEST	FRICTION μ_d(calib) ± $W_{\mu d}$	FRICTION μ_{dmax}	WEAR Dimensional Loss (Δ) (μin)	WEAR Wear Rate ($\frac{\mu in}{min.}$)
2A-A	0.330 ± 0.0555	0.335	127.0	31.8
3A-A	0.415 ± 0.0460	0.439	87.8	17.6
4A-A	0.180 ± 0.0130	0.754	167.0	22.2
5A-A	0.180 ± 0.0130	0.222	30.7	7.68
6A-A	0.288 ± 0.0394	0.417	72.0	36.0
7A-A	0.228 ± 0.0317	0.343	43.8	6.74
2A-V	0.450 ± 0.0613	0.581	14.9	0.903
3A-V	0.355 ± 0.0492	0.406	135.0	8.13
6A-V	0.393 ± 0.0531	0.770	>300.0*	>43.0
7A-V	0.390 ± 0.0527	0.675	278.0	21.4

Initial Film Thickness , 300-500 μ in.

*off scale, an estimation

TABLE D-3

TABULATED FRICTION CALCULATIONS AND RESULTS

TEST	Run time (min.)	M_p (in.-lb.)	$\Delta\phi$ (μin./in.)	Coefficient of Friction ($\mu_d \pm w_d$) Theoretical	Calibrated
2A-A	1.0	5.04	2360	0.328 ± 0.0231	0.327 ± 0.0454
	2.0	5.15	2420	0.336 ± 0.0237	0.334 ± 0.0463
	3.0	5.05	2375	0.330 ± 0.0232	0.327 ± 0.0454
	4.0	5.17	2435	0.338 ± 0.0238	0.335 ± 0.0463
2B-A	1.0	5.25	2265	0.315 ± 0.0218	0.341 ± 0.0476
	2.0	4.55	2130	0.296 ± 0.0209	0.296 ± 0.0398
	3.0	4.25	1970	0.274 ± 0.0193	0.276 ± 0.0374
	4.0	4.15	1920	0.267 ± 0.0186	0.269 ± 0.0368
	5.0	5.55	2620	0.364 ± 0.0250	0.361 ± 0.0547
	10.0	5.20	2440	0.339 ± 0.0233	0.338 ± 0.0468
	13.0	8.72	4170	0.580 ± 0.0400	0.567 ± 0.0798
2C-A	1.0	9.12	4360	0.605 ± 0.0426	0.592 ± 0.0810
3A-A	0.67	6.45	3060	0.425 ± 0.0299	0.418 ± 0.0557
	1.0	6.68	3160	0.438 ± 0.0309	0.439 ± 0.0586
	2.0	6.25	2960	0.412 ± 0.0289	0.406 ± 0.0542
	2.5	6.32	2990	0.415 ± 0.0293	0.410 ± 0.0547
	3.0	6.44	3050	0.423 ± 0.0298	0.417 ± 0.0556
	3.5	6.47	3065	0.426 ± 0.0300	0.419 ± 0.0559
	4.0	6.70	3085	0.428 ± 0.0301	0.434 ± 0.0579
	5.0	6.74	3090	0.429 ± 0.0302	0.436 ± 0.0582
3B-A	0.5	6.77	3215	0.446 ± 0.0314	0.439 ± 0.0585
	1.0	6.85	3245	0.450 ± 0.0318	0.444 ± 0.0592
	2.0	6.52	3095	0.429 ± 0.0302	0.423 ± 0.0565
	3.0	6.78	3225	0.448 ± 0.0316	0.440 ± 0.0587
	4.0	6.77	3215	0.446 ± 0.0314	0.439 ± 0.0584
	5.0	6.77	3215	0.446 ± 0.0314	0.439 ± 0.0584
4A-A	0.5	1.49	634	0.176 ± 0.0123	0.196 ± 0.0360
	1.0	2.40	1074	0.298 ± 0.0208	0.312 ± 0.0486
	1.5	3.22	1474	0.410 ± 0.0284	0.417 ± 0.0611
	2.0	4.00	1844	0.510 ± 0.0356	0.518 ± 0.0734
	2.5	3.70	1714	0.477 ± 0.0331	0.479 ± 0.0685
	3.0	3.63	1674	0.466 ± 0.0324	0.420 ± 0.0675
	3.5	4.04	1864	0.519 ± 0.0359	0.524 ± 0.0743
	4.0	4.16	1934	0.538 ± 0.0373	0.538 ± 0.0760
	4.5	4.82	2254	0.626 ± 0.0434	0.625 ± 0.0870
	5.0	5.21	2444	0.679 ± 0.0472	0.676 ± 0.0936
	5.5	5.32	2499	0.695 ± 0.0482	0.690 ± 0.0955
	6.0	5.40	2544	0.707 ± 0.0492	0.700 ± 0.0968
	6.5	5.62	2654	0.737 ± 0.0510	0.728 ± 0.100
	7.0	5.66	2664	0.741 ± 0.0514	0.734 ± 0.102
	7.5	5.75	2714	0.754 ± 0.0523	0.745 ± 0.103

TEST	Run time (min)	M_p (in.-lb.)	$\Delta \phi$ (μin/in)	Coefficient of Friction (μ_d) $\pm w_d$ Theoretical	Calibrated
4B-A	0.5	4.90	2300	0.639 ± 0.044	0.635 ± 0.0884
	1.0	4.80	2240	0.623 ± 0.0430	0.622 ± 0.0867
	1.5	5.02	2350	0.653 ± 0.0452	0.651 ± 0.0905
	2.0	5.10	2390	0.664 ± 0.0460	0.661 ± 0.0916
	2.5	5.10	2390	0.664 ± 0.0460	0.661 ± 0.0916
5A-A	0.25	1.55	640	0.177 ± 0.0125	0.200 ± 0.0365
	0.50	1.55	640	0.177 ± 0.0125	0.200 ± 0.0365
	1.0	1.55	640	0.177 ± 0.0125	0.200 ± 0.0365
	1.5	1.55	640	0.177 ± 0.0125	0.200 ± 0.0365
	2.0	1.61	680	0.189 ± 0.0133	0.209 ± 0.0374
	2.5	1.58	660	0.183 ± 0.0129	0.205 ± 0.0370
	3.0	1.61	680	0.189 ± 0.0133	0.209 ± 0.0374
	3.5	1.67	711	0.197 ± 0.0139	0.216 ± 0.0368
	4.0	1.85	800	0.222 ± 0.0155	0.240 ± 0.0405
5B-A	0.25	0.93	340	0.0945 ± 0.00682	0.120 ± 0.0296
	0.50	0.93	340	0.0945 ± 0.00682	0.120 ± 0.0296
	1.0	0.93	340	0.0945 ± 0.00682	0.120 ± 0.0296
	1.5	1.10	428	0.119 ± 0.00840	0.143 ± 0.0313
	2.0	2.43	1080	0.300 ± 0.0210	0.315 ± 0.0487
	2.5	2.83	1280	0.356 ± 0.0248	0.367 ± 0.0550
	3.0	2.83	1280	0.356 ± 0.0248	0.367 ± 0.0550
	3.5	2.83	1280	0.356 ± 0.0248	0.367 ± 0.0550
	4.0	2.90	1320	0.367 ± 0.0255	0.376 ± 0.0562
	4.5	2.90	1320	0.367 ± 0.0255	0.376 ± 0.0562
	5.0	2.95	1340	0.373 ± 0.0258	0.382 ± 0.0569
	5.5	4.40	2040	0.567 ± 0.0393	0.570 ± 0.0800
	6.0	2.90	1320	0.367 ± 0.0255	0.376 ± 0.0562
6A-A	0.5	7.05	3340	0.314 ± 0.0218	0.310 ± 0.0422
	1.0	6.02	2850	0.267 ± 0.0186	0.264 ± 0.0362
	1.5	8.70	4150	0.390 ± 0.0271	0.382 ± 0.0517
	2.0	9.50	4560	0.428 ± 0.0297	0.417 ± 0.0563
6B-A	0.5	6.85	3250	0.305 ± 0.0212	0.300 ± 0.0408
	1.0	6.75	3195	0.300 ± 0.0208	0.297 ± 0.0405
	1.5	7.14	3390	0.319 ± 0.0222	0.314 ± 0.0427
	2.0	7.30	3490	0.328 ± 0.0228	0.321 ± 0.0438
	2.5	7.65	3650	0.343 ± 0.0238	0.336 ± 0.0456
	3.0	8.35	3980	0.374 ± 0.0260	0.367 ± 0.0498
	3.5	9.17	4390	0.417 ± 0.0286	0.403 ± 0.0548

TEST	Run time (min)	M_p (in-lb)	$\Delta\phi$ (μin/in)	Coefficient of Friction ($\mu_d \pm \omega_d$) Theoretical	Calibrated
7A-A	0.25	3.65	1700	0.160 ± 0.0111	0.160 ± 0.0229
	0.50	4.15	1935	0.182 ± 0.0126	0.182 ± 0.0257
	1.0	4.45	2075	0.195 ± 0.0135	0.195 ± 0.0273
	1.5	4.70	2185	0.205 ± 0.0143	0.206 ± 0.0287
	2.0	4.70	2185	0.205 ± 0.0143	0.206 ± 0.0287
	2.5	4.80	2245	0.211 ± 0.0146	0.211 ± 0.0294
	3.0	5.05	2375	0.223 ± 0.0155	0.222 ± 0.0308
	3.5	5.30	2485	0.236 ± 0.0162	0.233 ± 0.0321
	4.0	5.42	2555	0.240 ± 0.0166	0.238 ± 0.0329
	4.5	5.48	2565	0.241 ± 0.0167	0.241 ± 0.0332
	5.0	6.05	2845	0.267 ± 0.0186	0.266 ± 0.0335
	5.5	6.60	3125	0.294 ± 0.0204	0.290 ± 0.0395
	6.0	7.10	3365	0.316 ± 0.0220	0.312 ± 0.0424
	6.5	7.80	3715	0.349 ± 0.0242	0.343 ± 0.0464
7B-A	0.25	7.95	3805	0.358 ± 0.0248	0.349 ± 0.0474
	0.5	9.35	4480	0.422 ± 0.0293	0.411 ± 0.0555
	1.0	10.12	4850	0.457 ± 0.0316	0.445 ± 0.0600
2A-V	0.25	7.05	3250	0.462 ± 0.0317	0.457 ± 0.0623
	0.50	7.05	3250	0.462 ± 0.0317	0.457 ± 0.0623
	1.0	7.60	3520	0.501 ± 0.0344	0.493 ± 0.0669
	1.5	6.75	3120	0.444 ± 0.0306	0.438 ± 0.0598
	2.0	6.75	3120	0.444 ± 0.0306	0.438 ± 0.0598
	2.5	7.20	3320	0.472 ± 0.0325	0.467 ± 0.0636
	3.0	6.43	2960	0.421 ± 0.0289	0.417 ± 0.0572
	3.5	6.67	3080	0.438 ± 0.0300	0.433 ± 0.0590
	4.0	6.55	3020	0.429 ± 0.0297	0.425 ± 0.0582
	4.5	6.47	2980	0.424 ± 0.0292	0.420 ± 0.0573
	5.0	--	--	--	--
	5.5	6.72	3100	0.441 ± 0.0303	0.436 ± 0.0594
	6.0	8.37	3880	0.552 ± 0.0380	0.543 ± 0.0736
	6.5	8.40	3900	0.555 ± 0.0381	0.545 ± 0.0738
	7.0	8.37	3800	0.552 ± 0.0380	0.543 ± 0.0594
	7.5	6.60	3045	0.433 ± 0.0298	0.428 ± 0.0584
	8.0	8.20	3800	0.540 ± 0.0370	0.532 ± 0.0713
	8.5	7.38	3400	0.483 ± 0.0318	0.479 ± 0.0651
	9.0	7.38	3400	0.483 ± 0.0318	0.479 ± 0.0651
	9.5	8.05	3720	0.529 ± 0.0363	0.522 ± 0.0707
	10.0	8.05	3720	0.529 ± 0.0363	0.522 ± 0.0707
	10.5	8.05	3720	0.529 ± 0.0363	0.522 ± 0.0707
	11.0	8.88	4130	0.587 ± 0.0404	0.576 ± 0.0776
	11.5	8.95	4160	0.592 ± 0.0407	0.581 ± 0.0779
	12.0	7.75	3585	0.510 ± 0.0350	0.503 ± 0.0683
	13.0	8.65	4020	0.572 ± 0.0394	0.561 ± 0.0759
	14.0	7.35	3400	0.483 ± 0.0318	0.477 ± 0.0650
	15.0	6.85	3160	0.449 ± 0.0304	0.444 ± 0.0605
	15.5	7.33	3380	0.481 ± 0.0330	0.476 ± 0.0648
	16.0	7.35	3400	0.483 ± 0.0318	0.477 ± 0.0649
	16.5	7.55	3480	0.495 ± 0.0340	0.490 ± 0.0665

TEST	Run time (min)	M_p (in.-lb)	$\Delta\phi$ (μin/in.)	Coefficient of Friction (μ_d)$\pm w_d$ Theoretical	Calibrated
2B-V	0.50	8.62	4000	0.569 ± 0.0391	0.559 ± 0.0757
	1.0	7.22	3340	0.475 ± 0.0327	0.468 ± 0.0637
	1.5	6.10	2800	0.398 ± 0.0274	0.396 ± 0.0542
	2.0	5.62	2580	0.367 ± 0.0253	0.365 ± 0.0502
	2.5	5.42	2480	0.353 ± 0.0233	0.352 ± 0.0483
	3.0	5.15	2360	0.336 ± 0.0230	0.334 ± 0.0462
	3.5	5.00	2280	0.324 ± 0.0223	0.324 ± 0.0440
	4.0	5.50	2520	0.358 ± 0.0246	0.357 ± 0.0493
	4.5	5.68	2600	0.370 ± 0.0254	0.369 ± 0.0508
	5.0	7.10	3280	0.466 ± 0.0320	0.461 ± 0.0628
	5.5	7.79	3600	0.512 ± 0.0352	0.505 ± 0.0685
	6.0	8.85	4120	0.586 ± 0.0403	0.574 ± 0.0776
	6.5	7.79	3600	0.512 ± 0.0352	0.505 ± 0.0685
	7.0	6.95	3200	0.455 ± 0.0304	0.451 ± 0.0614
	7.5	7.55	3480	0.495 ± 0.0340	0.490 ± 0.0667
	8.0	7.60	3520	0.500 ± 0.0343	0.493 ± 0.0669
	9.0	7.05	3160	0.449 ± 0.0303	0.457 ± 0.0622
	9.5	6.50	3000	0.427 ± 0.0293	0.421 ± 0.0575
	10.0	5.75	2640	0.375 ± 0.0258	0.373 ± 0.0513
	11.0	4.92	2240	0.319 ± 0.0218	0.319 ± 0.0443
	12.0	4.40	2000	0.284 ± 0.0196	0.285 ± 0.0400
	13.0	4.05	1820	0.259 ± 0.0178	0.263 ± 0.0371
3A-V	0.25	5.68	2600	0.370 ± 0.0254	0.369 ± 0.0508
	0.50	5.68	2600	0.370 ± 0.0254	0.369 ± 0.0508
	1.0	5.33	2440	0.347 ± 0.0238	0.346 ± 0.0478
	1.5	5.60	2560	0.364 ± 0.0250	0.363 ± 0.0500
	2.0	5.45	2500	0.356 ± 0.0244	0.354 ± 0.0488
	2.5	5.33	2440	0.347 ± 0.0238	0.346 ± 0.0478
	3.0	5.30	2420	0.344 ± 0.0237	0.344 ± 0.0475
	3.5	5.40	2480	0.353 ± 0.0233	0.350 ± 0.0483
	4.0	5.60	2560	0.364 ± 0.0250	0.363 ± 0.0500
	4.5	5.40	2480	0.353 ± 0.0233	0.350 ± 0.0483
	5.0	5.33	2440	0.347 ± 0.0238	0.346 ± 0.0478
	5.5	5.50	2520	0.358 ± 0.0246	0.357 ± 0.0493
	6.0	5.50	2520	0.358 ± 0.0246	0.357 ± 0.0493
	6.5	5.60	2560	0.364 ± 0.0250	0.363 ± 0.0500
	7.0	5.50	2520	0.358 ± 0.0246	0.357 ± 0.0493
	7.5	4.65	2120	0.301 ± 0.0207	0.302 ± 0.0421
	8.0	5.68	2600	0.370 ± 0.0254	0.369 ± 0.0508
	8.5	5.68	2600	0.370 ± 0.0254	0.369 ± 0.0508
	9.0	5.17	2360	0.336 ± 0.0231	0.335 ± 0.0464
	9.5	5.33	2440	0.347 ± 0.0238	0.346 ± 0.0478

TEST	Run time (min)	M_p (in-lb)	$\Delta\phi$ (μin/in)	Coefficient of Friction ($\mu_d \pm w_d$) Theoretical	Calibrated
3A-V (Cont.)	10.0	5.68	2600	0.370 ± 0.0254	0.369 ± 0.0508
	10.5	5.25	2400	0.341 ± 0.0235	0.341 ± 0.0472
	11.0	5.40	2480	0.353 ± 0.0233	0.350 ± 0.0483
	11.5	5.50	2520	0.358 ± 0.0246	0.357 ± 0.0493
	12.0	5.92	2720	0.387 ± 0.0266	0.384 ± 0.0528
	13.0	5.40	2480	0.353 ± 0.0233	0.350 ± 0.0483
	14.0	6.25	2880	0.410 ± 0.0282	0.406 ± 0.0555
	15.0	5.50	2520	0.358 ± 0.0246	0.357 ± 0.0493
	16.0	5.60	2560	0.364 ± 0.0250	0.363 ± 0.0500
	16.5	5.60	2560	0.364 ± 0.0250	0.363 ± 0.0500
3B-V	0.25	5.42	2480	0.353 ± 0.0233	0.352 ± 0.0483
	0.50	5.67	2600	0.370 ± 0.0254	0.368 ± 0.0508
	1.0	5.30	2420	0.344 ± 0.0237	0.344 ± 0.0475
	1.5	5.85	2680	0.381 ± 0.0262	0.380 ± 0.0522
	2.0	5.12	2340	0.333 ± 0.0229	0.332 ± 0.0460
	2.5	5.07	2320	0.330 ± 0.0227	0.329 ± 0.0457
	3.0	4.75	2160	0.307 ± 0.0212	0.308 ± 0.0430
	3.5	4.75	2160	0.307 ± 0.0212	0.308 ± 0.0430
	4.0	5.50	2520	0.358 ± 0.0246	0.357 ± 0.0493
	4.5	5.50	2520	0.358 ± 0.0246	0.357 ± 0.0493
	5.0	4.66	2120	0.301 ± 0.0207	0.302 ± 0.0422
	5.5	5.50	2520	0.358 ± 0.0246	0.357 ± 0.0493
	6.0	4.81	2200	0.313 ± 0.0215	0.312 ± 0.0435
	6.5	6.10	2800	0.398 ± 0.0274	0.396 ± 0.0542
	7.0	5.00	2280	0.324 ± 0.0223	0.324 ± 0.0440
	7.5	6.25	2880	0.410 ± 0.0282	0.406 ± 0.0555
	8.0	5.25	2400	0.341 ± 0.0235	0.341 ± 0.0472
	8.5	5.00	2280	0.324 ± 0.0223	0.324 ± 0.0440
	9.0	5.25	2400	0.341 ± 0.0235	0.341 ± 0.0472
	9.5	4.88	2220	0.316 ± 0.0217	0.317 ± 0.0430
	10.0	4.88	2220	0.316 ± 0.0217	0.317 ± 0.0430
	10.5	4.40	2000	0.284 ± 0.0196	0.285 ± 0.0400
	11.0	5.13	2340	0.333 ± 0.0229	0.333 ± 0.0462
	11.5	6.25	2880	0.410 ± 0.0282	0.406 ± 0.0555
	12.0	3.75	1680	0.239 ± 0.0164	0.243 ± 0.0348
	12.5	4.07	1840	0.262 ± 0.0180	0.264 ± 0.0374
	13.0	7.00	3240	0.461 ± 0.0310	0.454 ± 0.0622
6A-V	0.25	7.95	3680	0.355 ± 0.0240	0.350 ± 0.0485
	0.5	7.35	3400	0.328 ± 0.0223	0.323 ± 0.0435
	1.0	8.45	3920	0.378 ± 0.0255	0.371 ± 0.0500
	1.5	8.90	4160	0.401 ± 0.0271	0.392 ± 0.0529
	2.0	8.60	4000	0.385 ± 0.0261	0.378 ± 0.0511
	2.5	9.18	4270	0.411 ± 0.0279	0.417 ± 0.0561

TEST	Run time (min)	M_p (in.-lb.)	$\Delta\xi$ (μin/in)	Coefficient of Friction (μ_d) $\pm \omega_d$ Theoretical	Calibrated
6A-V (Cont.)	3.0	9.90	4605	0.444 ± 0.0301	0.435 ± 0.0587
	3.5	9.70	4520	0.436 ± 0.0295	0.427 ± 0.0575
	4.0	11.45	5360	0.516 ± 0.0350	0.504 ± 0.0678
	4.5	12.95	6050	0.582 ± 0.0395	0.570 ± 0.0766
	5.0	14.25	6680	0.644 ± 0.0437	0.628 ± 0.0843
	5.5	15.75	7400	0.712 ± 0.0483	0.694 ± 0.0930
	6.0	16.10	7560	0.728 ± 0.0494	0.710 ± 0.0950
	6.5	16.60	7800	0.752 ± 0.0509	0.732 ± 0.0978
	7.0	17.47	8200	0.790 ± 0.0535	0.770 ± 0.103
7A-V	0.25	6.15	2840	0.274 ± 0.0186	0.271 ± 0.0372
	0.50	7.60	3520	0.339 ± 0.0229	0.334 ± 0.0453
	1.0	8.28	3840	0.370 ± 0.0250	0.364 ± 0.0492
	1.5	9.15	4280	0.413 ± 0.0279	0.403 ± 0.0545
	2.0	10.05	4690	0.452 ± 0.0308	0.442 ± 0.0595
	2.5	9.32	4360	0.420 ± 0.0285	0.410 ± 0.0553
	3.0	8.28	3840	0.370 ± 0.0250	0.364 ± 0.0492
	3.5	9.32	4360	0.420 ± 0.0285	0.410 ± 0.0553
	4.0	8.95	4160	0.400 ± 0.0271	0.394 ± 0.0532
	4.5	9.55	4440	0.428 ± 0.0291	0.420 ± 0.0568
	5.0	8.35	3880	0.374 ± 0.0254	0.367 ± 0.0498
	5.5	8.28	3840	0.370 ± 0.0250	0.364 ± 0.0492
	6.0	8.05	3720	0.359 ± 0.0242	0.354 ± 0.0481
	6.5	8.80	4080	0.394 ± 0.0267	0.387 ± 0.0523
	7.0	8.52	3960	0.382 ± 0.0259	0.375 ± 0.0508
	7.5	9.20	4280	0.413 ± 0.0279	0.405 ± 0.0548
	8.0	9.55	4440	0.428 ± 0.0291	0.420 ± 0.0566
	8.5	9.70	4520	0.436 ± 0.0295	0.427 ± 0.0575
	9.0	10.05	4690	0.452 ± 0.0306	0.442 ± 0.0596
	9.5	11.95	5600	0.540 ± 0.0365	0.526 ± 0.0708
	10.0	12.80	6000	0.578 ± 0.0391	0.563 ± 0.0756
	10.5	15.35	7200	0.694 ± 0.0470	0.675 ± 0.0905
	11.0	11.95	5600	0.540 ± 0.0365	0.526 ± 0.0708
	11.5	11.95	5600	0.540 ± 0.0365	0.526 ± 0.0708
	12.0	13.42	6290	0.607 ± 0.0410	0.591 ± 0.0793
	12.5	15.07	7080	0.683 ± 0.0463	0.663 ± 0.0890
	13.0	15.35	7200	0.694 ± 0.0470	0.675 ± 0.0905

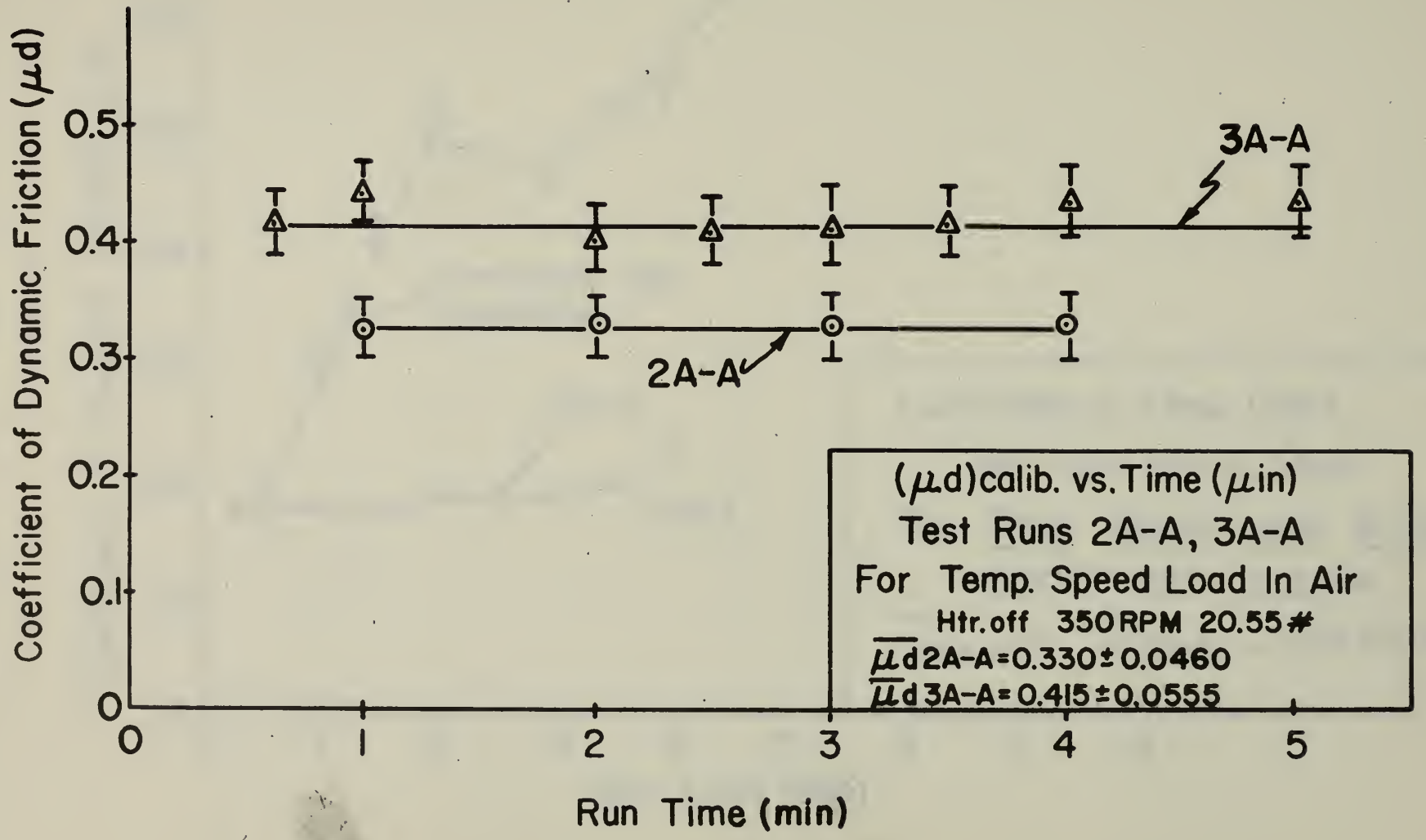
Coefficient of Dynamic Friction (μd)
0.5
0.4
0.3
0.2
0.1
0
0
1
2
3
4
5
Run Time (min)
3A-A
2A-A
(μd)calib. vs. Time (μin)
Test Runs 2A-A, 3A-A
For Temp. Speed Load In Air
Htr. off 350 RPM 20.55#
μd 2A-A = 0.330 ± 0.0460
μd 3A-A = 0.415 ± 0.0555

Figure D-1

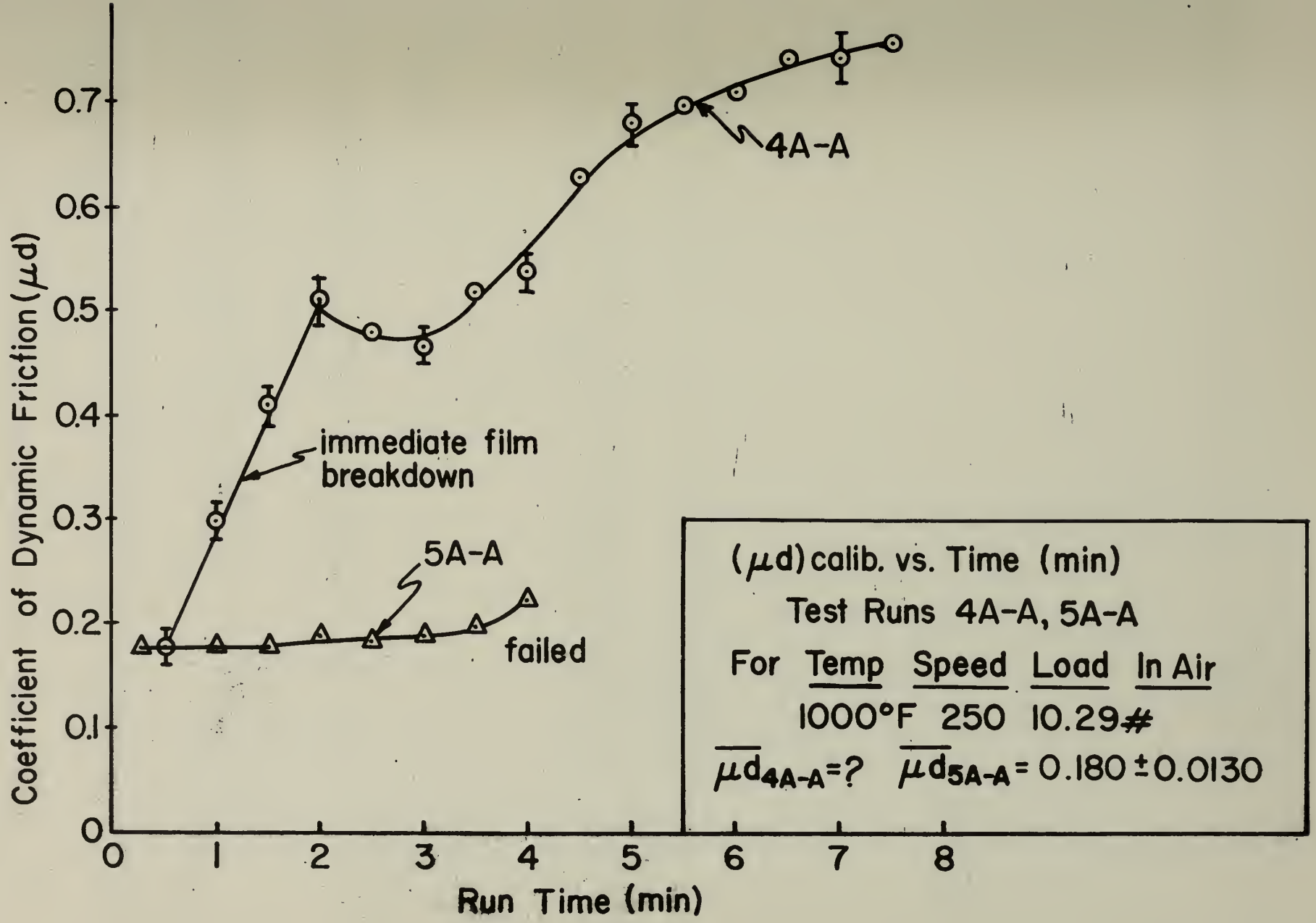
Coefficient of Dynamic Friction (μd)
0
0.1
0.2
0.3
0.4
0.5
0.6
0.7
0
1
2
3
4
5
6
7
8
Run Time (min)
4A-A
immediate film breakdown
5A-A
failed
(μd) calib. vs. Time (min)
Test Runs 4A-A, 5A-A
For Temp Speed Load In Air
1000°F 250 10.29#
$\overline{\mu d}_{4A-A}$=? $\overline{\mu d}_{5A-A}$ = 0.180 ± 0.0130

Figure D-2

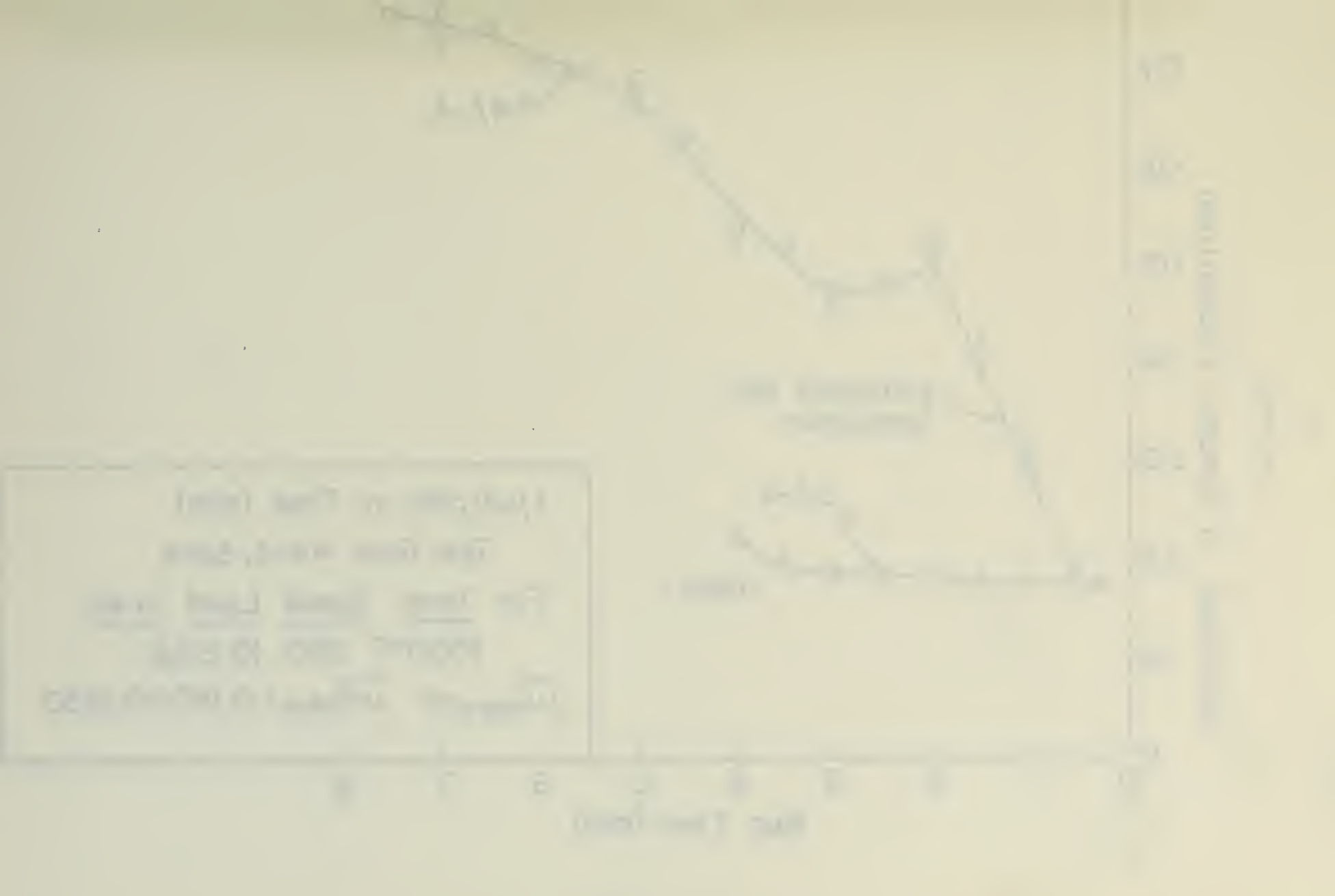

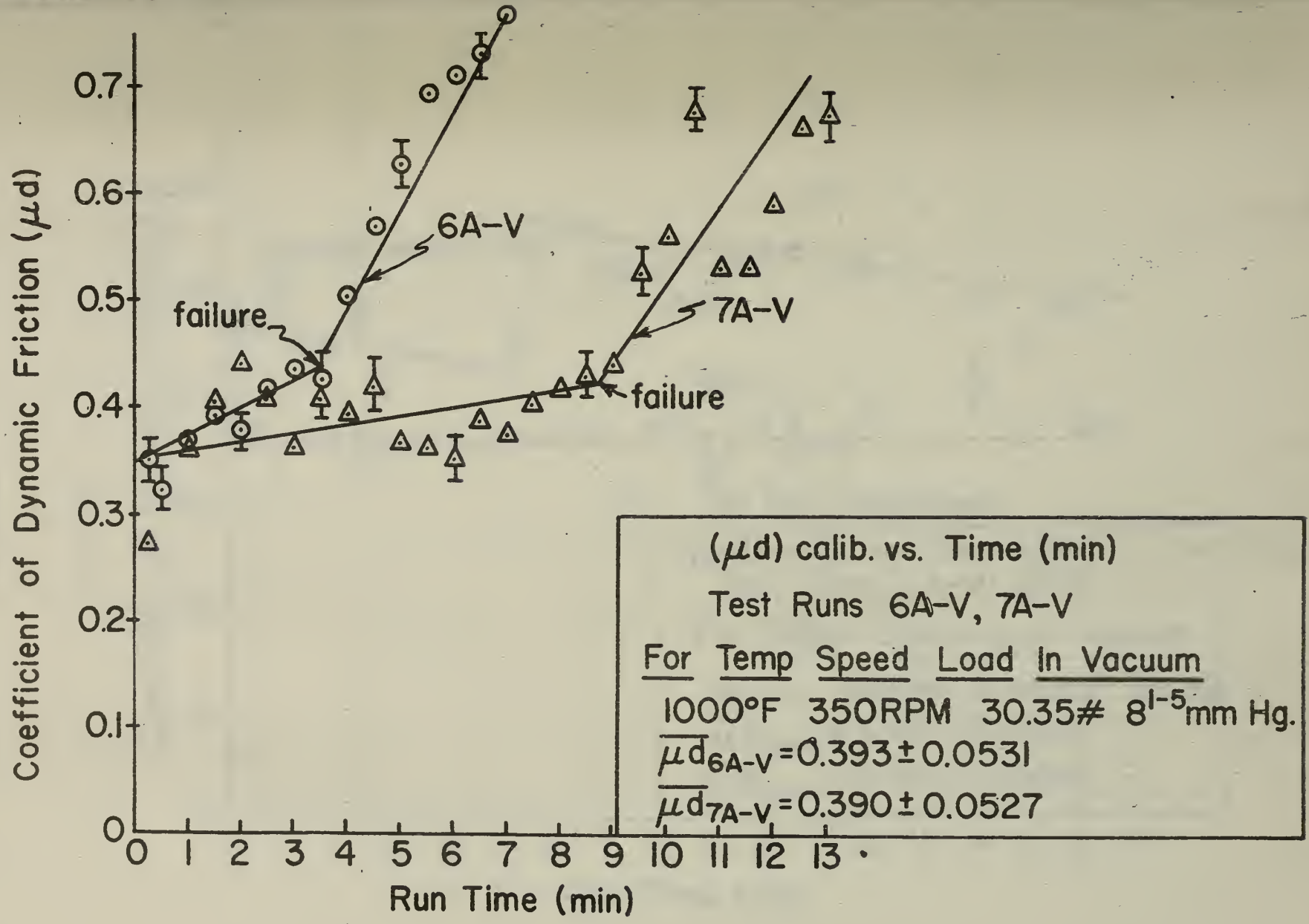
Coefficient of Dynamic Friction (μd)
0.7
0.6
0.5
0.4
0.3
0.2
0.1
0
0 1 2 3 4 5 6 7 8 9 10 11 12 13
Run Time (min)
6A-V
7A-V
failure
failure
(μd) calib. vs. Time (min)
Test Runs 6A-V, 7A-V
For Temp Speed Load In Vacuum
1000°F 350RPM 30.35# 8^1-5 mm Hg.
μd6A-V = 0.393 ± 0.0531
μd7A-V = 0.390 ± 0.0527

Figure D-3

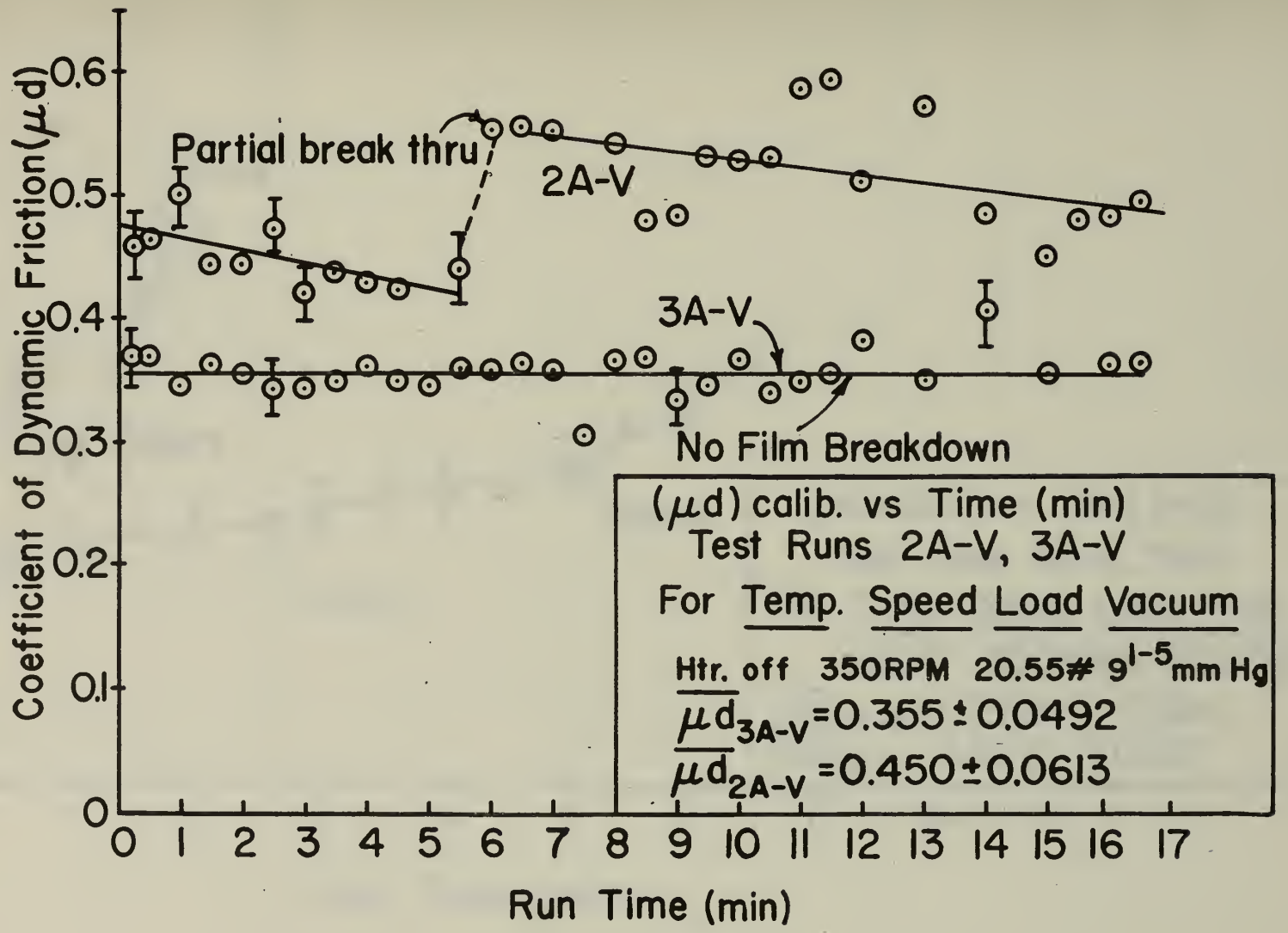
Coefficient of Dynamic Friction(μd)
0.6
0.5
0.4
0.3
0.2
0.1
0
Partial break thru
2A-V
3A-V
No Film Breakdown
(μd) calib. vs Time (min)
Test Runs 2A-V, 3A-V
For Temp. Speed Load Vacuum
Htr. off 350RPM 20.55# 9^{1-5}mm Hg
$\overline{\mu d}_{3A-V}$=0.355±0.0492
$\overline{\mu d}_{2A-V}$=0.450±0.0613
0 1 2 3 4 5 6 7 8 9 10 11 12 13 14 15 16 17
Run Time (min)

Figure D-4

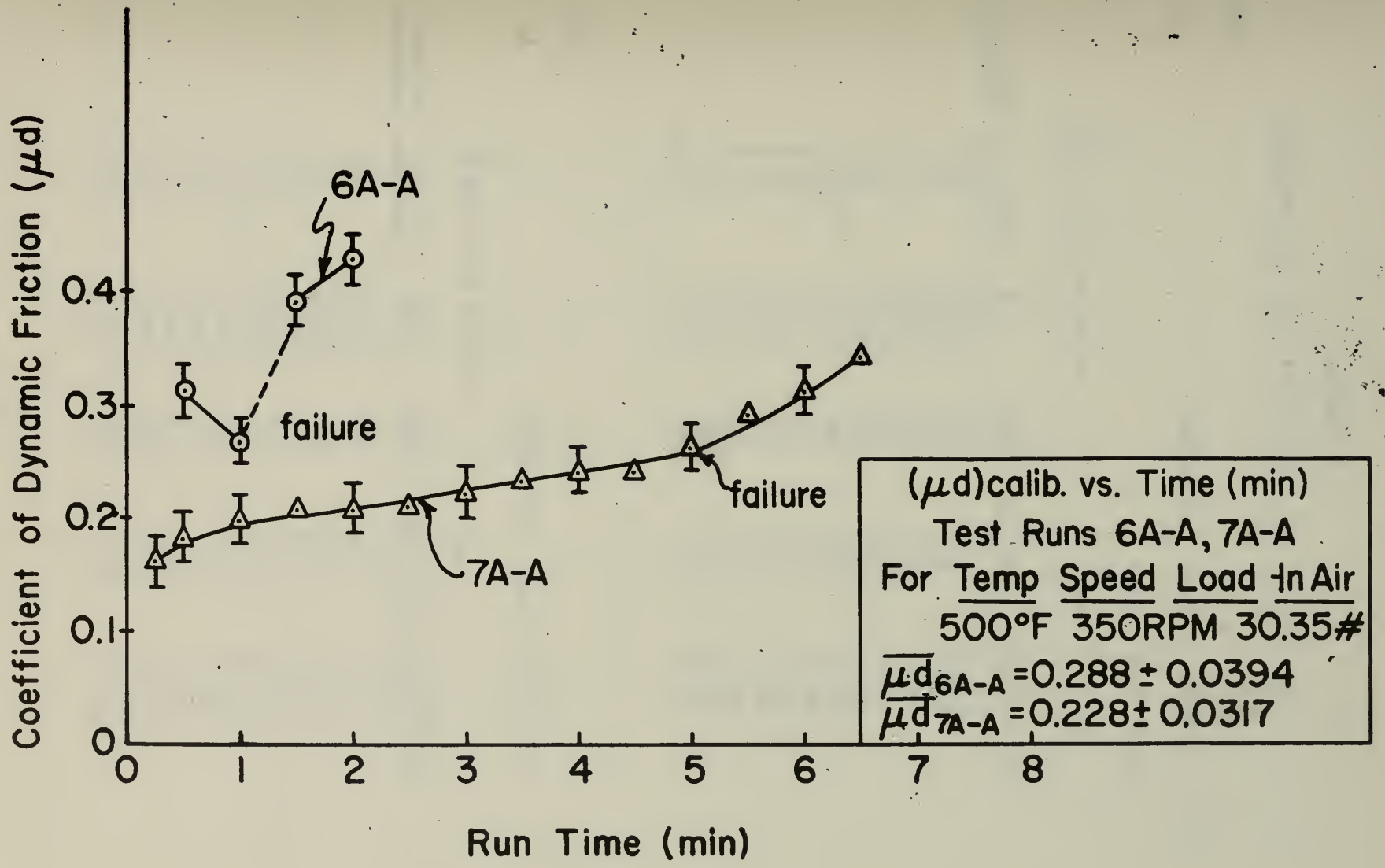
Coefficient of Dynamic Friction (μd)
0
0.1
0.2
0.3
0.4
0 1 2 3 4 5 6 7 8
Run Time (min)
6A-A
failure
7A-A
failure
(μd)calib. vs. Time (min)
Test Runs 6A-A, 7A-A
For Temp Speed Load In Air
500°F 350RPM 30.35#
$\overline{\mu d}_{6A-A}$ = 0.288 ± 0.0394
$\overline{\mu d}_{7A-A}$ = 0.228 ± 0.0317

Figure D-5

TABLE D-4

FRICTION DATA AND CALCULATIONS FOR TEFLON (TFE)

TEST #1

VARIABLES: Speed - 350 RPM (in air)
Load - 10.29 lbs.
Temp - Htr. off

$\mathcal{E}_b$ - 17,735 μin/in.

Friction	Time (min.)	$\mathcal{E}_a$	$\Delta\mathcal{E}$	M_p (in-lb)	(μ_d) calib.
	0.25	17035	700	1.65	0.214
	0.5	16975	760	1.78	0.230
	1.0	17075	660	1.58	0.205
	2.0	17123	612	1.47	0.191
	3.0	17115	620	1.50	0.194
	4.0	17115	620	1.50	0.194
	5.0	17115	620	1.50	0.194
	6.0	17123	612	1.47	0.191
	7.0	17155	580	1.40	0.181
	8.0	17194	541	1.33	0.172
	9.0	17194	541	1.33	0.172
	10.0	17155	580	1.40	0.181

TEST #2

VARIABLES: (same as Test #1)

$\mathcal{E}_b$ - 17,694 μin/in.

Friction	Time (min.)	$\mathcal{E}_a$	$\Delta\mathcal{E}$	M_p (in-lb)	(μ_d) calib.
	0.25	17041	652	1.66	0.215
	0.5	17060	633	1.53	0.198
	1.0	17049	644	1.55	0.201
	2.0	17060	633	1.53	0.198
	3.0	17049	644	1.55	0.201
	4.0	17070	613	1.51	0.196
	5.0	17070	613	1.51	0.196
	6.0	17060	633	1.53	0.198
	7.0	17093	600	1.45	0.188
	8.0	17093	600	1.45	0.188
	9.0	17121	572	1.40	0.180
	10.0	17121	572	1.40	0.180

TEST

#3

VARIABLES: Speed = 350 RPM (in air)

Load = 30.35 lbs.

Temp = Htr. off

ε_b - 17,700 μ in/in.

Friction	Time (min)	ε_a	$\Delta\varepsilon$	M_p (in-lb)	(μ_d) calib.
	0.25	15840	1860	4.02	0.177
	0.5	15880	1820	3.92	0.172
	1.0	15900	1800	3.88	0.171
	2.0	15840	1860	4.02	0.177
	3.0	15840	1860	4.02	0.177
	4.0	15840	1860	4.02	0.177
	5.0	15880	1820	3.92	0.172

TEST

#4

VARIABLES: (same as Test #3)

ε_b - 17,725 μ in/in.

Friction	Time (min)	ε_a	$\Delta\varepsilon$	M_p (in-lb)	(μ_d) calib.
	0.25	15545	2180	4.67	0.205
	0.50	15645	2080	4.45	0.196
	1.0	15745	1980	4.25	0.187
	2.0	15875	1850	4.00	0.176
	3.0	15905	1820	3.92	0.172
	4.0	15975	1750	3.00	0.167
	5.0	15905	1820	3.92	0.172

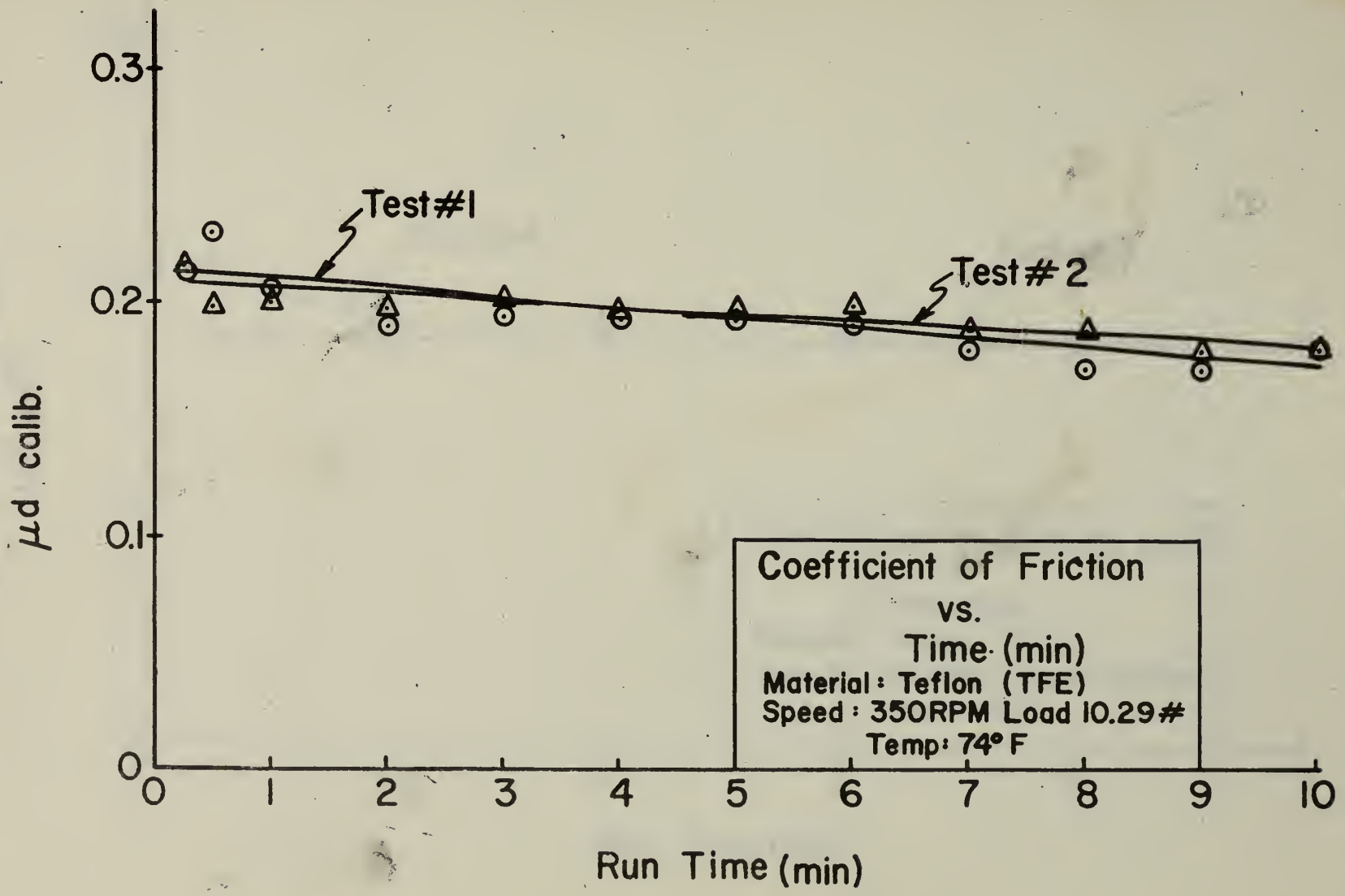
0.3
0.2
0.1
0
μd calib.
Test#1
Test#2
Coefficient of Friction
vs.
Time (min)
Material: Teflon (TFE)
Speed: 350RPM Load 10.29#
Temp: 74° F
0
1
2
3
4
5
6
7
8
9
10
Run Time (min)

Figure D-6

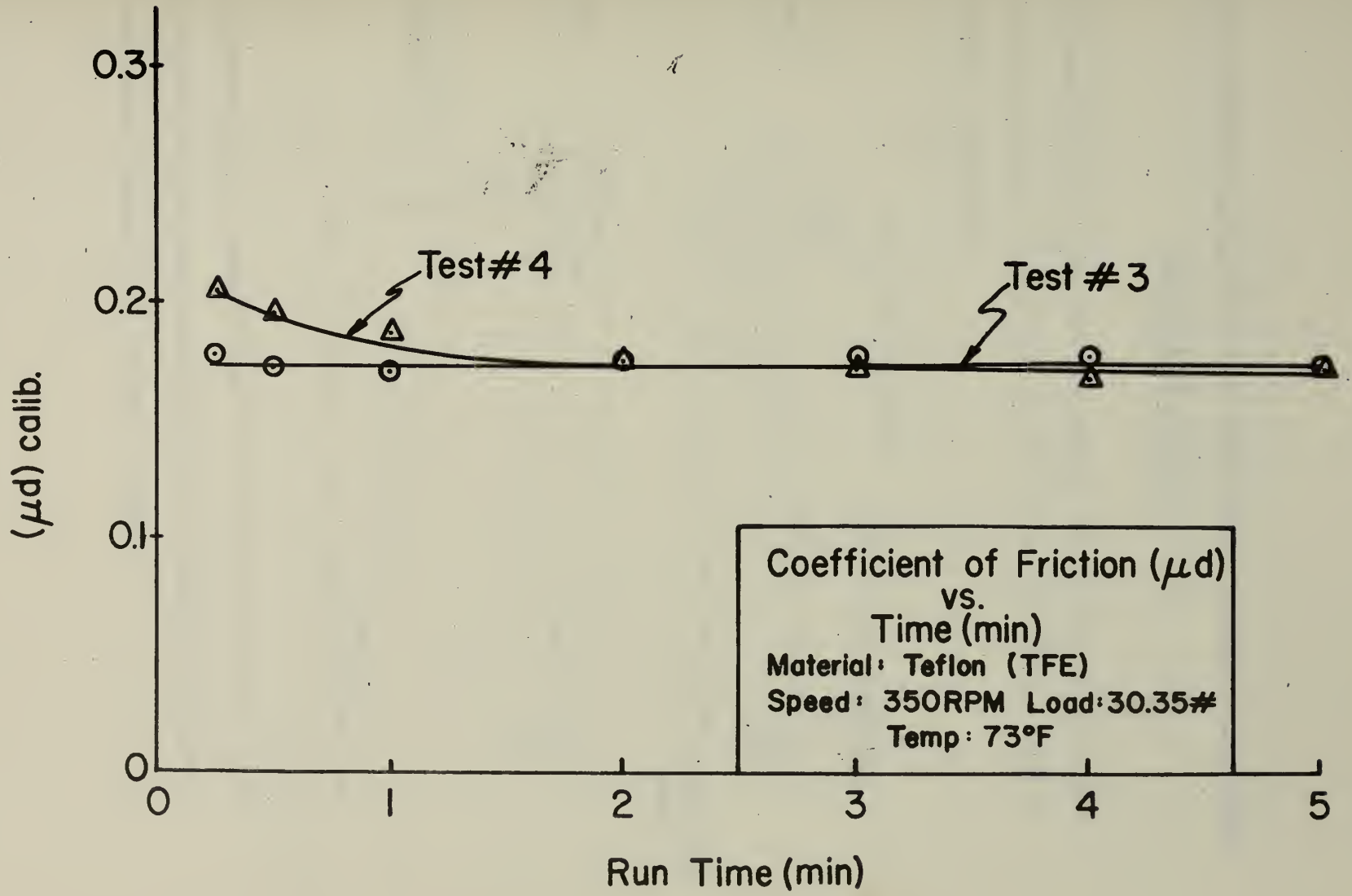
0.3
0.2
0.1
0
(μd) calib.
Test#4
Test #3
Coefficient of Friction (μd)
vs.
Time (min)
Material: Teflon (TFE)
Speed: 350RPM Load: 30.35#
Temp: 73°F
0
1
2
3
4
5
Run Time (min)

Figure D-7

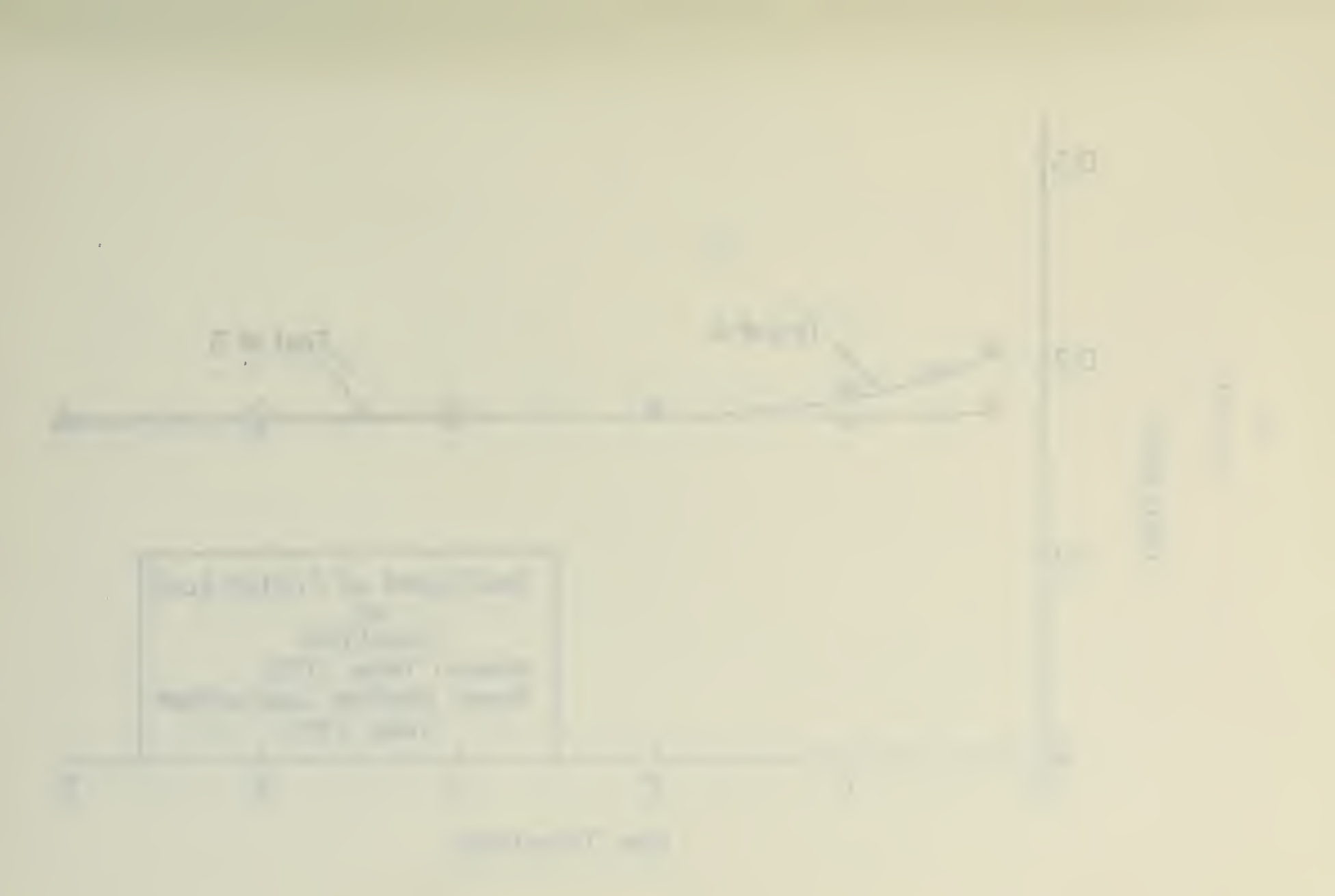

Analytical Development for the Dynamic Coefficient of Friction including Uncertainty Analysis

This analysis will show that the dynamic coefficient of friction (μ_d) can be calculated by multiplying the net strain reading ($\Delta\varepsilon$) by a suitable constant (K).

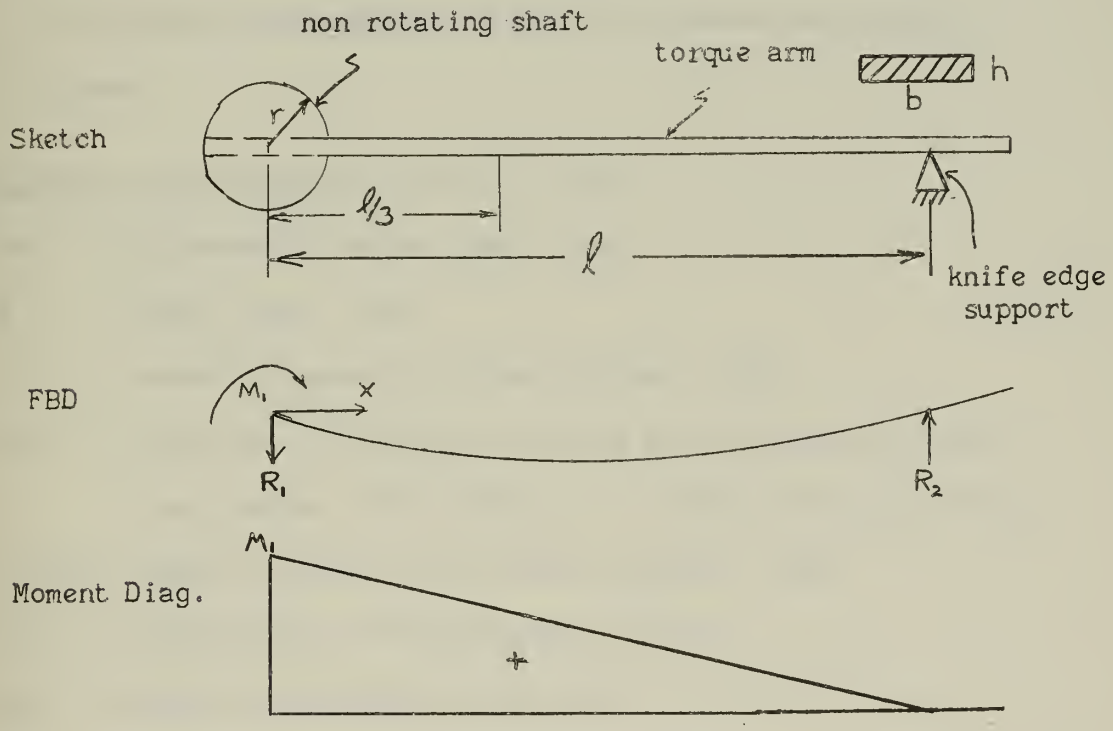

The moment (M_1) is readily found by subtracting the frictional moment produced at the lower non-rotating shaft bearing, from the frictional moment generated at the wear surfaces.

The Frictional Moment (M_f)

An expression for the frictional moment at the wear surface depends on three assumptions. They are

1. The dynamic coefficient of friction is independent of rubbing velocity [1].
2. The wear over the annular surfaces is uniform [21].
3. The wear is proportional to applied pressure and rubbing speed.

Nomenclature Used in Analysis (see Fig. E-1)

dW = differential normal load (lbs.)

W = normal load (lbs.)

p = "apparent" pressure on wear surface (psi)

dA = $\rho\, d\rho\, d\theta$ - differential surface area expressed in polar coordinates (in^2) where, ρ = radius (in) ($r_1 \leq \rho \leq r_2$)

r_1, r_2 = inner and outer radii of wear specimen (in.)

dF_f = differential frictional force (lbs.)

μ_d = dynamic coefficient of friction

dM_f = differential frictional moment (in. lbs.)

M_f = frictional moment (in. lbs.)

$\bar{r}$ = arithmetic mean radius (in.)

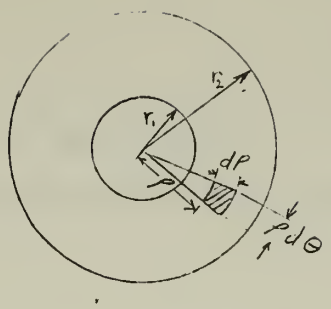

Figure E-1

Schematic Drawing of Lower Wear Sample

Analysis

$$dW = pdA = p\rho d\rho d\theta$$

from assumption 3, $p\rho$ = constant = C

Integrating twice over suitable limits, we have

$$W = \int_0^{2\pi}\int_{r_1}^{r_2} C d\rho d\theta = 2\pi C (r_2 - r_1)$$

where,

$$C = W/2\pi(r_2 - r_1)$$

Since the frictional force (F_f) can be related to the coefficient of friction and the normal load applied, we have

$$dF_f = \mu_d dW = \mu_d C d\rho d\theta$$

and the differential frictional moment is expressed as

$$dM_f = \rho dF_f = \mu_d C \rho d\rho d\theta$$

Performing a double integration, using appropriate limits, yields

$$M_f = \int_{r_1}^{r_2}\int_0^{2\pi} \mu_d C \rho d\rho d\theta$$

whence,

$$M_f = 2\pi\mu_d C\left[\frac{r_2^2}{2} - \frac{r_1^2}{2}\right] = \frac{2\pi\mu_d W}{2\pi(r_2 - r_1)}\left[\frac{(r_2+r_1)(r_2-r_1)}{2}\right]$$

95

or, $$M_f = \mu_d W \bar{r} \quad \text{(in. lbs.)} \quad (1)$$

The resisting frictional torque at the lower bearing can also be expressed as

$$M_b = \mu_{SB} R_1 d/2 \quad \text{(in. lbs.)} \quad (2)$$

where, μ_{SB} = bearing static coefficient of friction

R_1 = shaft reaction (lbs.)

d = shaft diameter (in.)

Thus,

$$M_1 = M_f - M_b \quad \text{(in. lbs.)} \quad (3)$$

To avoid a solution for the dynamic coefficient of friction to be in quadratic form, let

$$R_1 \sim \mu_d W \bar{r}/\ell \quad \text{(lbs.)} \quad (4)$$

where, ℓ = effective length of torque arms (in.)

Thus, by substituting equation (4) into (2) and subtracting this expression from equation (1), equation (3) can be expressed as

$$M_1 = \mu_d W \bar{r} - \mu_{SB} \mu_d W \bar{r} d/2\ell$$

or,

$$M_1 = \left[W (r_1+r_2) \mu_d (\ell - \mu_{SB} r)\right]/2\ell \quad \text{(in. lbs.)} \quad (5)$$

where, r = non-rotating shaft diameter (in.)

r_1, r_2 = inner and outer radii of wear specimen (in.)

The moment equation for the beam is simply

$$M_x = M_1 - R_1 x \quad \text{(in. lbs.)} \quad (6)$$

At $x = \ell/3$ (mean position of strain gages) we have

$$M_{\ell/3} = M_1 - \frac{M_1}{\ell}\frac{\ell}{3} = \frac{2}{3} M_1 \qquad (7)$$

Substituting equation (5) into (7) yields

$$M_{\ell/3} = \left[W(r_1+r_2)\mu_d(\ell - \mu_{sB} r)\right]/3\ell \qquad (8)$$

The longitudinal strain at $\ell/3$ of the torque arm will be derived from simple strength of materials theory [22].

Useful expressions are

$$\sigma = E\epsilon \qquad \text{(psi)}$$

$$\sigma = \frac{Mc}{I} \qquad \text{(psi)}$$

$$I = \frac{bh^3}{12} \qquad (\text{in}^4)$$

where, σ = tensile or compressive stress

E = Young's Modulus of elasticity (psi)

ϵ = longitudinal strain (in/in)

I = transverse moment of inertia

b = base of torque arm (in)

h = height of torque arm (in)

C = distance from neutral axis to outermost fiber of the arm (in)

M = bending moment (in. lbs.)

from which

$$\epsilon = \frac{6M}{Ebh^2} \qquad (9)$$

The longitudinal strain at $\ell/3$ is obtained by substiting equation (8) into (9), thus yielding

$$\epsilon_{\ell/3} = \frac{2W(r_1+r_2)\mu_d(\ell - \mu_{sB} r)}{bh^2 \ell E 10^{-6}} \quad [\mu\text{in./in.}] \qquad (10)$$

Since four (4) high temperature strain gages composed the external bridge, strain readings are four times the actual strain. Therefore, solving for μ_d from (10) and letting the net strain be

$$\Delta\epsilon = 4\epsilon_{l/3}$$

we have

$$\mu_d = \frac{E b h^2 \ell \Delta\epsilon 1^{-6}*}{8W(r_1+r_2)(\ell-\mu_{SB}r)} \qquad (11)$$

Because the strain gages are not located at the outermost fibers of the torque arm, equation (11) must be modified by a correction factor.

Let ΔC = distance from outer fiber of beam to strain gage

Then, by similar triangles

$$\mu_d = \left(\frac{c}{c+\Delta C}\right)\frac{E b h^2 \ell \Delta\epsilon 1^{-6}}{8W(r_1+r_2)(\ell-\mu_{SB}r)} \qquad (12)$$

All quantities in equation (12) are either known (k), measured (m) or estimated (e), except the net strain ($\Delta\epsilon$).

This constant can be evaluated for various normal loads (W), and operating temperatures (T), and is found in Table E-1.

*For compactness, $1 \times 10^{-6} = 1^{\backslash -6}$

Data for Constant (K) Evaluation

$C = 0.0252$ in. (m)

$b = 0.50$ in. (m)

$h = 0.0504$ in. (m)

$\ell = 5.00$ in. (m)

$E = 28.75 \times 10^6$ psi at 400°F [22] (k)

29.25×10^6 psi at 300°F

29.80×10^6 psi at 200°F

30×10^6 psi at 70°F

$W = 10.29$, 20.55, and 30.35 lbs. (m)

$r_1 + r_2 = 1.50$ in. (m)

$\Delta C = 0.003$ in. (m)

$\mu_{sB} \cong 0.1$ (e)

$r = 0.50$ in. (e)

TABLE E-1

Tabulated Values of $K^{1/4}$

	Weights (lbs)		
Temp.(°F)	10.29	20.55	30.35
70	2.84	1.42	0.964
200	2.82	1.41	0.956
300	2.72	1.39	0.940
400	2.70	1.36	0.924

Thus, it has been shown that the dynamic coefficient of friction can be determined from a theoretical basis, and in final form this expression for μ_d is

$$\mu_d = K \Delta\varepsilon \tag{13}$$

where, K is the calculated constant appearing in Table E-1 and, $\Delta\varepsilon$ is the net strain as read from the strain indicator (μ in/in).

Uncertainty Analysis

The uncertainty ($w_{\mu d}$) in the value of the dynamic coefficient of friction can be expressed as [20]

$$w_{\mu d} = \left[\left(\frac{\partial \mu_d}{\partial K}\right)^2 w_K^2 + \left(\frac{\partial \mu_d}{\partial \Delta\varepsilon}\right)^2 w_{\Delta\varepsilon}^2 \right]^{1/2} \tag{14}$$

Since, $\mu_d = K \Delta\varepsilon$

the first derivative of μ_d with respect to K and $\Delta\varepsilon$ are

$$\frac{\partial \mu_d}{\partial K} = \Delta\varepsilon \qquad \text{and} \qquad \frac{\partial \mu_d}{\partial \Delta\varepsilon} = K$$

Therefore, equation (14) simplifies to

$$w_{\mu d} = \left[(\Delta\varepsilon)^2 w_K^2 + (K)^2 w_{\Delta\varepsilon}^2 \right]^{1/2} \tag{15}$$

The net strain reading ($\Delta\varepsilon$), and the particular value of (K) are known for each test. Thus, it remains to evaluate the uncertainties in ($\Delta\varepsilon$) and (K) to complete the analysis.

1. The Uncertainty in ($\Delta\varepsilon$) $w_{\Delta\varepsilon}$

   Recalling that, $\Delta\varepsilon = \varepsilon_b - \varepsilon_a$

   it follows that the expression for $w_{\Delta\varepsilon}$ is

$$w_{\Delta\varepsilon} = \left[\left(\frac{\partial \Delta\varepsilon}{\partial \varepsilon_b}\right)^2 w_{\varepsilon_b}^2 + \left(\frac{\partial \Delta\varepsilon}{\partial \varepsilon_a}\right)^2 w_{\varepsilon_a}^2 \right]^{1/2}$$

or

$$w_{\Delta\ell} = \left[w_{\ell b}^2 + w_{\ell a}^2 \right]^{1/2} \qquad (16)$$

Letting $w_{\ell b} = w_{\ell a} = \pm 5$ Min/in. we have

$$w_{\Delta\ell} = \pm 7.1 \text{ Min/in.}$$

2. The Uncertainty in (K) w_K

If it is assumed that $l >> u_{sB} r$ then the constant (K) can be expressed as

$$K \sim \frac{A b h^2 E^{1-6}}{16 W \bar{r}}$$

where for simplicity

$$A = \frac{C}{C + \Delta C}$$

Thus, it follows that

$$w_K = \left[\left(\frac{\partial K}{\partial A}\right)^2 w_A^2 + \left(\frac{\partial K}{\partial b}\right)^2 w_b^2 + \left(\frac{\partial K}{\partial h}\right)^2 w_h^2 + \left(\frac{\partial K}{\partial E}\right)^2 w_E^2 + \left(\frac{\partial K}{\partial W}\right)^2 w_W^2 + \left(\frac{\partial K}{\partial \bar{r}}\right)^2 w_{\bar{r}}^2 \right]^{1/2} \qquad (17)$$

where,

$$\frac{\partial K}{\partial A} = \frac{b h^2 E^{1-6}}{16 W \bar{r}} \quad , \quad \frac{\partial K}{\partial b} = \frac{A h^2 E^{1-6}}{16 W \bar{r}}$$

$$\frac{\partial K}{\partial h} = \frac{A b h E^{1-6}}{8 W \bar{r}} \quad , \quad \frac{\partial K}{\partial E} = \frac{A h^2 b^{1-6}}{16 W \bar{r}}$$

$$\frac{\partial K}{\partial W} = \frac{-A b h^2 E^{1-6}}{16 W^2 \bar{r}} \quad , \quad \frac{\partial K}{\partial \bar{r}} = \frac{-A b h^2 E^{1-6}}{16 W \bar{r}^2}$$

The following parameters were measured and the uncertainties estimated.

$A = 0.89 \pm 0.05$

$b = 0.500 \pm 0.001$ (in)

$h = 0.0504 \pm 0.001$ (in)

$E = 28.75^{1}\!/_{6} \pm 0.5^{1}\!/_{6}$ (psi) at 400°F [22]

$29.25^{1}\!/_{6} \pm 0.5^{1}\!/_{6}$ (psi) at 300°F

$29.80^{1}\!/_{6} \pm 0.5^{1}\!/_{6}$ (psi) at 200°F

$30^{1}\!/_{6} \pm 0.5^{1}\!/_{6}$ (psi) at 70°F

$W = 10.29$, 20.55, and 30.35 ± 0.05 (lbs)

$\bar{r} = 0.75 \pm 0.10$ (in)

TABLE E-2

Evaluation of the Uncertainty in K*

	Weights (lbs.)		
	10.29	20.55	30.35
$\left(\frac{\partial K}{\partial A}\right)$	3.00×10^{-4}	1.50×10^{-4}	1.02×10^{-4}
$\left(\frac{\partial K}{\partial A}\right)^2 \omega_A^2$	22.5×10^{-11}	5.63×10^{-11}	2.58×10^{-11}
$\left(\frac{\partial K}{\partial b}\right)$	5.35×10^{-4}	2.68×10^{-4}	1.82×10^{-4}
$\left(\frac{\partial K}{\partial b}\right)^2 \omega_b^2$	28.6×10^{-14}	7.17×10^{-14}	3.29×10^{-14}
$\left(\frac{\partial K}{\partial h}\right)$	10.6×10^{-3}	5.32×10^{-3}	3.60×10^{-3}
$\left(\frac{\partial K}{\partial h}\right)^2 \omega_h^2$	112.0×10^{-12}	28.3×10^{-12}	12.9×10^{-12}
$\left(\frac{\partial K}{\partial E}\right)$	9.14×10^{-12}	4.58×10^{-12}	3.10×10^{-12}
$\left(\frac{\partial K}{\partial E}\right)^2 \omega_E^2$	20.9×10^{-12}	5.26×10^{-12}	2.41×10^{-12}
$\left(\frac{\partial K}{\partial W}\right)$	-13.0×10^{-7}	-6.52×10^{-7}	-4.42×10^{-7}
$\left(\frac{\partial K}{\partial W}\right)^2 \omega_W^2$	4.23×10^{-15}	1.06×10^{-15}	0.488×10^{-15}
$\left(\frac{\partial K}{\partial F}\right)$	-3.55×10^{-5}	-1.78×10^{-5}	-1.21×10^{-5}
$\left(\frac{\partial K}{\partial F}\right)^2 \omega_F^2$	12.6×10^{-12}	5.60×10^{-12}	1.46×10^{-12}

Substituting the evaluated parameters from Table E-2 into equation (17) yields the uncertainty of K as shown below.

$\omega_K = 19.3\times10^{-6}$, for W = 10.29 (lbs.)

$\omega_K = 9.77\times10^{-6}$, for W = 20.55 (lbs.)

$\omega_K = 6.52\times10^{-6}$, for W = 30.35 (lbs.)

*Young's Modulus (E) is considered constant and equal to E at 300°F.

Recalling that

$$\omega_{ud} = \left[(\Delta \xi)^2 \omega_K^2 + (K)^2 \omega_{\Delta \xi}^2 \right]^{1/2}$$

we have the following formula tabulation for ω_{ud}

TABLE E-3

T(°F)	10.29 (lbs.)	20.55 (lbs)	30.35 (lbs)
70	$(371\times10^{-12}\ \Delta\xi^2 + 40.3\times10^{-7})^{\frac{1}{2}}$	$(95.5\times10^{-12}\ \Delta\xi^2 + 10.1\times10^{-7})^{\frac{1}{2}}$	$(42.6\times10^{-12}\ \Delta\xi^2 + 4.65\times10^{-7})^{\frac{1}{2}}$
200	$(371\times10^{-12}\ \Delta\xi^2 + 39.7\times10^{-7})^{\frac{1}{2}}$	$(95.5\times10^{-12}\ \Delta\xi^2 + 9.93\times10^{-7})^{\frac{1}{2}}$	$(42.6\times10^{-12}\ \Delta\xi^2 + 4.57\times10^{-7})^{\frac{1}{2}}$
300	$(371\times10^{-12}\ \Delta\xi^2 + 37.0\times10^{-7})^{\frac{1}{2}}$	$(95.5\times10^{-12}\ \Delta\xi^2 + 9.61\times10^{-7})^{\frac{1}{2}}$	$(42.6\times10^{-12}\ \Delta\xi^2 + 4.41\times10^{-7})^{\frac{1}{2}}$
400	$(371\times10^{-12}\ \Delta\xi^2 + 36.4\times10^{-7})^{\frac{1}{2}}$	$(95.5\times10^{-12}\ \Delta\xi^2 + 9.22\times10^{-7})^{\frac{1}{2}}$	$(42.6\times10^{-12}\ \Delta\xi^2 + 4.26\times10^{-7})^{\frac{1}{2}}$

Determination of the Dynamic Coefficient of Friction by the Calibration Method Including Uncertainty Analysis

Torque Arm Calibration

A known moment was applied to the non-rotating shaft using a C-clamp as the lever arm and steel discs for loading. A "frictionless" ball bearing pulley enabled the calibration to be conducted with the shaft in the normal vertical position. Flexible nylon fishing line (monofilament - 20 lbs. test) connected the weights to the clamp. For every moment applied to the shaft, the net strain was recorded, and a calibration curve of net strain versus moment was constructed. To verify the strain readings, an analytical treatment was conducted. The largest per cent error was two per cent, while most runs yielded percentage errors less than one. The calibration curve was determined at 80°F and 166°F (using an industrial blower with temperature monitoring by a thermocouple). This curve was found to be linear for $4 \leq M_p \leq 12$ (in.lbs.)

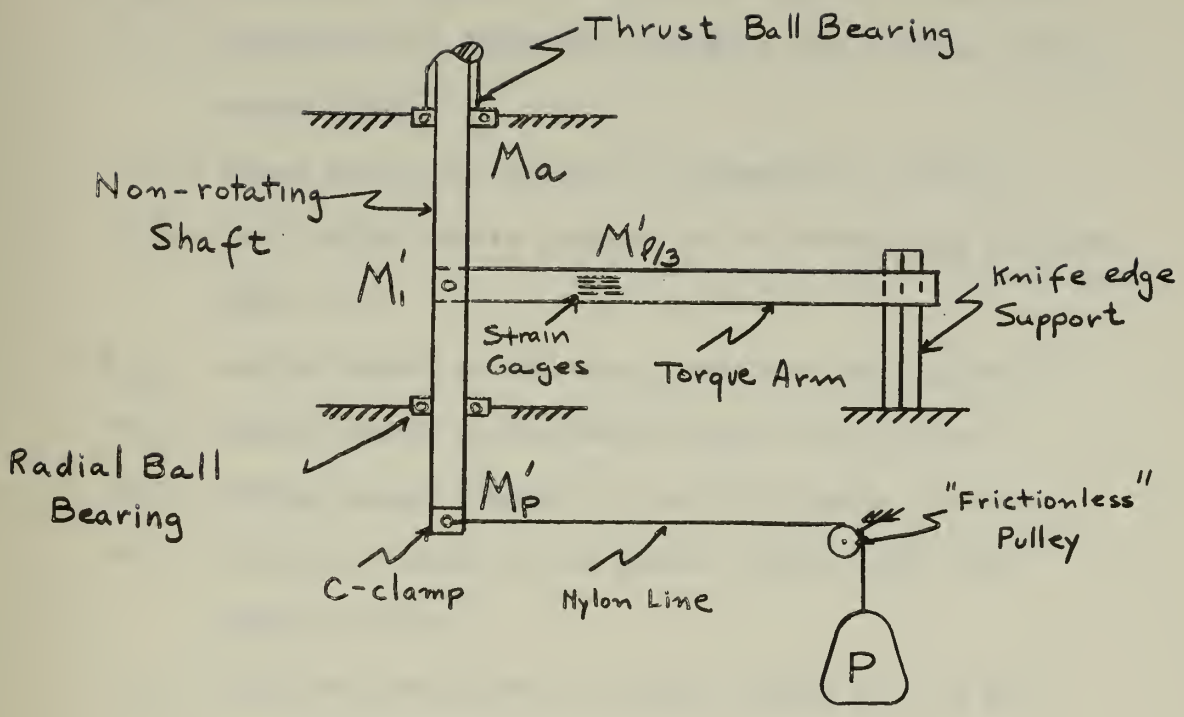

Figure F-1

Calibration Loading Diagram

Nomenclature

$\Delta\varepsilon$ = net corrected strain gage reading (μin./in.)

C = distance from neutral axis of torque arm to outer fiber (in.)

ΔC = distance the strain gages are above the outer fiber of the arm (in.)

b = base of the torque arm (in.)

h = height of the torque arm (in.)

μ_{BB} = static coefficient of friction of the ball bearings

E = Young's Modulus of Elasticity (psi.)

ℓ' = C-clamp lever arm (in.)

P = force of gravity acting on weights (lbs.)

r_{BB} = "effective" radius of the friction forces in the ball bearings (in.) (measured from shaft center line to ball center line)

W' = normal weight of the shaft, C-clamps, etc. (lbs.)

$\epsilon_{\ell/3}$ = longitudinal strain produced at the strain gage position (μin./in.)

$M_{\ell/3}$ = bending moment at the strain gage position (in.lbs.)

M_l' = bending moment at the shaft center line (in.lbs.)

M_p' = bending moment produced by loaded C-clamps (in.lbs.)

M_r = frictional torque due to radial load in lower ball bearing (in.lbs.)

M_a = frictional torque due to thrust loading (W') in the upper ball bearing (in.lbs.)

Known or Measured Data

μ_{BB} = 0.1 (assumed)

W' = 1.71 (lbs.)

E = 30^{6} (psi.) at 70°F

C = 0.0252 (in.)

ΔC = 0.003 (in.)

ℓ' = 3.81 (in.)

r_{BB} = 0.50 (in.)

b = 0.50 (in.)

An Analysis to Verify the Calibration Test

The following assumptions were made:

1. All the weight of the vertical shaft acted on the upper ball bearing.
2. The ball bearing used in the calibration test was frictionless.
3. The lower ball bearing absorbed all the radial loading applied to the shaft.
4. The "effective" coefficients of friction for the shaft bearings were considered to be equal. (0.1)
5. Each strain gage contributed 25 per cent of the total output reading.
6. The "effective" length of the torque arm (ℓ) was from the shaft center line to the knife edge support.

Summing the moments yields

$$M'_p = M_r + M_a + M_1 \quad \text{(in.lbs.)} \quad (18)$$

where

$$\begin{aligned} M'_p &= P\ell' \\ M_r &= \mu_{BB} P r_{BB} \\ M_a &= \mu_{BB} W' r_{BB} \end{aligned} \quad (19)$$

Substituting equations (19) into (18) we have

$$M'_1 = P\ell' - \mu_{BB} r_{BB} (P + W') \quad \text{(in.lbs.)} \quad (20)$$

at $x = \ell/3$ of the torque arm, $M'_{\ell/3} = 2/3\, M'_1$ (21)

The longitudinal strain produced (from simple theory) yields

$$\epsilon'_{\ell/3} = \frac{M'_{\ell/3} C}{I E} = \frac{6 M'_{\ell/3}}{b h^2 E 10^{-6}} \quad (\mu \text{in./in.}) \quad (22)$$

Placing the expression for M_1' into equation (21), equation (22) takes the form of

$$\epsilon'_{\ell/3} = \frac{4\left[P\ell' - \mu_{BB} r_{BB}(P+W')\right]}{bh^2 E^{-6}} \qquad (\mu\text{in./in.}) \quad (23)$$

Since the strain gages are not located at the outermost fibers of the torque arm, a correction must be introduced.

Let, $$\epsilon'_{\ell/3}\ \text{corr.} = \left(\frac{C+\Delta C}{C}\right)\epsilon'_{\ell/3} \qquad (24)$$

The four gages compose an external bridge; thus the output from the strain indicator will be four times the corrected strain.

$$\Delta\mu = 4\epsilon'_{\ell/3}\ \text{corr.} = 4\left(\frac{C+\Delta C}{C}\right)\left[\frac{4\left(P\ell' - \mu_{BB} r_{BB}(P+W')\right)}{bh^2 E^{-6}}\right]$$

or $$\Delta\mu = \frac{4(C+\Delta C)\left[P\ell' - \mu_{BB} r_{BB}(P+W')\right]}{C^3 b E^{-6}} \qquad (\mu\text{in./in.}) \quad (25)$$

After substituting numerical values, we have

$$\Delta\mu = 470(3.81P - 0.05(P+1.71)) \qquad (\mu\text{in./in.}) \quad (26)$$

Calibration data and results follow, verified by analytical results.

Table F-1

Calibration Data

P (lbs.)	M'_p (in.lbs.)	$\mathcal{E}$ b(μin./in.)	$\mathcal{E}$ a(μin./in.)	Temp.(°F)
1.0	3.81	11371	9630	80
		11364	9625	
		11369	9640	
		11370	9640	
1.5	5.72	11360	8733	80
		11360	8720	
		11360	8730	
		11360	8730	
2.0	7.62	11365	7871	80
		11361	7859	
		11361	7865	
		11360	7855	
2.5	9.54	11361	6902	80
		11364	6886	
		11359	6921	
		11361	6900	
3.0	11.42	11369	5993	80
		11362	6018	
		11367	6000	
		11362	5997	
1.0	3.81	11318	9550	166
		11319	9562	
		11318	9563	
		11317	9541	
1.5	5.72	11318	8613	166
		11318	8631	
		11318	8631	
		11314	8628	
2.0	7.62	11317	7680	166
		11318	7712	
		11319	7670	
		11313	7676	
2.5	9.54	11312	6742	166
		11310	6740	
		11311	6752	
		11311	6742	

Calibration Data (Cont.)

P (lbs.)	M'_p (in.lbs.)	ε_b (μin./in.)	ε_a (μin./in.)	Temp.(°F)
3.0	11.42	11310	5860	166
		11310	5836	
		11308	5842	
		11308	5836	

Table F-2

Calibration Results

P(lbs.)	M'_p (in.lbs.)	T(°F)	ε_b (μin./in.)	ε_a (μin./in.)	$\Delta\varepsilon$ Calib.	$\Delta\varepsilon$ Theor.	% Error
1.0	3.81	80	11369	9634	1735	1725	0.58
1.5	5.72	80	11360	8728	2632	2610	0.84
2.0	7.62	80	11362	7870	3492	3490	0.06
2.5	9.54	80	11361	6902	4459	4380	1.8
3.0	11.42	80	11365	6002	5363	5260	1.9
1.0	3.81	166	11318	9554	1764	1760	0.23
1.5	5.72	166	11317	8626	2691	2670	0.78
2.0	7.62	166	11317	7685	3632	3560	2.0
2.5	9.54	166	11311	6744	4567	4480	1.9
3.0	11.42	166	11309	5844	5465	5370	1.7

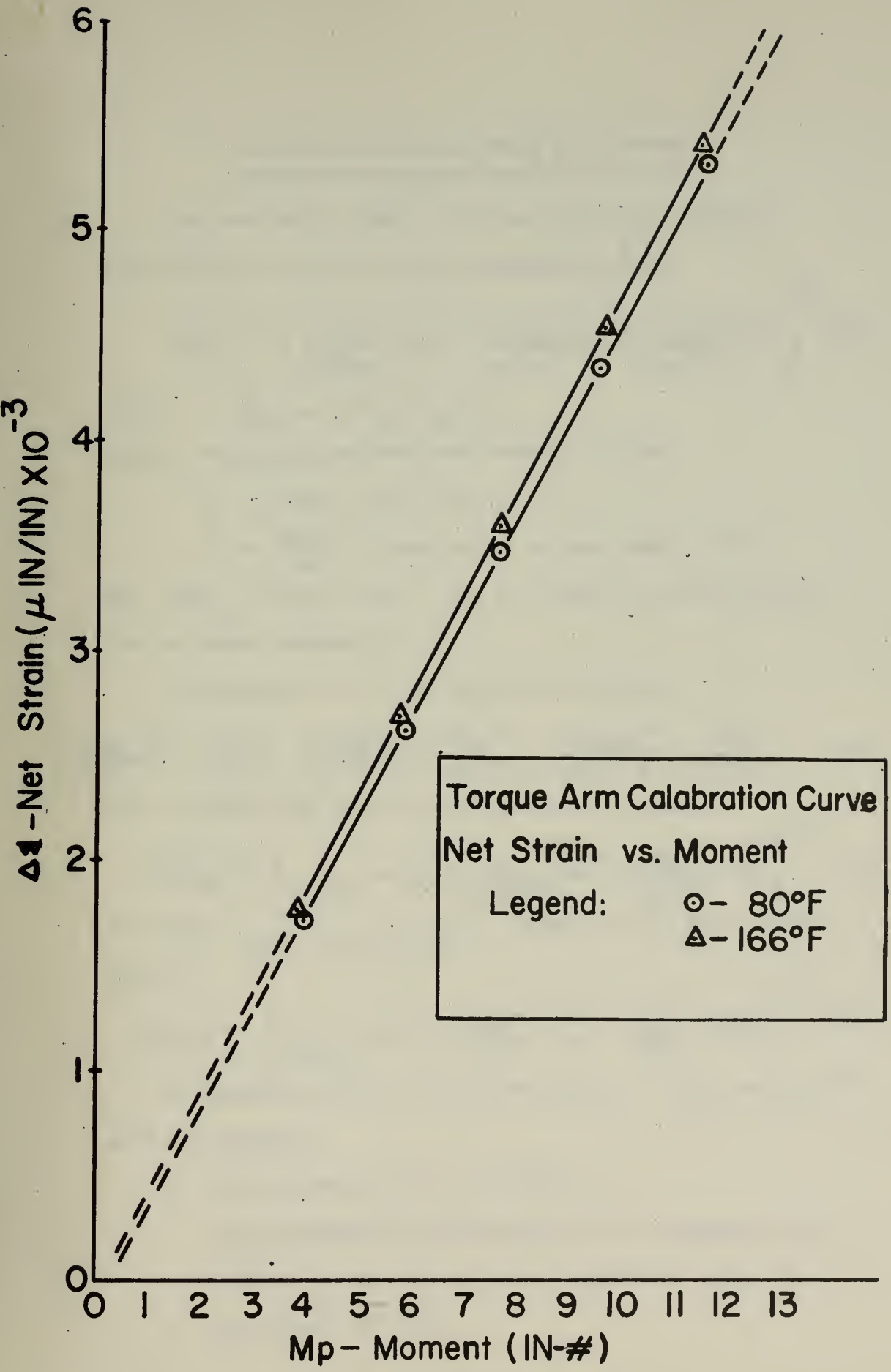
Δ1 - Net Strain (μIN/IN) X10^-3
0
1
2
3
4
5
6
0 1 2 3 4 5 6 7 8 9 10 11 12 13
Mp - Moment (IN-#)
Torque Arm Calabration Curve
Net Strain vs. Moment
Legend:
⊙ - 80°F
Δ - 166°F

Figure F-2

Uncertainty Analysis for μ_d Calibrated

The uncertainty (w_{μ_d}) in the value of the dynamic coefficient of friction can be expressed as [20].

$$w_{\mu_d} = \left(\left(\frac{\partial \mu_d}{\partial M_p}\right)^2 w_{M_p}^2 + \left(\frac{\partial \mu_d}{\partial W}\right)^2 w_W^2 + \left(\frac{\partial \mu_d}{\partial \bar{r}}\right)^2 w_{\bar{r}}^2 \right)^{1/2} \quad (27)$$

since, $\mu_d = M_p / W\bar{r}$

where, M_p = applied frictional moment (in.lbs.)

W = normal load (lbs.)

$\bar{r} = \frac{r_1 + r_2}{2}$ = mean radius of wear sample (in.)

and, w_{M_p}, w_W, $w_{\bar{r}}$ are the respective uncertainties for the above parameters.

The square of the first derivatives yields

$$\left(\frac{\partial \mu_d}{\partial M_p}\right)^2 = \frac{1}{W^2\bar{r}^2} \; ; \left(\frac{\partial \mu_d}{\partial W}\right)^2 = \frac{M_p^2}{W^4\bar{r}^2} \; ; \left(\frac{\partial \mu_d}{\partial \bar{r}}\right)^2 = \frac{M_p^2}{W^2\bar{r}^4} \quad (28)$$

Thus, substituting equation (28) into (27) we have

$$w_{\mu_d} = \left(\frac{1}{W^2\bar{r}^2} w_{M_p}^2 + \frac{M_p^2}{W^4\bar{r}^2} w_W^2 + \frac{M_p^2}{W^2\bar{r}^4} w_{\bar{r}}^2 \right)^{1/2} \quad (29)$$

but since $\mu_d^2 = M_p^2 / W^2\bar{r}^2$, equation (27) can be simplified to

$$w_{\mu_d} = \left(\frac{1}{W^2\bar{r}^2} w_{M_p}^2 + \frac{\mu_d^2}{W^2} w_W^2 + \frac{\mu_d^2}{\bar{r}^2} w_{\bar{r}}^2 \right)^{1/2} \quad (30)$$

To proceed further, the uncertainties in M_p, W, and $\bar{r}$ must be evaluated.

1. The Uncertainty in M_p (w_{M_p})

   It is assumed that uncertainty in the simulated calibration moment and the actual frictional moment is equal when $M_p' = M_p$.

Thus, $M_p' = P\ell'$ (in.lbs.) from which

$$w_{M_p} = \left(\left(\frac{\partial M_p'}{\partial P} \right)^2 w_P^2 + \left(\frac{\partial M_p'}{\partial \ell'} \right)^2 w_{\ell'}^2 \right)^{1/2} \qquad (31)$$

where,

$$\left(\frac{\partial M_p'}{\partial P} \right)^2 = \ell'^2, \text{ and } \left(\frac{\partial M_p'}{\partial \ell'} \right)^2 = P^2$$

whence,

$$w_{M_p} = \left(\ell'^2 w_P^2 + P^2 w_{\ell'}^2 \right)^{1/2} \qquad (32)$$

If, $\ell' = 3.81 \pm 0.01$ (in.)

$P = 1.0, 1.5, 2.0, 2.5,$ and 3.0 ± 0.05 (lbs.)

then, $w_{M_p} = \left(0.0363 + P^2 \times 10^{-4} \right)^{1/2}$ (33)

The following table gives the uncertainty in the frictional moment (M_p).

Table F-3

M_p(in.lbs.)	w_{M_p}	% uncertainty*
3.81	0.1910	5.02
5.72	0.1912	3.35
7.62	0.1917	2.51
9.54	0.1922	2.01
11.42	0.1930	1.67

*% uncertainty $= \frac{w_{M_p}}{M_p} \times 100$

2. The Uncertainty in W (W_W)

The smallest weight division on the scale used was 0.1 (lb.) Thus $W_W = \pm 0.05$ (lb.)

3. The Uncertainty in $\bar{r}$ $(W_{\bar{r}})$

By visually inspecting the wear specimen after each run, it was possible to estimate the uncertainty in $\bar{r}$. Thus, $W_{\bar{r}} = \pm 0.1$ (in.)

Since W_{M_P} does not vary greatly with moment, a mean uncertainty of 0.192 will be used. Substituting all known or calculated parameters into equation (30) yields

$$W_{\mu_d} = \left(\frac{6.55}{W^2} 10^{-2} + \frac{2.50}{W^2} 10^{-3} \mu_d^2 + 1.78 \times 10^{-2} \mu_d^2 \right)^{1/2} \quad (34)$$

The following table lists the uncertainty in the dynamic coefficient of friction for three loadings.

Table F-4

W (lbs.)	W_{μ_d}
10.29	$(6.18 \times 10^{-4} + 178 \times 10^{-4} \mu_d^2)^{\frac{1}{2}}$
20.55	$(1.56 \times 10^{-4} + 178 \times 10^{-4} \mu_d^2)^{\frac{1}{2}}$
30.35	$(0.712 \times 10^{-4} + 178 \times 10^{-4} \mu_d^2)^{\frac{1}{2}}$